WELL AND RESERVOIR MANAGEMAENT FOR MERCURY
CONTAMINATED WASTE DISPOSAL

Miss Manisa Rangponsumrit

การศึกษาการกำจัดของเสียที่มีการปนเปื้อนของปรอทลงสู่หลุมเจาะและแหล่งกักเก็บ

นางสาวมานิษา แรงผลสัมฤทธิ์

Thesis Title   WELL AND RESERVOIR MANAGEMAENT FOR
         MERCURY CONTAMINATED WASTE DISPOSAL

By   Manisa Rangponsumrit
Field of Study   Petroleum Engineering
Thesis Advisor   Suwat Athichanagorn, Ph.D.
Thesis Co-advisor Thotsaphon Chaianansutcharit, Ph.D.

Accepted by the Faculty of Engineering, Chulalongkorn University in Partial Fulfillment of the Requirements for the Master's Degree

…………………………… Dean of the Faculty of Engineering

(Professor Direk Lavansiri, Ph.D.)

THESIS COMMITTEE

…………………………… Chairman

(Associate Professor Yingyos Khemayodhin)

…………………………… Thesis Advisor

(Suwat Athichanagorn, Ph.D.)

…………………………… Thesis Co-advisor

(Thotsaphon Chaianansutcharit, Ph.D.)

…………………………… Member

(Jirawat Chewaroungroaj, Ph.D.)

มานิษา แรงผลสัมฤทธิ์ : การศึกษาการกำจัดของเสียที่มีการปนเปื้อนของปรอทลงสู่หลุมเจาะและแหล่งกักเก็บ (WELL AND RESERVOIR MANAGEMAENT FOR MERCURY CONTAMINATED WASTE DISPOSAL) อาจารย์ที่ปรึกษา : ดร. สุวัฒน์ อธิชนากร, อาจารย์ที่ปรึกษาร่วม : ดร. ทศพล ชัยอนันต์สุจริต, จำนวน 155 หน้า, ISBN 974-17-6088-4

ของเสียที่มีการปนเปื้อนของปรอทเป็นผลผลิตหนึ่งจากการผลิตก๊าซในหลายแหล่งก๊าซในอ่าวไทย   วิธีการหนึ่งที่ใช้ในการกำจัดของเสียคือการอัดของเสียที่มีการปนเปื้อนของปรอทเข้าไปสู่แหล่งกักเก็บที่ไม่สามารถทำการผลิตได้แล้วผ่านทางหลุมเจาะ   ประโยชน์ของวิธีการนี้คือสามารถกำจัดของเสียได้ในปริมาณมากและเป็นการกำจัดอย่างถาวร   โครงสร้างที่เหมาะสมที่สุดในการกำจัดของเสียในแหล่งก๊าซที่ทำการศึกษาคือบริเวณเอ็มเอ็นซึ่งเป็นโครงสร้างปิดและอยู่ในระยะสุดท้ายของการผลิต   เนื่องจากแหล่งกักเก็บที่ถูกเลือกยังมีความสามารถในการผลิตก๊าซ จึงต้องทำการผลิตก๊าซก่อน และจำเป็นต้องหากลยุทธ์ที่เหมาะสมที่สุดในการผลิตและกำจัดของเสียที่มีการปนเปื้อนของปรอท โปรแกรมสร้างแบบ จำลองแหล่งกักเก็บ 3 มิติ ได้ถูกในมาใช้ในการหากลยุทธ์ในการผลิตก๊าซ และกำจัดของเสียให้ได้ปริมาณมากที่สุด

แบบจำลองแหล่งกักเก็บสำหรับแหล่งกักเก็บในบริเวณเอ็มเอ็นสร้างมาจากข้อมูลคลื่นไหวสะเทือน ข้อมูลหลุมเจาะ และข้อมูลจากการวิเคราะห์ตัวอย่างชิ้นหิน สภาวะเริ่มต้นของแหล่งกักเก็บและคุณสมบัติของของไหลถูกกำหนดขึ้นในแบบจำลอง   และทำการปรับคุณสมบัติของแบบจำลองโดยทำให้ความสามารถในการผลิตและความดันของแหล่งกักเก็บในแบบจำลองเท่ากับประวัติการผลิตที่เกิดขึ้นจริง   หลังจากนั้นทำการหากลยุทธ์ที่ดีที่สุดในการผลิต   โดยการปรับเปลี่ยนแผนการเจาะผ่านแหล่งกักเก็บและแรงดันที่ใช้ควบคุมการผลิต สุดท้ายจึงทำการหากลยุทธ์ที่ดีที่สุดในการกำจัดของเสียที่มีการปนเปื้อนของปรอท   โดยการปรับเปลี่ยนความหนาแน่นของของเหลวที่จะกำจัด อัตราเร็วในการอัดของเสีย และความหนืดของของเหลว รวมถึงศึกษาอิทธิพลของตัวแปรต่างๆนี้ต่อความสามารถในการกำจัดของเสีย กลยุทธ์ที่ดีที่สุดต้องการเวลาน้อยที่สุดในการกำจัดของเสียโดยที่แรงดันในการอัดของเหลวไม่มากเกินไปจนก่อให้เกิดรอยแยกในชั้นหิน

ภาควิชาวิศวกรรมเหมืองแร่และปิโตรเลียม	ลายมือชื่อนิสิต..
สาขาวิชาวิศวกรรมปิโตรเลียม	ลายมือชื่ออาจารย์ที่ปรึกษา...................................
ปีการศึกษา 2547	ลายมือชื่ออาจารย์ที่ปรึกษาร่วม..............................

Mercury contaminated waste is one of the byproducts from hydrocarbon production in many gas fields in the Gulf of Thailand. One method to dispose the waste is to inject mercury contaminated waste into confined depleted reservoirs through a depleted well. The advantages of this approach are high disposal capacity and permanent waste elimination. In the field selected for this study, the most suitable structure called the MN compartment, which is a confined and in the last stage of production, was chosen. Since the selected reservoirs are not completely depleted, gas should first be produced. Thus, there is a need to optimize both the production and waste disposal strategy. In this study, a 3D reservoir simulator is used to maximize gas production and Hg contaminated waste disposal.

The reservoir simulation model for the reservoirs in the MN compartment was constructed from seismic, well logging, and special core analysis data. Initial reservoir conditions and fluid properties were entered into the model, and history matching on production performance and reservoir pressure was performed to fine tune the reservoir model. After that, reservoir simulation was performed to optimize hydrocarbon production by varying perforation plan and wellhead production pressure. Finally, mercury contaminated slurry injection was optimized by performing sensitivity simulation on slurry density, injection rate, and slurry viscosity. The effect of these parameters on injection capability was also investigated. The optimal injection criterion is minimum injection time under a condition that the injection pressure is not high enough to create any fracture in the reservoirs.

Department of Mining and Petroleum Engineering   Student's signature……………...

Field of study: Petroleum Engineering   Advisor's signature……………...

Academic year: 2004   Co-advisor's signature…………..

Acknowledgments

I would like to express my graceful thank to Dr. Suwat Athichanagorn, my thesis advisor, for useful discussion and invaluable advice for this work. I also am grateful to Dr. Thotsaphon Chaianansutcharit, my co-advisor, for creative suggestion and invaluable advice. I would like to gratefully thank Dr. Vinit Harnsamutr, Chief Reservoir Engineer (PTTEP Co., Ltd.) for providing guideline, reservoir simulation software, data used in this work, invaluable recommendations and encouragement. I wish to give my special thank to Mr. Rangsun Bhengbhun, Chief geologist (PTTEP Co., Ltd.) for providing the geological model for the study and important knowledge.

I would like to give my special thank to everyone in the Reservoir engineering group at PTTEP Co., Ltd. for invaluable discussions, encouragement, and friendship.

I would like to express my deep appreciation to my family who gives me their sympathy, endless love, encouragement, and support

I wish to thank the thesis committee members for their comments and recommendations.

Contents

Contents (continued)

Contents (continued)

List of Tables

List of Figures

List of Figures (continued)

List of Figures (continued)

List of Figures (continued)

Nomenclature

A cross-section area

B formation volume factor

$\vec{g}$ gravity force

g_c conversion constant

k permeability

k_{rg} gas relative permeability

k_{rw} water relative permeability

k_{ro} oil relative permeability

M_x mass flux in or out of control volume

p pressure

p_c capillary pressure

p_{cow} water-oil capillary pressure

p_{cog} gas-oil capillary pressure

Q mass injection or production

q fluid flow rate

R_{so} solution gas oil ratio

R_{sw} solution gas water ratio

S saturation

u_x flow velocity

V fluid volume

GREEK LETTER

ϕ porosity

ρ fluid density

μ fluid viscosity

Δ difference operator

λ fluid mobility

Nomenclature (continued)

SUPERSCRIPTS

n current time level

$n+1$ new time level

SUBSCRIPTS

g gas

i grid block location

o oil

sc standard condition

w water
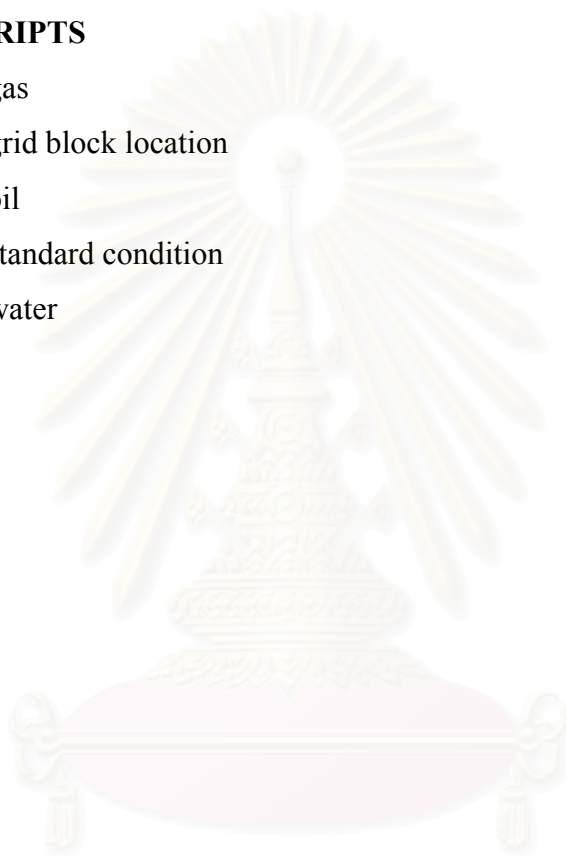
CHAPTER I

INTRODUCTION

The production of oil and gas from hydrocarbon reservoirs may generate hazardous waste such as mercury(Hg), lead(Pb), cadmium(Cd), zinc(Zn), chromium(Cr), copper(Cu), etc. These metals, especially mercury, can affect and harm the environment. In order to protect the environment, this hazardous waste should be properly disposed of.

Mercury (Hg) is originated from volcanic rocks that underlie hydrocarbon reservoir and naturally associated with the production of hydrocarbon [1]. Due to it hazard, mercury should be separated from the hydrocarbon. Mercury contaminated waste is one of the byproducts from gas production in one of the petroleum fields in the Gulf of Thailand. We will call this field the M field. Approximately 100 tons of Hg-contaminated waste is generated each year, about 50 tons from production and the balance from yearly cleaning of condensate vessel of the floating storage offloading (FSO). The sour process platform (SPP), planned to be in operation in 2005, will create additional 150 to 200 tons of Hg solid-base waste each year. This calls for a need to manage 250-300 tons of contaminated waste a year.

Currently, Hg-contaminated waste from the M field is exported for treatment in the Netherlands. Pure Hg is separated and then sold in the market. However, the demand of Hg is likely to reduce. So, the treatment cost should increase in the future.

There are several techniques to dispose Hg-contaminated waste. One technique is to bury it in an abandoned well. This method is not suitable due to limitation of capacity. Another method is to fill Hg-contaminated waste in drums and stored in a warehouse located in a remote area. This method also has limitation in storage area. A recent technique is to inject Hg-contaminated waste into confined depleted reservoirs through a depleted well. The advantages of this approach are high disposal capacity and permanent waste elimination. In this method, the Hg-contaminated sludge is ground to fine particles and then mixed with seawater. The slurry is then injected into the depleted well.

Waste disposal into a depleted reservoir was successfully implemented in the Gulf of Thailand by Unocal Thailand, Ltd. in August/September 2001. The slurry was prepared by mixing ground sludge, viscosifier, and seawater until it had a viscosity of 40-70 cp and density of 9 to 10 ppg. The preparation and injection of slurry was done in batches. One batch yielded 30-40 barrels of slurry prepared from 10-15 drums of Hg-contaminated waste. The injection rate of slurry was 2 to 3 barrels/minute. After each batch of injection, the slurry was chased out from the wellbore area by seawater injection. The slurry and seawater was alternatively injected until 1,666 drums of sludge were slurrified and disposed into depleted reservoirs. The success of this case has proven that subsurface injection of Hg-contaminated slurry is an environmentally and economically attractive disposal method.

To handle a large quantity of Hg-contaminated waste generated in the M field, the depleted reservoir disposal method was selected and scheduled to be implemented in 2005. An appropriate reservoir should be selected based on the following criteria: confined structure, fully depleted reservoir, high injectivity, and high capacity reservoir. After an integrated team of engineers and geologists had finished reviewing and studying the M field, the most suitable structure called the MN compartment, which is confined and in the last stage of production, was chosen. The compartment MN is multi-layered reservoir consisting of 22 gas reservoirs. Since the selected reservoirs are not completely depleted, hydrocarbon production and Hg-contaminated waste disposal strategy should be optimized. In this study, a 3D reservoir simulator called ECLIPSE is used to maximize hydrocarbon production and Hg-contaminated waste disposal.

1.1 Outline of Methodology

This thesis is to optimize hydrocarbon production and slurry injection strategy to dispose Hg-contaminated waste into a depleted reservoir using a reservoir simulator. The following tasks are performed :

1) Determine representative fluid and rock properties using available PVT and special core analysis (SCAL) data.

2) Build a reservoir model based on a geological model that was constructed from sand map, well logs, and special core analysis data. The geological model has a total of 50,000 - 70,000 grid blocks.

3) Perform history matching based on the production data.

4) Perform reservoir simulation to optimize strategy for hydrocarbon production and slurry injection to meet the following conditions:

   (a) Since there are several layers intersected by the well, the well will be perforated in two batches from the bottom up.

   (b) The well will be used for alternate production and injection until it is completely depleted and reaches injection capacity. After the first batch of perforation, the well will be on production for two years or until the reservoirs are completely depleted. Then, Hg-contaminated slurry will be injected. Then, the zones will be plugged, and the second batch of reservoirs is perforated.

   (c) Hg-contaminated slurry will be injected every two years for a maximum injection period of two weeks.

5) Analyze the results and make conclusion.

1.2 Thesis Outline

This thesis paper consists of seven chapters.

Chapter 2 outlines a list of related work of mercury contaminated waste disposal and reservoir simulation that has been previously conducted.

Chapter 3 describes the principle of reservoir simulation and its application that related to this study.

Chapter 4 discusses the steps involved in the construction of the geological model of the disposal reservoir. The geological reservoir model was constructed based on sand map, well log, and available special core analysis data. Essential parameters which are porosity, permeability, and water saturation were defined for each grid block.

Chapter 5 discusses the process of history matching. The production data of the well MN-1 starting from the initial production in June 1996 until October 2003

were used in history matching. When performing history matching, the absolute permeability, relative permeability, aquifer volume, and original gas in place were adjusted.

Chapter 6 discusses the prediction of hydrocarbon production and mercury contaminated waste injection obtained from reservoir simulation. Reservoir simulation was used to optimize hydrocarbon production and slurry injection. The optimized variables are perforation plan, maximum gas rate, Hg sludge concentration, Hg-contaminated slurry viscosity, and injection rate. Simulation runs for all the cases were performed based on an assumption that there is no particle filtration effect.

Chapter 7 makes conclusion and provides recommendation for future works.

CHAPTER II

LITERATURE REVIEW

This chapter discusses some of related works on mercury contaminated waste disposal. Some works on reservoir simulation and history matching are also outlined.

2.1 Previous Works on Hazardous Waste Management

Mercury occurs naturally during gas production in certain fields. It is one of the major problems in the petroleum industry. Several techniques such as ordinary physical cleaning, physical cleaning in association with chemical treatment, and deep-well disposal have been deployed in order to eliminate Hg. The following literatures discuss some related works on Hg disposal.

Mussig *et.al* [1] discussed about methods to remove Hg from sale gas and method to dispose it. The methods to remove Hg from sale gas are low temperature separation (LTS) or amalgamation with other metals. Hg-contaminated waste, removed from sale gas, can be treated on-site using high temperature oxidation (HTO) process or mixing it with cement and then pumping it down into the borehole or filling it into cylindrical containers. Another method is downhole disposal which carries Hg-contaminated sludge and scales into a depleted formation.

Wilhelm and McArthur [2] reviewed mercury contamination in the gas processing industry and introduced chemical and thermal methods for clean-up and disposal of mercury waste. Chemical treatments can be applied to the equipment decontamination and soil remediation. This method uses non-aqueous solvents to remove mercury from equipment surfaces and certain soils. Then, mercury solution is filtrated or precipitated to obtain elemental mercury. The thermal process is to heat a complex mixture containing mercury to allow mercury to vaporize. Then, mercury vapor is condensed and collected in a relatively pure form.

Soponkanabhorn and Killing [3] presented a procedure to treat Hg-contaminated seawater to meet strict criteria set by the Royal Thai Government (mercury < 5 ppb) by using chemical precipitation, coagulation, and activated carbon adsorption methods.

Yod-In-Lom and Doyle [4] presented a method to dispose Hg sludge by deep well injection. This method was approved by the Department of Mineral Resources and performed in a safe, environmental friendly and cost effective manner. The slurry disposal process consists of grinding, slurry mixing, and injection.

Pongsiri [5] discussed about an origination of mercury in Gulf of Thailand. After the mercury contaminated sludge is recovered from hydrocarbon production, it was proposed to be injected into depleted reservoirs. The injecting process consists of crushing, slurring, stirring, and pumping.

Chaianansutcharit [6] presented a well selection process for Hg waste disposal in Bongkot field in Thailand by considering four criteria; reservoir confinement, depleted reservoir, high injectivity, and high capacity.

2.2 Previous Works on Reservoir Simulation and History Matching

As mentioned earlier, the selected method for Hg waste disposal in the M field is to re-inject it into a depleted reservoir. Reservoir simulation is used for this study to optimize hydrocarbon production and Hg waste injection. The reservoir simulation process consists of reservoir model construction, history matching, and prediction. Many authors have proposed effective workflows for reservoir simulation as well as benefits and shortcomings of reservoir simulation for reservoir management.

Dimitrakopoulos [7] presented a simple and effective geostatistical method to determine the absolute horizontal and vertical effective permeabilities for reservoir grid blocks from core data. The concept is to define block permeability as a function of the permeability variogram, the average volume, and a power averaging constant.

Aly *et.al.* [8] presented a case study of using geostatistics to develop a 3D model by integrating well log, geologic, and core data. The completed model honors the exact well data and imposes spatial continuity relations derived from variography. After applying this technique, a three dimensional porosity distribution was generated by ordinary kriging. The permeability realizations were generated from permeability-porosity correlation, which was obtained from core data analysis. The geostatistical reservoir model is more heterogeneous and better representative than the conventional geological model.

Saleri and Toronyi [9] presented application of reservoir simulation and its three key shortcomings which are lacking of established industry standards, non-uniqueness of model solutions, and inherent uncertainties in the modeling. The general methodology for conducting reservoir simulation was also proposed. It starts with statement and prioritization of objectives, reservoir characterization, model selection, model construction, validation, and finally documentation.

Thomas [10] discussed roles of reservoir simulators for initial reservoir development, optimization of future production plans, and EOR project design. The use of reservoir simulation in the initial reservoir development can minimize the number of alternatives. Simulation can be used for sensitivity analysis to observe the effects of uncertainties in reservoir description and fluid data. If reservoir description and fluid properties are reasonably defined, reservoir simulation can be very useful for assigning well location. For reservoir development, history matching needs to be carried out to calibrate the reservoir model. The history matched model is then suitable for production planning and prediction.

Sanchez, Martinez and Rattia [11] presented a process flow for reservoir simulation step by step to achieve exceptional simulation results. Three major steps were proposed. The first step is initialization of the reservoir model. The second step is history matching, which is to match simulation production data with historical data. The last step is prediction of future performance such as effects of well location and spacing, effects of production or injection rate variations, and additional recovery using an enhanced oil recovery process.

Williams and Keating [12] proposed a technique for performing history matching. Four hierarchical levels of history matching are (1) global or fieldwide, (2) flow units or layer group, (3) individual layers, and (4) individual wells. There are seven steps in this approach: (1) gathering data, (2) preparing analysis tools, (3) identifying key wells, (4) interpreting reservoir behavior from observed data, (5) running model, (6) comparing model results to observe data, and (7) adjusting model parameters. This method provides guidance for reservoir management as well as improves its efficiency. This method has been successfully used in many complex

simulation studies, reducing the time spent in history matching and improving the integrity of the match.

In the literatures reviewed in this study, several techniques have been used to decontaminate mercury from sale gas, seawater, soil, and equipments. The mercury decontamination methods are chemical treatment, thermal treatment, LTS, coagulation, and activated carbon adsorption. Using thermal process and precipitation process, mercury can be collected in the form of pure element. Pure mercury can be reused in some industries. However, mercury waste may remain in a sludge form and should be disposed by a proper method. There are several techniques to dispose the waste such as mixing it with cement and then pump it down into the borehole, storing it in drums or disposing it into depleted reservoirs. As mentioned in Chapter 1, to handle Hg-contaminated waste generated in the M field, the depleted reservoir disposal method is selected because it is an effective method which can permanently eliminate Hg-contaminated waste. This disposal method consists of grinding, slurring, and injecting. The criteria for choosing a disposal reservoir are reservoir confinement, depleted reservoir, high injectivity, and high capacity.

Reservoir simulation and history matching processes were reviewed to obtain a guideline for this study. Reservoir simulation should start from objective defining, reservoir characterization, model construction, history matching, and prediction. Geostatistical techniques should be applied for geological model construction since they provide better representation than the conventional geological model. The simulation production data should be matched with historical data. After completing history matching, the model is ready for prediction of future reservoir performance.

CHAPTER III

RESERVOIR SIMULATION

Reservoir simulation is a powerful technique for reservoir management. To perform reservoir simulation, a reservoir model is constructed and used to predict reservoir performance under different operating scenarios. Reservoir simulation model is a numerical model of reservoir made up of a large number of cells and uses numerical equations to simulate reservoir performance. The numerical reservoir model is representative of a real geological structure. The equations are solved to examine the reservoir performance in terms of pressure and flow rate. Reservoir simulation can be used to predict future performance in order to make a decision on optimum development strategies.

To perform reservoir simulation, the reservoir is divided into a number of blocks. Basic data are required in each grid block. The wells are positioned within the arrangement of blocks. The required flow in/out rate is specified as a function of time. The appropriate equations are solved for pressures and saturations of each block as well as the production of each phase for each well.

3.1 Formulation of Simulation Equations

The basic equations of reservoir simulation are obtaining by combining conservation of mass (material balance equation) with conservation of momentum (Darcy's Law). These equations along with appropriate constraints, constitutive relations, and initial conditions can be solved by approximate numerical techniques to predict the performance of reservoirs under different operating conditions.

3.1.1 Mass conservation

Mass conservation in a representative elementary volume or grid block is achieved by equating the accumulation of mass in the block with the difference between the mass leaving the block and the mass entering the block.

For one dimension,
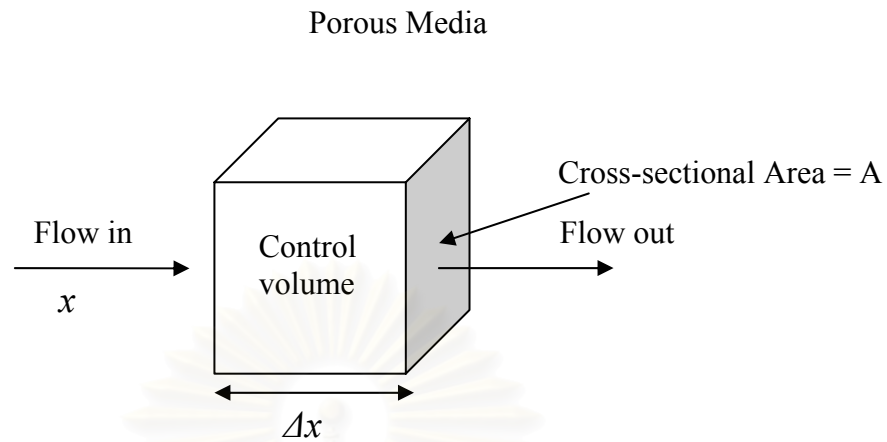
Porous Media

Figure 3.1: Fluid flow in porous media.

From Fig. 3.1,

$$\text{Volume of control volume} = A\Delta x \qquad (m^3) \qquad (3.1)$$

$$\text{Rock porosity in control volume} = \phi(t) \qquad (3.2)$$

$$\text{Fluid density (mass/volume)} = \rho(x,t) \qquad (3.3)$$

$$\text{Mass of fluid in control volume} = \rho\phi A\Delta x = \rho\phi\Delta V \qquad (3.4)$$

Mass balance equation

Over the time interval Δt, the material balance equation is

Mass in – Mass out = Mass accumulation* + Mass injection or production   (3.5)

* The mass accumulation is due to compressibility as the pressure change.

$$\text{Mass in} = M_x\big|_x A\Delta t \qquad (3.6)$$

$$\text{Mass out} = M_x\big|_{x+\Delta x} A\Delta t \qquad (3.7)$$

Accumulation = [mass in place at time $t + \Delta t$] - [mass in place at time t]

$$= \left[\rho\phi A\Delta x\right]_{t+\Delta t} - \left[\rho\phi A\Delta x\right]_t \qquad (3.8)$$

where M_x = mass flux in or out of control volume = mass flow/area/time

Then,

$$\left[M_x|_x - M_x|_{x+\Delta x}\right]A\Delta t = \left[\rho\phi A\Delta x\right]_{t+\Delta t} - \left[\rho\phi A\Delta x\right]_t + QA\Delta x\Delta t \tag{3.9}$$

where Q = mass injection (-) or production (+) = mass flow/volume/time

Dividing Eq. 3.9 by $A\Delta x\Delta t$, then

$$\frac{\left\lfloor M_x|_x - M_x|_{x+\Delta x}\right\rfloor}{\Delta x} = \frac{\rho\phi|_{t+\Delta t} - \rho\phi|_t}{\Delta t} + Q \tag{3.10}$$

Taking limit as $\Delta x \to 0$, $\Delta t \to 0$, then

$$-\frac{\partial M_x}{\partial x} = \frac{\partial}{\partial t}(\phi\rho) + Q \tag{3.11}$$

3.1.2 Momentum conservation

Momentum conservation is modeled using Darcy's law. This assumption means that the model does not accurately represent turbulent flow in a reservoir or near the wellbore.

$$\text{Mass flux} = M_x = \rho u_x \tag{3.12}$$
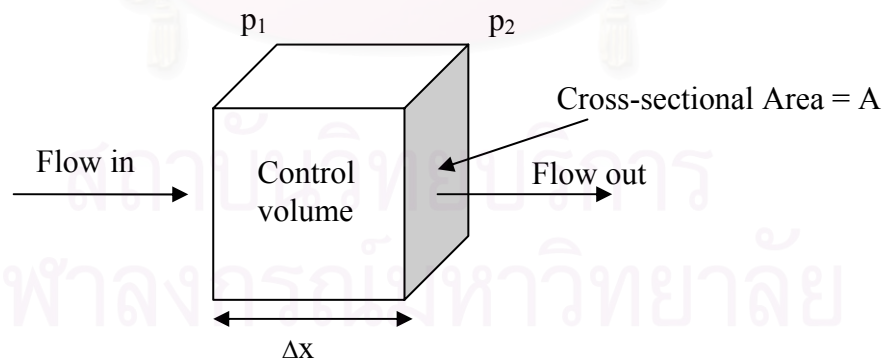
Figure 3.2: Linear flow in porous media.

From Fig. 3.2, Darcy's law is described as

$$u_x = -\frac{k}{\mu}\frac{\partial p}{\partial x}$$

(3.13)

where k = permeability

For three dimensional single phase flow,

$$\vec{u} = -\frac{k}{\mu}\left[\nabla p + \rho\frac{\vec{g}}{g_c}\right]$$

(3.14)

where $\vec{g}$ = gravity force

g_c = conversion constant

$$\rho\frac{\vec{g}}{g_c} = \rho\frac{g}{g_c}\nabla z = \gamma\nabla z$$

(3.15)

Note z is positive in the downward direction.

Thus, Darcy's law can be written in the vector form as

$$\vec{u} = -\frac{k}{\mu}[\nabla p - \gamma\nabla z]$$

(3.16)

3.1.3 Combining material balance equation with Darcy's law

Substituting u_x in the definition of M_x and substituting M_x in Eq. 3.11, one gets

$$-\frac{\partial(\rho u_x)}{\partial x} = \frac{\partial}{\partial t}(\rho\phi) + Q$$

(3.17)

In three dimensions,

$$-\nabla(\rho\vec{u}) = \frac{\partial}{\partial t}(\rho\phi) + Q$$

(3.18)

Substituting $\vec{u}$ from Eq. 3.16, we obtain

$$-\nabla\left(\frac{\rho k}{\mu}(\nabla p - \gamma\nabla z)\right) = \frac{\partial}{\partial t}(\rho\phi) + Q$$

(3.19)

3.1.4 Simulation flow equation

Now if we divide Eq. 3.20 by ρ_{sc} and define the formation volume factor as

$B = \dfrac{V_{res}}{V_{sc}}$, then

$$-\nabla[\lambda(\nabla p - \gamma\nabla z)] = \frac{\partial}{\partial t}\left(\frac{\phi}{B}\right) + q \tag{3.20}$$

where V_{res} = fluid volume calculated at reservoir condition

V_{sc} = fluid volume calculated at standard condition

$$\lambda = \frac{k}{\mu B} \quad \text{and} \quad q = \left(\frac{Q}{\rho_{sc}}\right) \tag{3.21}$$

q = fluid flow rate

Three phase simulation flow equations can be described as follows:

Water phase

$$-\nabla[\lambda_w(\nabla p_w - \gamma_w\nabla z)] = \frac{\partial}{\partial t}\left(\phi\frac{S_w}{B_w}\right) + q_w \tag{3.22}$$

where S_w = water saturation

B_w = water formation volume factor

q_w = water flow rate

Oil phase

$$-\nabla[\lambda_o(\nabla p_o - \gamma_o\nabla z)] = \frac{\partial}{\partial t}\left(\phi\frac{S_o}{B_o}\right) + q_o \tag{3.23}$$

where S_o = oil saturation

B_o = oil formation volume factor

q_o = oil flow rate

Gas phase

$$-\nabla\left[R_{so}\lambda_o\left(\nabla p_o - \gamma_o\nabla z\right) + R_{sw}\lambda_w\left(\nabla p_w - \gamma_w\nabla z\right) + \lambda_g\left(\nabla p_g - \gamma_g\nabla z\right)\right]$$ (3.24)

$$= \frac{\partial}{\partial t}\left(\phi\left(R_{so}\frac{S_o}{B_o} + R_{sw}\frac{S_w}{B_w} + \frac{S_g}{B_g}\right)\right) + R_{so}q_o + R_{sw}q_w + q_g$$

where S_g = gas saturation

B_g = oil formation volume factor

q_g = oil flow rate

R_{so} = solution gas-oil ratio

R_{sw} = solution gas-water ratio

The transmissibility for phase i is

$$\lambda_i = \frac{kk_{ri}}{\mu_i B_i}$$ (3.25)

For a three-phase simulation, there are six unknowns which are p_o, S_o, p_w, S_w, p_g, and S_g. Thus, three additional relationships from the saturation equation and capillary pressure equations are required to solve for the six unknowns.

The saturation equation is expressed as

$$S_o + S_w + S_g = 1$$ (3.26)

The capillary pressure equations are

$$p_{cow} = p_o - p_w = f(S_w)$$ (3.27)

$$p_{cog} = p_g - p_o = f(S_g)$$ (3.28)

where p_{cow} = water-oil capillary pressure

p_{cog} = gas-oil capillary pressure

After knowing the reservoir properties, fluid properties, initial reservoir conditions, time step and grid block sizes, we can solve Eqs. 3.22 to 3.28 for the six unknowns.

3.2 Simulation Solution Procedure

Fluid flow equations for reservoir simulation are a set of nonlinear partial differential equations. The partial derivatives are converted to finite differences, which can be solved more easily. Then, the unknown parameters can be calculated in the domain of discrete element (grid blocks) and discrete time step.

We may replace $\frac{\partial}{\partial x}$ and $\frac{\partial}{\partial t}$ at specific points in space and time using Taylor's series, which can be written as

$$f(x_0 + \Delta x) = f(x_0) + \frac{\Delta x}{1!}\frac{\partial f(x_0)}{\partial x} + \frac{(\Delta x)^2}{2!}\frac{\partial^2 f(x_0)}{\partial x^2} + \frac{(\Delta x)^3}{3!}\frac{\partial^3 f(x_0)}{\partial x^3} + \ldots \qquad (3.29)$$

From Taylor's series, three finite difference forms to approximate the partial differential equations can be determined. The finite difference equations in the space domain for one dimension are given as:

Forward difference $\quad \dfrac{\partial f}{\partial x} = \dfrac{f(x + \Delta x) - f(x)}{\Delta x}$

Backward difference $\quad \dfrac{\partial f}{\partial x} = \dfrac{f(x) - f(x - \Delta x)}{\Delta x}$

Central difference $\quad \dfrac{\partial f}{\partial x} = \dfrac{f(x + \Delta x) - f(x - \Delta x)}{2\Delta x}$

The example of finite difference simulation equation for the oil phase in the x-direction is shown as follows:
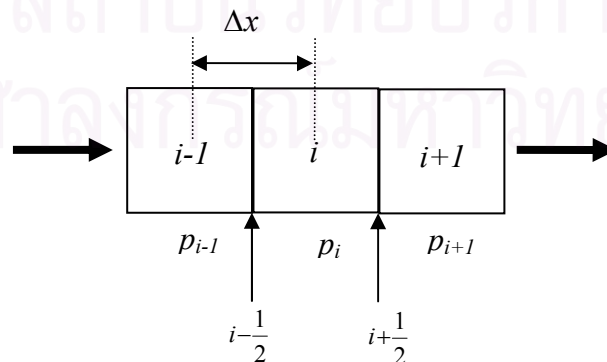
Figure 3.3: One dimension simulation grid.

From Eq. 3.23, by neglecting the gravity term, the flow equation for the oil phase in the x-direction at block i is expressed as

$$-\frac{\partial}{\partial x}\left(\lambda_{o,i}\left(\frac{\partial p_o}{\partial x}\right)_i\right) = \frac{\partial}{\partial t}\left(\phi_i\frac{S_o}{B_o}\right)_i + q_o \qquad (3.30)$$

where

$$\left(\frac{\partial p_o}{\partial x}\right)_i = \left(\frac{\partial p_o}{\partial x}\right)_{i+\frac{1}{2}} - \left(\frac{\partial p_o}{\partial x}\right)_{i-\frac{1}{2}} \qquad (3.31)$$

Then,

$$-\frac{1}{\Delta x}\left[\lambda_{o,i}\left(\frac{\partial p_o}{\partial x}\right)_{i+\frac{1}{2}} - \lambda_{o,i}\left(\frac{\partial p_o}{\partial x}\right)_{i-\frac{1}{2}}\right] = \frac{\phi_i}{B_{o,i}}\left(\frac{\partial S_o}{\partial t}\right)_i + q_o \qquad (3.32)$$

Finally, the finite difference form of the flow equation for the oil phase in the x-direction at block i can be written as

$$-\frac{\lambda_{o,i}}{\Delta x}\left[\left(\frac{p_{o,i+1}-p_{o,i}}{\Delta x_i}\right)_{i+\frac{1}{2}} - \left(\frac{p_{o,i}-p_{o,i-1}}{\Delta x_i}\right)_{i-\frac{1}{2}}\right] = \frac{\phi_i}{B_{o,i}\Delta t}\left(S_{o,i}^{n+1} - S_{o,i}^n\right) + q_o \qquad (3.33)$$

where n = current time level

$n+1$ = new time level

Δt = time step

Two approaches can be used to solve this system of equations. Fig. 3.4 shows the flow chart of the two techniques.

1. Fully implicit or implicit pressure implicit saturation method. This approach uses saturations at the old time step (S^n) to implicitly calculate pressures and saturations at the new time step (p^{n+1} and S^{n+1}). The pressures and saturations at the new time level are determined simultaneously. The fully implicit method is totally stable, i.e., no limit for the time step size. However, numerical dispersion, an error in calculating the movement of saturation front becomes more pronounced when the time step size increases.

2. IMPES or Implicit Pressure and Explicit Saturation method. This approach uses saturations and pressures at the old time step (p^n) to implicitly calculate pressures at the new time step (p^{n+1}), then uses saturations at the old time step (S^n) and the pressures at the current time step (p^{n+1}) to explicitly calculate saturations at the new time step (S^{n+1}). The IMPES method has a few severe stability constraints such as a throughput for a grid block cannot exceed 10% of the pore volume and time step lengths cannot be large.

The fully implicit technique does more calculations in a time step than the IMPES procedure, but is stable over longer time steps. The unconditional stability of the fully implicit technique means that a fully implicit simulator can solve problems faster than the IMPES technique by taking a significantly longer time step.
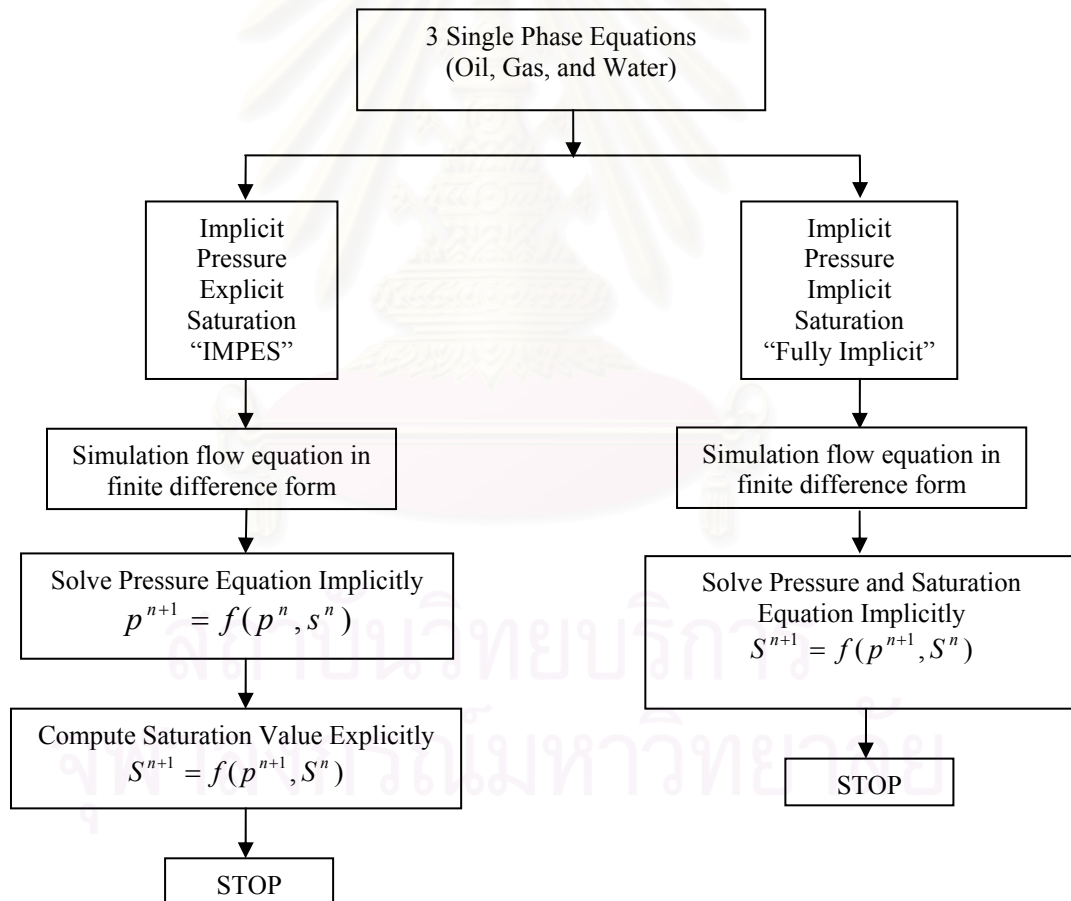
Figure 3.4: Flow chart for solving fluid flow simulation equations.

3.3 Reservoir Simulation Workflow

A typical workflow of reservoir simulation can be organized into 3 main steps which are reservoir model construction, history matching, and prediction. A rough detail of each step is described as follows:

3.3.1 Reservoir model construction

To construct a reservoir model, the following tasks are performed:

1. Describe the physical properties of the reservoir such as reservoir structure, gross and net thickness, well location, and perforation interval.

2. Design reservoir grid and define reservoir/fluid properties such as porosity, permeability, fluid properties, initial fluid saturation, initial pressure, initial temperature, and fluid contact. The basic data required for a simulation study and source of data are listed below:
   - Porosity from core analysis and logging.
   - Permeability from core analysis, logging, and well testing.
   - Relative permeability from core analysis.
   - Capillary pressure from core analysis.
   - Initial fluid saturation from well data, logging, and core analysis.
   - Pore compressibility from core analysis.
   - Initial pressure from repeated formation test (RFT) and drill stem test (DST).
   - Initial temperature from RFT and logging.
   - Fluid properties (oil, water, and gas) such as B, μ, oil-gas ratio from PVT analysis.
   - Grid dimensions defined by users.
   - Well producing interval and productivity from field performance history.
   - Aquifer description from seismic and material balance calculations.
   - Observed pressure vs. time from field performance history.

3. Select an appropriate simulation model. Reservoir simulator is classified as different types based on the following characteristics:
   - Fluid description
     - o Black oil

- o Equation of state (EOS) –compositional
- o Chemical
- Temperature
  - o Isothermal
  - o Thermal
- Simulation solution method
  - o IMPES
  - o Fully implicit
- Coordinates systems
  - o Cartesian
  - o Radial
  - o Spherical

In this study, the reservoir simulator ECLIPSE 100 is used. ECLIPSE 100 is a black oil and isothermal simulator. The fully implicit method was selected as simulation solution method since it is a stable technique. The selected grid system is Cartesian coordinate.

3.3.2 History matching

The objective of history matching is to fine tune parameters in the model until the simulated performance matches with the historical information. History matching is an inverse problem as shown in Fig. 3.5. For an inverse problem, the model equation and output are known but the input parameters are not known. Typically, trial and error is used to accomplish model matching.
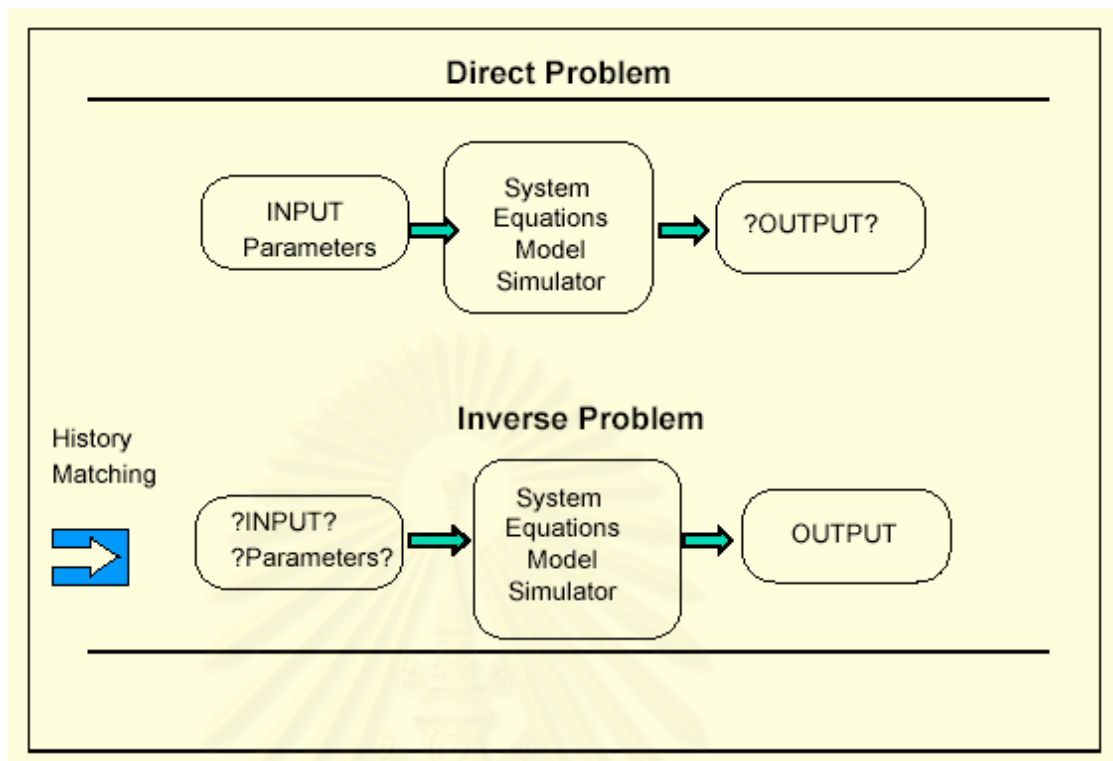
Figure 3.5: Direct problem vs. inverse problem (Pinisetti, 2004).

Adjusting variables

The following variables are often considered to have high uncertainties, so they are prior to be adjusted in the history matching process:

- o Pore volume
- o Permeability
- o Transmissibility
- o k_v/k_h ratio
- o Relative permeability
- o Aquifer properties

The following variables are often considered to be determined properties (having low uncertainties), so they should not be adjusted without any confidence:

- o Gross thickness
- o Net thickness
- o Structure (reservoir top/bottom)

o Fluid properties

o Rock compressibility

o Capillary pressure

o Original fluid contact

o Production rates

History matching procedure

History matching is performed in the following manners:

(1) Match volume (original hydrocarbon in place). The significant parameters affecting the volume are pore volume and fluid contact.

(2) Match reservoir pressure. The significant parameters affecting the reservoir pressure are pore volume, hydrocarbons in place, and aquifer properties which are size and direction.

(3) Match production or injection history. The significant parameters affecting the production or injection profile are relative permeabilities and the absolute permeability.

(4) Match well flowing pressure. The significant parameters affecting the well flowing pressure are *kh* and skin.

Acceptable error on the matching of each parameter depends on the objective of the study, quality of the historical data, and the model resolution.

3.3.3 Prediction

After fine tuning the parameters in the history matching process, the reservoir model can now be used to simulate the behavior of different scenarios in the prediction mode. The detail of prediction depends on the nature of a particular field and the objective of the study. In general, this process starts form defining a base case; then, parameters or conditions to be varied are designed. Sensitivity analysis of defined variables is performed to compare results of different simulation cases. The best case is selected based on the objective of the study such as the highest productivity, the highest injectivity, or the latest water breakthrough.

In summary, reservoir simulation is a process to simulate the reservoir performance by solving numerical equations of reservoir simulation model. The numerical equations are solved for pressures and saturations of each grid block as well as the production of each phase for each well. Reservoir simulation equations are formulated from conservation of mass (Material balance equation) and conservation of momentum (Darcy's law). There are two approaches in solving reservoir simulation equations: IMPES and fully implicit. In the IMPES method, the pressures at the new time step are solved using saturations at the old time step; then, the pressures at the new time level are used to explicit calculate saturations at the new time step. In the fully implicit method, the pressures and saturations at the new time step are determined simultaneously. The fully implicit method is selected as the simulation solution method in this study since it is a stable technique.

A typical workflow of reservoir simulation consists of 3 main steps which are reservoir model construction, history matching, and prediction. Workflow for reservoir model construction consists of (1) describing reservoir characteristic, (2) designing simulation grid and defining properties, (3) selecting an appropriate simulation model, and (4) constructing the model. History matching is then performed to fine tune the reservoir model in an attempt to match simulation performance with historical data. The history matched model can be used as a representation of a real reservoir. After obtaining the representative model, prediction of reservoir performance can be performed.

CHAPTER IV

RESERVOIR MODEL BUILDING

To optimize hydrocarbon production and Hg waste injection into a compartment using 3D reservoir simulation requires the assembly of a geocellular model to represent its geometry and petrophysical properties. This chapter discusses the detail of the disposal reservoir and workflow for reservoir model construction. The data required for model construction are structural depth map, well log data, and special core analysis data. The structural model was constructed using structural depth map with fault polygons. Gridding and layering were performed to choose an appropriate grid block size. The Sequential Gaussian Simulation technique was applied to determine petrophysical property distribution. Finally, basic reservoir properties were entered into the model to complete the reservoir model.

4.1 Review of Targeted Reservoirs

As mentioned in Chapter 1, mercury contaminated waste is a byproduct from gas production in one of the field in the Gulf of Thailand, renamed M in this study . The M field is located offshore and covers approximately 4600 km^2 in area. Natural gas and condensate accumulation is found in multi-faulted sandstone reservoirs made up of channels and bars in a fluvio-deltaic and coastal environment. Hydrocarbon reserves are found from the depth of 800 to 3,000 m TVD below the sea level. Currently, this field produces approximately 575 MMSCFD. After the working team had reviewed geological structure and production status, the compartment MN, shown in Fig. 4.1 was found to be the most suitable for Hg-contaminated waste disposal since it is confined and in the last stage of production.

There are 22 gas reservoirs located in the compartment MN and two wells penetrating through the compartment. The two wells are depicted in Fig. 4.1. The first well is well MN-1 which had been on production since June 1996 until October 2003. Well MN-1 is a monozone completion well. This well was drilled through 22 reservoirs, shown in Fig. 4.2. Reservoir 355 is the uppermost reservoir, located in the

top zone which is formation 2D. Reservoirs 405 to 710 are located in the middle zone which is formation 2C. Reservoirs 720 to 840 are located in the bottom zone which is formation 2B. These formations are categorized by sediment characteristics that can be defined from seismic data correlating with sonic log. No packers were set between different gas reservoirs. The tubing size is 3 ½ inches OD (2.991 inches ID). Well MN-1 is 3755 m MD or 1969 m TVD MSL. Initially, 18 gas reservoirs (480 to 840) were perforated, producing 10.9 MMSCFD of gas, 180 BPD of condensate, and 25 BPD of water. Two years later additional three reservoirs (355, 440, and 475) were perforated. After the second perforation, the productivity of gas and water increased. Due to high water rate, water shut-off by coiled tubing on reservoir 515 was performed one year later. Before abandonment in October 2003, the cumulative production was 6.67 BSCF of gas, 0.06 MMSTB of condensate, and 0.42 MMSTB of water.

In February, 2000, fine sand/$CaCO_3$ scale was detected in well MN-1. During an attempt to remove the scale, a bailer/wire line tool was stuck and left in the well at an estimated depth of 760 m MD. In order to avoid such obstruction in the injection process, the sidetrack well MN-2 was drilled to duplicate well MN-1 in December 2003. Well MN-2 will be used for an alternate hydrocarbon production and mercury contaminated slurry disposal.
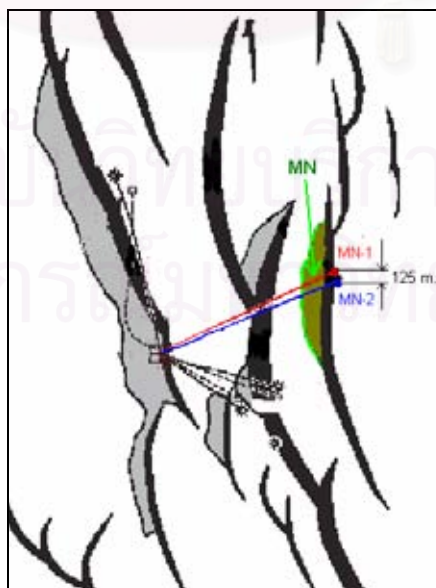
Figure 4.1: The MN compartment and well location map.

COMPARTMENT: MN

Formation	Reservoir	MN-1		
		Net Pay (m)	Perf.	Top (mTVDSS)
2D	355	1.2	2	1387.7
	380			
2C	405	11.6/ 4.0 /3.3 ✕		1430.5
	440	2.8	2	1465.1
	475	1.0	2	1502.7
	480	2.2	1	1506.9
	485			1515.6
	495	3.3	1	1523.1
	515	2.8	▥	1542.6
	525	0.6	1	1552.7
	535	2.3	1	1562.4
	545			
	560	1.4	1	1581.7
	570	5.8	1	1593.6
	585	1.3	1	1612.1
	600			1625.3
	605	0.8	1	1634.4
	620	1.8	1	1650.3
	625	0.6	1	1659.9
	660			1683.9
	675	4.5	1	1703.9
	700	2.0	1	1715.4
	710	0.9	1	1727.8
2B	720			1744.7
	740	8.3	1	1761.4
	760	4.6	1	1790.8
	830	4.7	1	1861.7
	840	1.4	1	1874.0

Not perforated ✕
March 1996   1
October 1998 2

2.0	Reservoir with only gas (2.0 m gas net pay)
11.0/ 1.0 /2.0	Reservoir with GOC and OWC (11.0 m net sand / 1.0 m oil net pay / 2.0 m gas net pay)
▥	Isolation#1 (i.e. CSG patch, Cement&Chemical Squeezing)

Figure 4.2: Reservoir chart for well MN-1.

4.2 Reservoir Model Construction

The reservoir model for the MN compartment was built using a 3D geological modeling software called PETREL. The model was constructed based on structural depth maps, well log data, and special core analysis data.

4.2.1 Input data for model construction

The data required for initial model construction are structural depth maps with fault polygons, well log data, and special core analysis data such as porosity, permeability, and capillary pressure.

a) Structural depth maps with fault polygons

Structural depth maps with fault polygons of the main horizons were initially loaded into PETREL to construct the main surfaces and faults of the geological model. Horizon is a rock layer characterized by a particular assemblage of fossils. The structural maps of horizon and fault polygons were built from seismic data. The horizons, used for the model construction, are H30, H33, H37, H40, and H44. Fig. 4.3 shows sample of seismic reflection data used to indicate horizons.
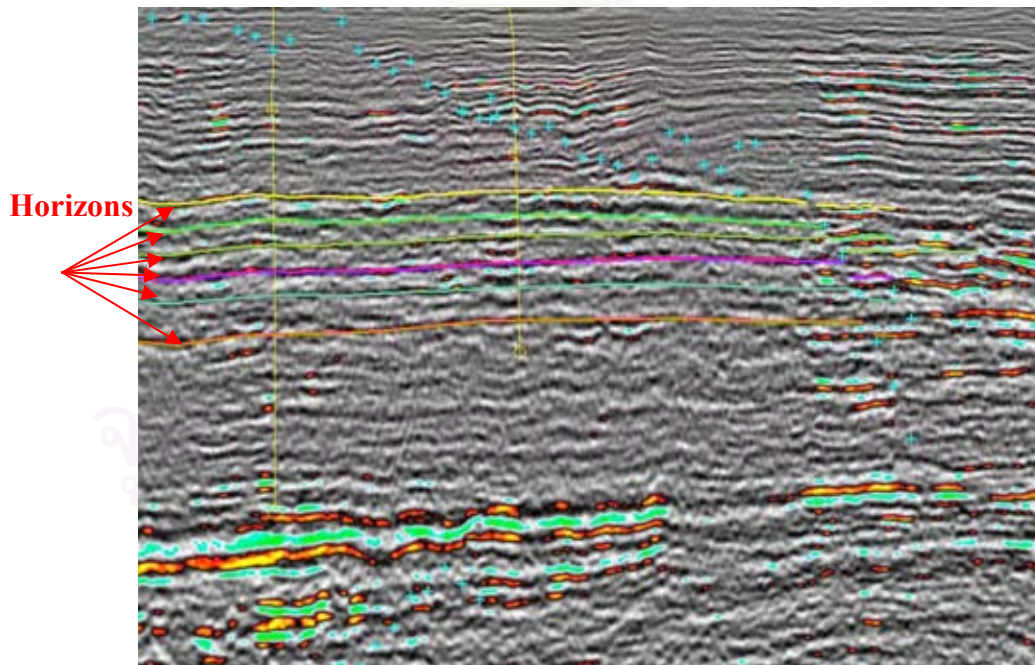
Figure 4.3: Seismic reflection and horizons.

b) Well log data

The required well log data are porosity, top and base reservoir depth, and lithology. For petrophysical modeling, the Sequential Gaussian Simulation technique was applied to estimate the property distribution from the sample points. A good representative model should be constructed from many sample points which cover the area being modeled. Since there are only 2 wells in the compartment MN, there are not enough data for model construction. In order to build the geological model, 20 nearby wells as shown in Fig. 4.4 were used. The model constructed covers the entire B5 area as shown in Fig. 4.5.
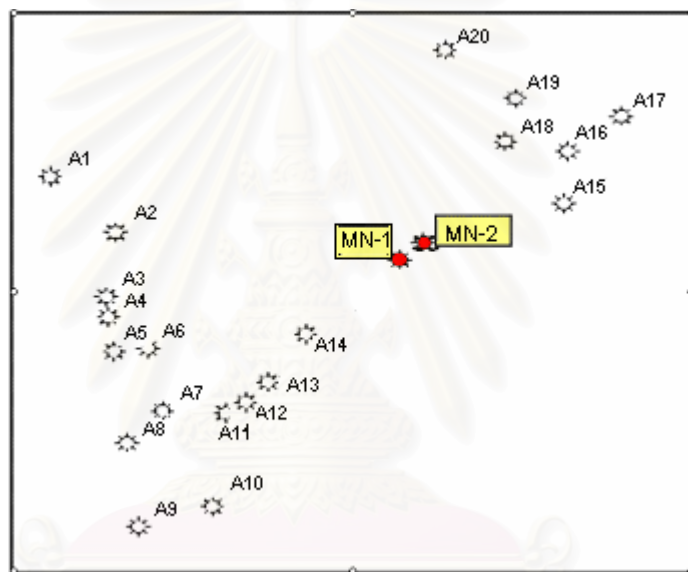
Figure 4.4: Wells in the same vicinity with well MN-1 and well MN-2.
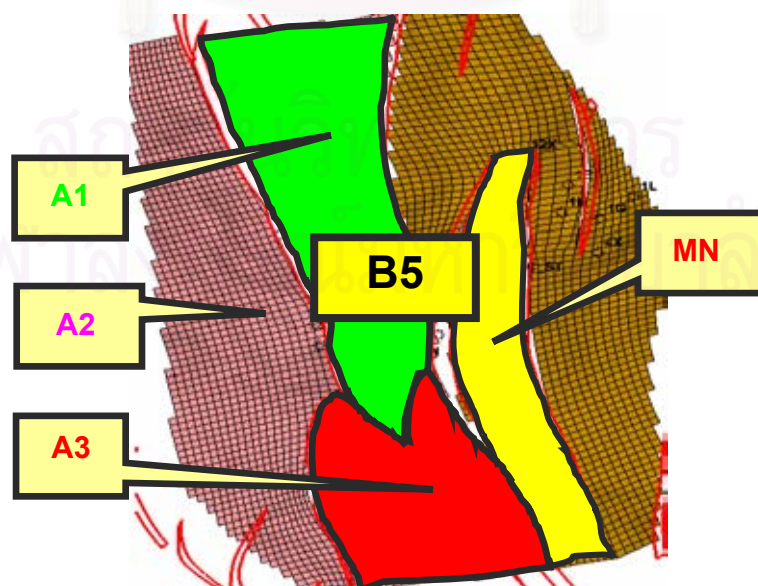
Figure 4.5: B5 modeling area**.**

c) Special core analysis data

Special core analysis has never been carried out for samples in the compartment MN (well MN-1 and MN-2). So, the data were borrowed from other available data for the M field. The data from special core analysis are porosity, permeability, relative permeability and capillary pressure. Permeability vs. porosity correlation was used for permeability modeling. The capillary pressure curve was used in the model to generate a transition zone between gas and water.

4.2.2 The reservoir model construction workflow

The following processes were performed to build a model for the compartment MN:

- Fault modeling
- Gridding
- Surface making
- Zone making
- Well log up-scaling
- Grid block layering
- Facies modeling
- Petrophysical modeling
- PETREL to ECLIPSE model transferring
- Reservoir model initialization

a) Fault modeling

The fault model was built by constructing the fault pillars following the fault polygon patterns in structural depth maps of main horizons. After that, the fault planes were created as shown in Fig. 4.6. In this study, eleven faults were constructed.
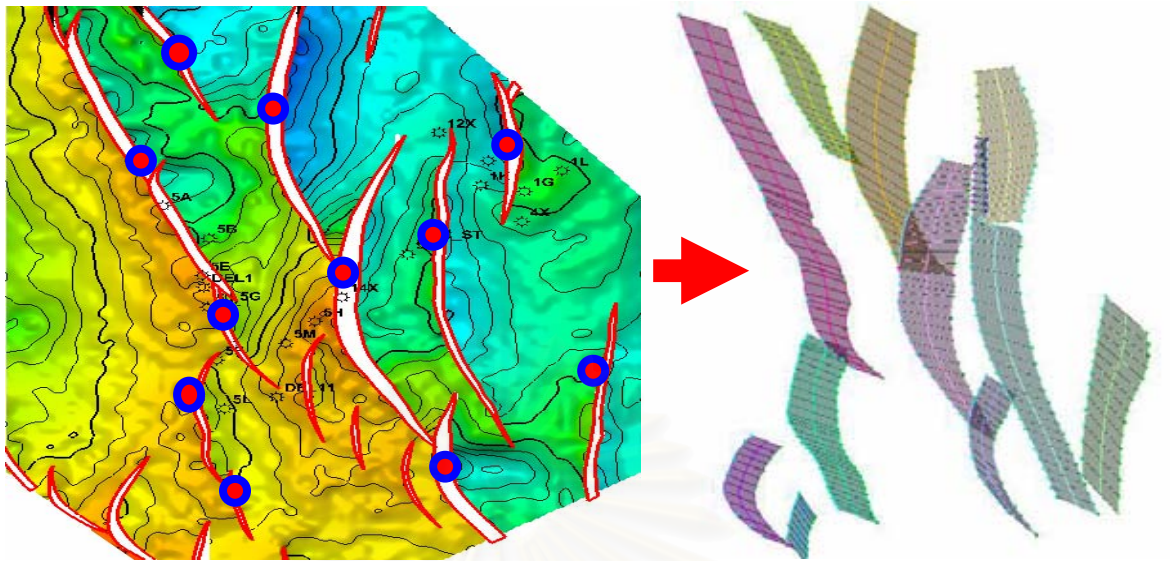
Figure 4.6: Fault modeling.

b) Gridding

In a normal grid block, ΔX and ΔY is 100 m. × 100 m. In an area near the wellbore (250 m. around the wellbore), the grid block is refined to 25 m. × 25 m.

c) Surface making

Twelve surfaces (M355, Top C, M455, M475, M515, M570, M600, M655, Top B, M825, M860, and Top A) were generated using the structural depth maps and surface depths from well log data. The structural depth maps were loaded into PETREL along with the reference surface depths from well log. Then, the surface model was constructed as shown in Fig. 4.7.
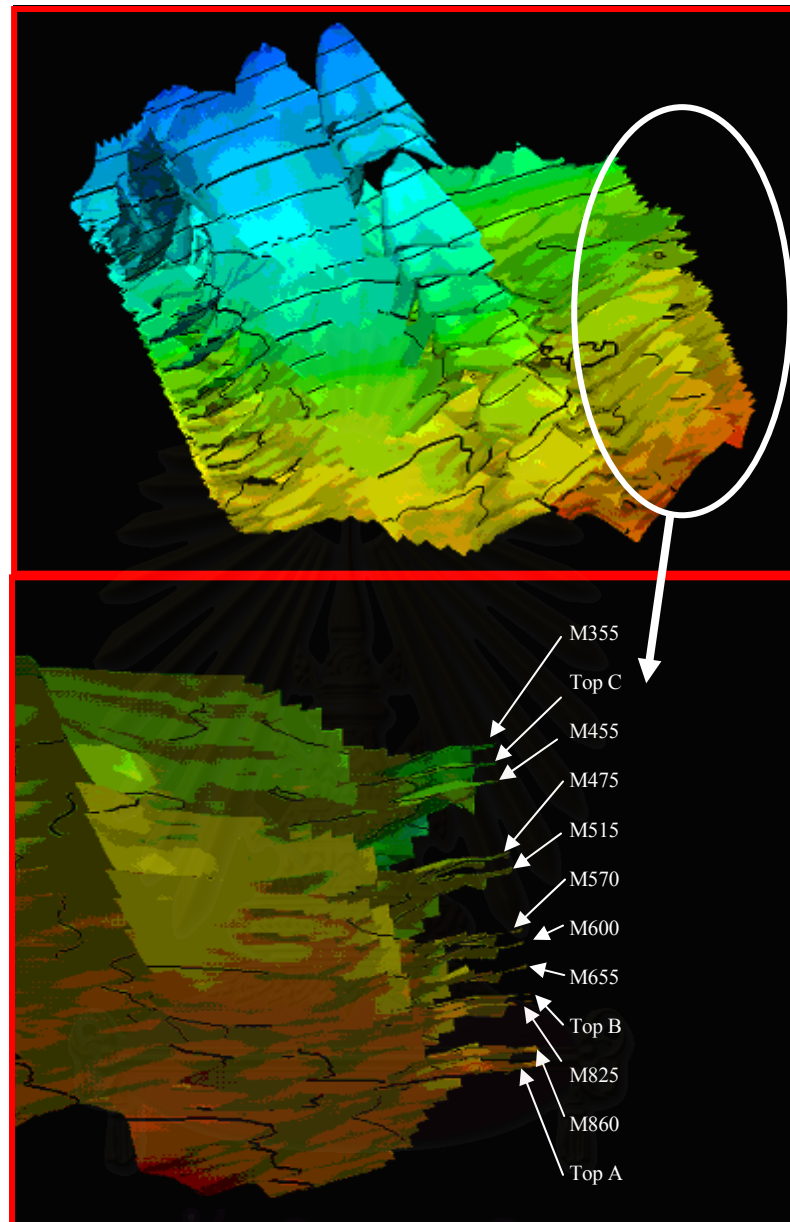
Figure 4.7: Surface making

c) Zone making

All top and base reservoir maps were constructed in PETREL using 12 surfaces and well log data of top and base depths for each reservoir. To construct a new surface map, one reference surface was selected from an available 12 surfaces. New surface was then constructed following the feature of the selected surface and fitted with the well log data of top and base depths for each reservoir. The process was performed until all top and base reservoir maps were generated. Then, zones were defined from each pair of nearby surfaces. Fig.4.8 shows the zones that were constructed in this study.
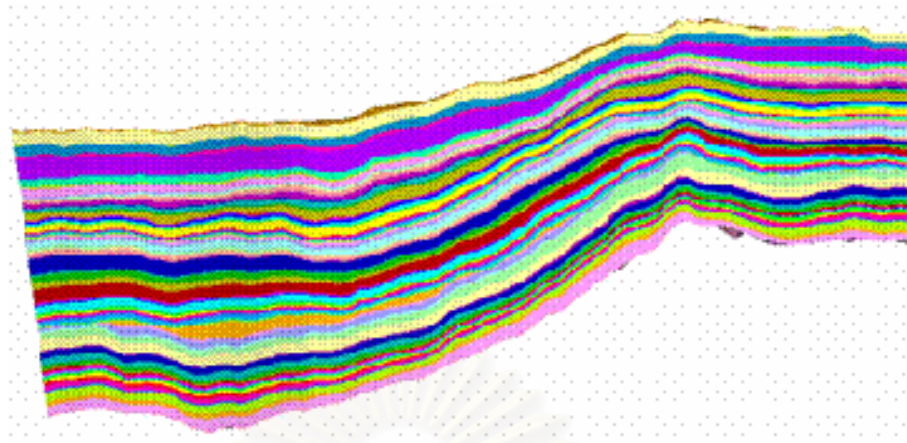
Figure 4.8: Zones making.

d) Well logs up-scaling

The thickness of geological grid blocks is normally larger than the well log sampling frequency which is 0.152 m/record. As a result, the well log data must be scaled up to the resolution of the 3D grid before performing any modeling. In this study, the arithmetic averaging method was used for the scale-up process.

e) Grid block layering

The compartment MN is multi-layer reservoirs with alternate sand and shale sequences. The thickness of shale layers ranges from 3 m. to 77 m. Shale layers are not what we are interested, so one grid block was used for each shale zone. Bar sands are less than three meters thick, so one grid block for each bar sand was designed. Channel sands are thicker than three meters. A grid block thickness of one meter was used in these zones.

The grid block was constructed at the same scale as the simulation scale. So, model upscaling was not required. There are a total of 991,600 geologic cells for the whole B5 model and 204,240 geologic or simulation cells [30 × 46 ×148] for the MN compartment.

f) Facies modeling

Three facie types (shale, channel sand, and bar sand) were defined from wire line log and net sand maps. Facies model is shown in Fig. 4.9. As seen in the figure, most of

the reservoirs in the compartment MN are bar sands. The identification of facies is used later for petrophysical property modeling.
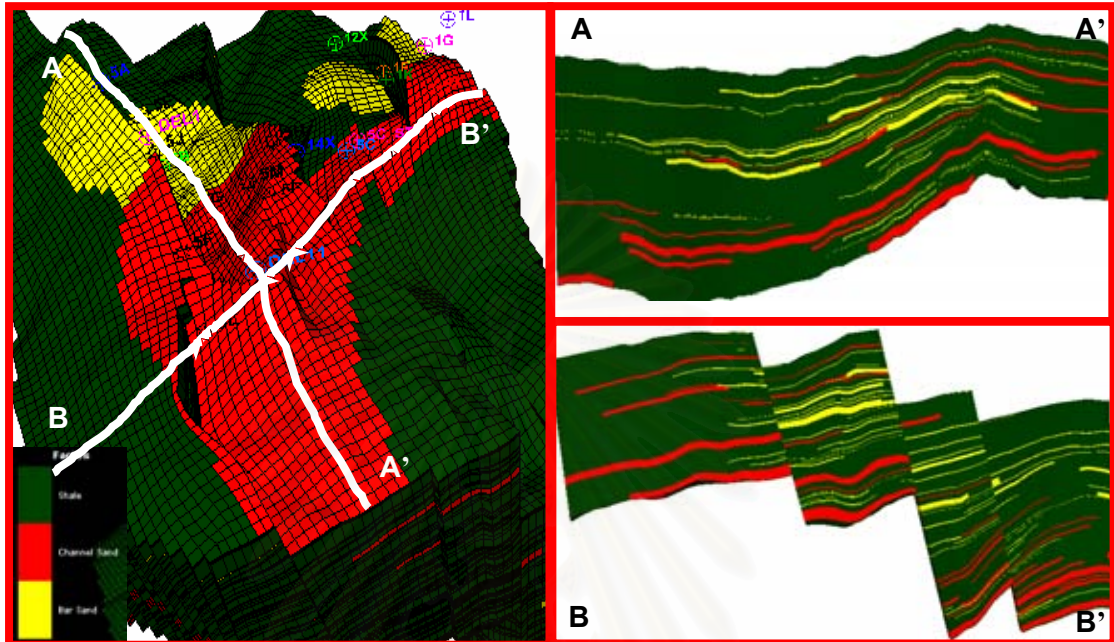
Figure 4.9: Facies model.

g) Petrophysical modeling

There are two petrophysical properties (porosity and permeability) generated in this process.

▪ **Porosity modeling**

The formation that is considered to be the reservoir should has clay content less than 40% and porosity greater than 10%. The values of porosity were determined by interpreting the well log data and verified with the data from special core analysis. Fig. 4.10 shows the comparison between log and core porosities of well A5. There is a good agreement between log porosity and core porosity. Then, the porosity data were distributed into the whole model by applying the Sequential Gaussian Simulation (SGS) technique. The porosity model obtained from the process is shown in Fig. 4.11.
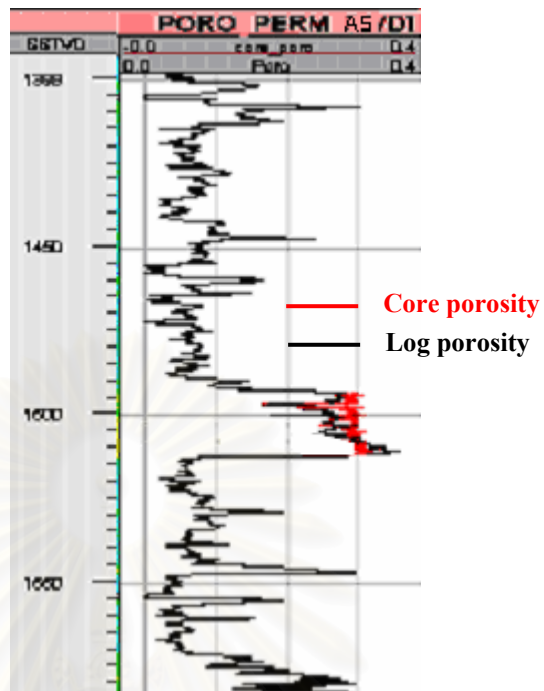
Figure 4.10: Well A5 log porosity and core porosity comparison.
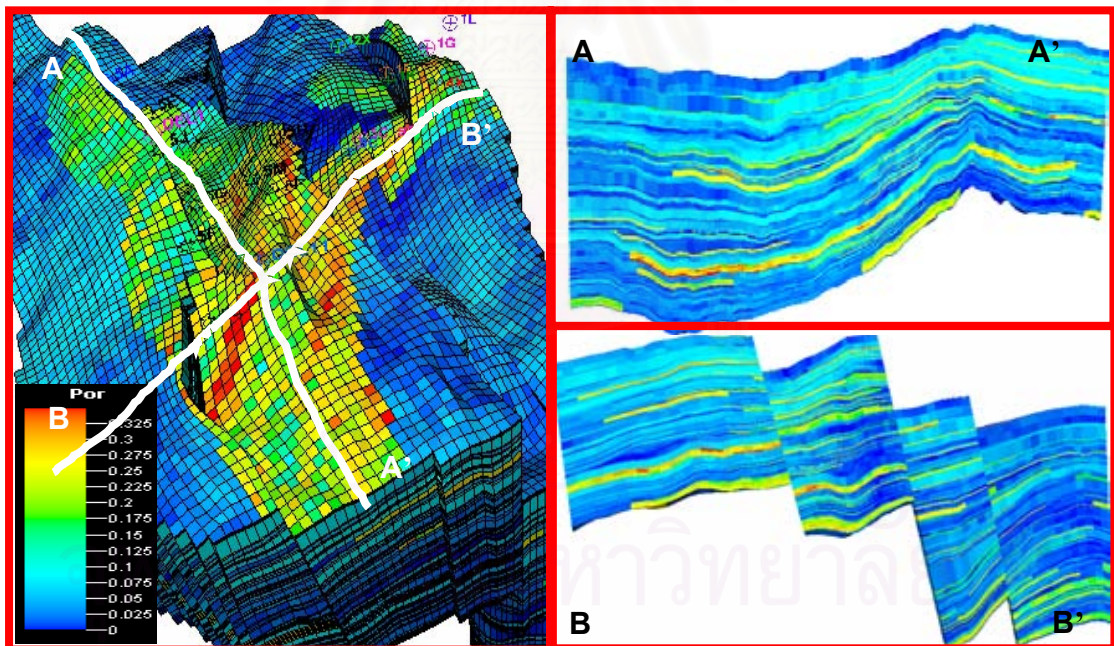
Figure 4.11: Porosity model.

- **Permeability modeling**

Both horizontal and vertical permeability were generated in the model. First, horizontal permeability was generated; then, ten percent of the horizontal permeability was used as the vertical permeability. The horizontal permeability model

was generated using horizontal permeability-porosity correlation. The correlation was derived from special core analysis of wells in formation 2B and 2C of the M field.

From a scatter plot between horizontal permeability-porosity as shown in Fig. 4.12, a correlation can be determined for each facies: 2B channel sand, 2C channel sand, and bar sand. With the same porosity, the channel sand in unit 2B has the highest permeability value. The channel sand in unit 2C and the bar sand have close values of permeability. The horizontal permeability, converted from porosity log, is verified with data from special core analysis and DST obtained from well MN-DEL1 and well MN-DEL2 as shown in Fig. 4.13. For well MN-DEL1 (the left chart in Fig. 4.13), there is good agreement for all sources of data. For well MN-DEL2 (the right chart in Fig. 4.13), the log permeability is a little bit less than the permeabilities obtained from special core analysis and DST data. The cause of error is uncertainty of the data. The effect of uncertainty was already accounted in the variance of permeability data. It was incorporated when performing geostatistical permeability propagation. Fig. 4.13 shows the horizontal permeability model, established by applying SGS technique.
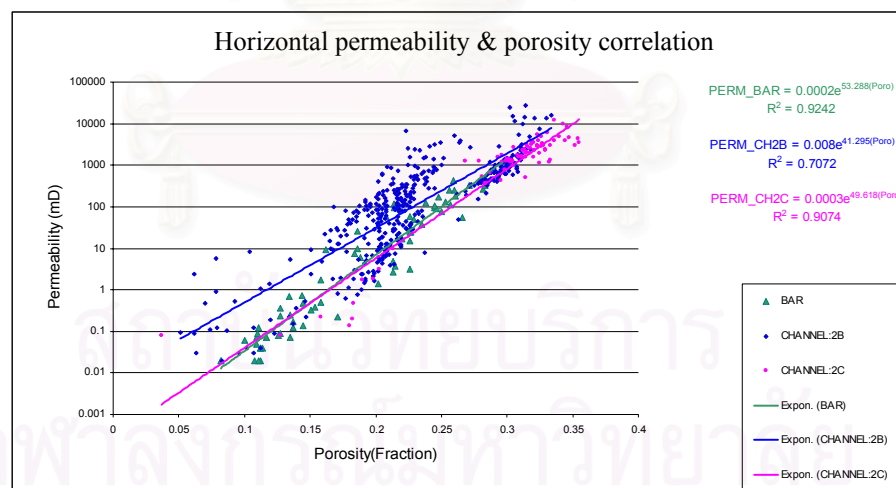
Figure 4.12: Horizontal permeability and porosity correlation plot.
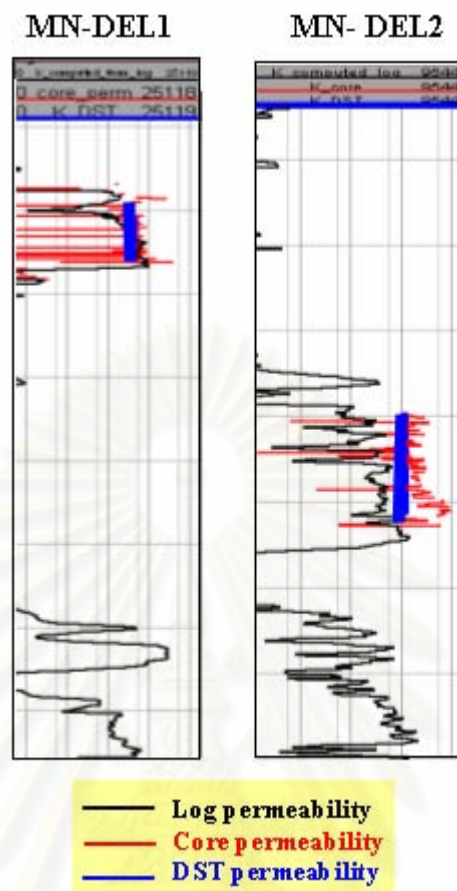
Figure 4.13: Comparison of correlation permeability, core permeability, and DST permeability.
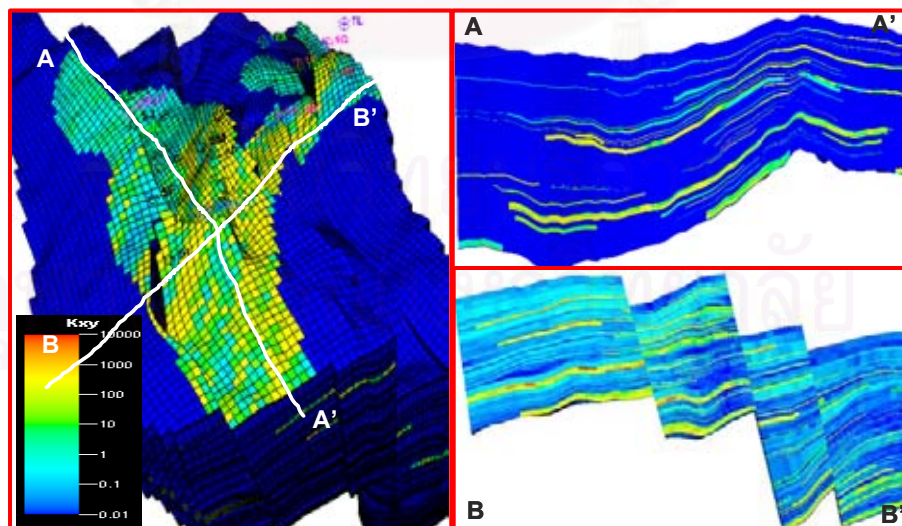
Figure 4.14: Horizontal permeability model.

h) PETREL to ECLIPSE model transferring

The model for the area of interest, the compartment MN, was transferred from PETREL to ECLIPSE in order to run reservoir simulation. The exported model comprises the grid file with coordinate and corner point geometry for ECLIPSE and basic grid properties which are porosity and permeability.

After exporting the model from PETREL to ECLIPSE, the model was evaluated by comparing pore volume from both softwares. There is good agreement between the two values as reported in Table 4.1. All basic data such as well data, initial water saturation, and other fluid properties were entered to complete the model.

Table 4.1: Pore volume comparison (PETREL vs. ECLIPSE).

Formation	Pore Volume(10^6 m^3)	
	Petrel	Eclipse
2D	0.40	0.40
2C	37.42	36.94
2B	7.58	7.34
Total MN	45.40	44.68

i) Reservoir model initialization

Model initialization is the process to prepare an initial pressure and fluid saturation for each grid block. In this process, the fluid pressure (p_g, p_o, p_w) at initial conditions is prepared using the defined fluid density, vaporized oil concentration, and a formation pressure at each depth. After that, the capillary pressure can be obtained as follows:

$$p_{cow} = p_o - p_w$$
$$p_{cog} = p_g - p_o$$

where p_{cow} = water-oil capillary pressure

p_{cog} = gas-oil capillary pressure

Then, water saturation is determined by inverse look-up of the defined water capillary pressure table.

Incorporation of remaining basic reservoir characteristics such as initial reservoir pressure and temperature, reservoir fluid properties, rock property, aquifers, and well completion data is also included in this section.

♦ **Initial water saturation**

To define initial water saturation, GWC, capillary pressure data, and relative permeability curves for each reservoir were entered into the model.

▪ **Input data**

o **Gas-water contact**

From wire line log data, only GWC of reservoir 475 was observed. For the remaining reservoirs, only the lowest proved gas (LPG) is defined. GWC and LPG for each reservoir are shown in Table 4.2. In case that gas–water contact (GWC) has not been found from well log data, the LPG is the lowest gas depth that can be seen. First, LPG was used as the equivalent GWC but it was allowed to be increased in order to calibrate S_w (model) as mentioned earlier.

Table 4.2: Original gas-water contact depth.

Reservoir Name	GWC (m)
355	1389
405	1438
440	1468
475	1514
480	1520
495	1541
515	1550
525	1558
535	1570
560	1609
570	1604
585	1613
605	1660
620	1652
625	1661
685	1709
700	1724
710	1729
740	1773
760	1795
830	1904
840	1875

o **Capillary pressure vs. water saturation**

The special core analysis was not conducted for core from the compartment MN. The capillary pressure data were borrowed from available special core analysis data conducted for wells in formations 2B and 2C of the M field. Fig. 4.15 shows the initial p_c model (p_c1) used in this study. The initial p_c model was constructed from averaging the available data.
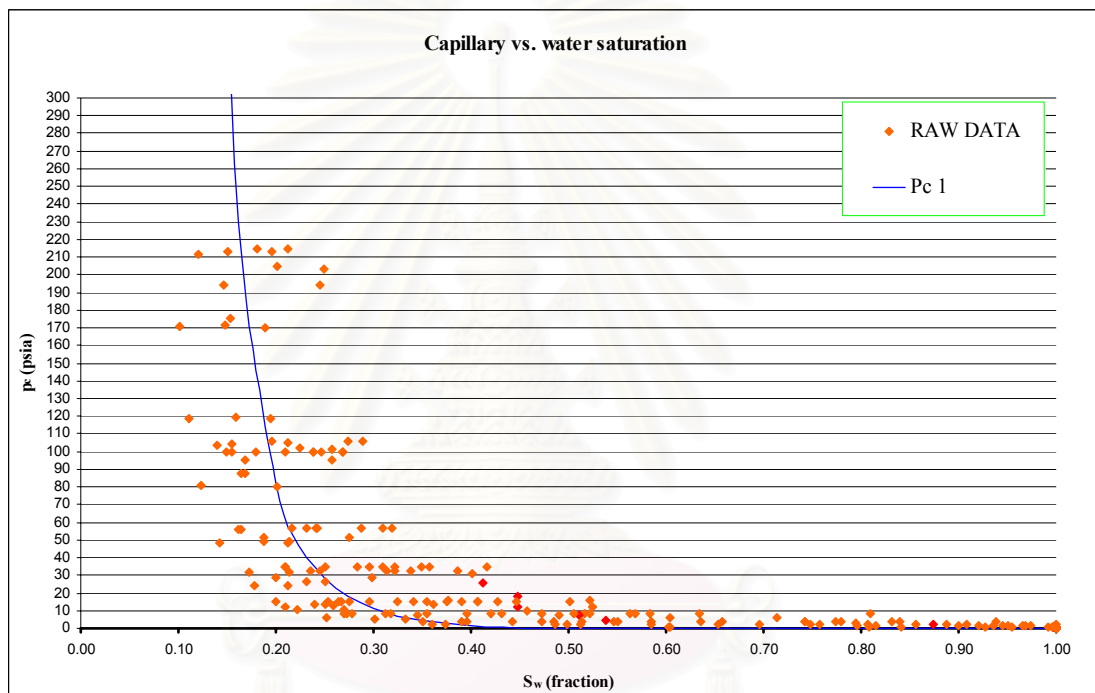
Figure 4.15: Capillary pressure model.

o **Relative permeability curves**

The plot of gas relative permeability vs. gas saturation of special core analysis data of the M field is shown in Fig. 4.16, and the plot of water relative permeability vs. water saturation is shown in Fig. 4.17. The initial gas relative permeabilities model (Krg1) and water relative permeabilities model (Krw1) were constructed from averaging the available data. Then, the end points of fluid saturations were defined.

There are no data of oil relative permeability in the M field, so the initial oil relative permeability curves were constructed using

Corey function. The residual oil saturation input into the function is 0.3 and Corey oil exponent is three. The oil relative permeability curves are shown in Fig. 4.18.
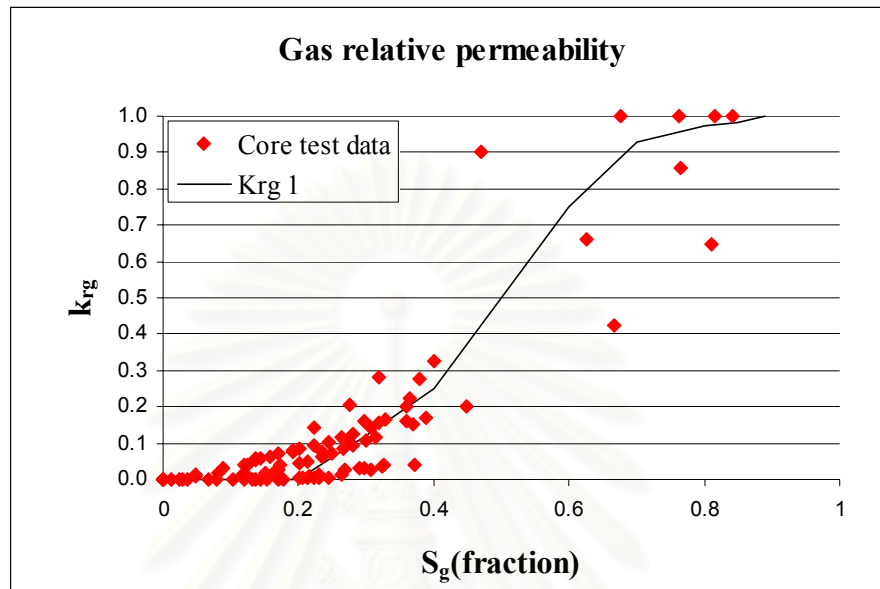
Figure 4.16: Gas relative permeability.
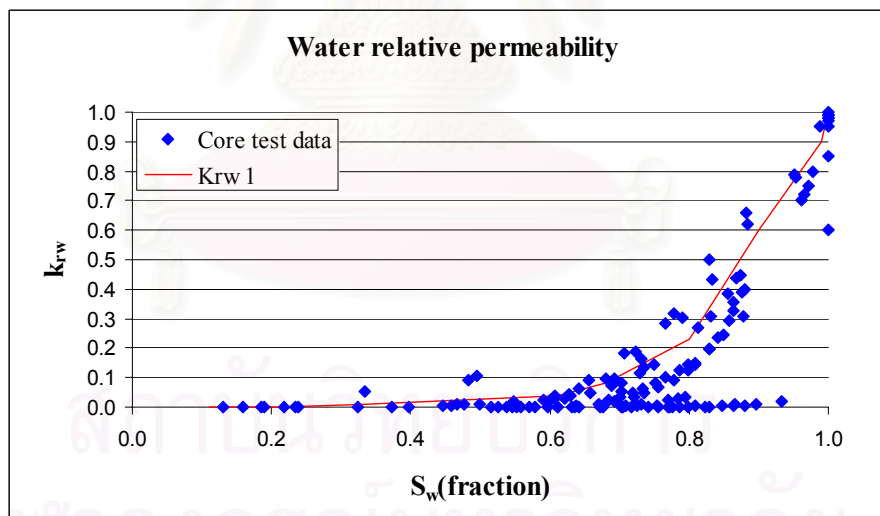
Figure 4.17: Water relative permeability.
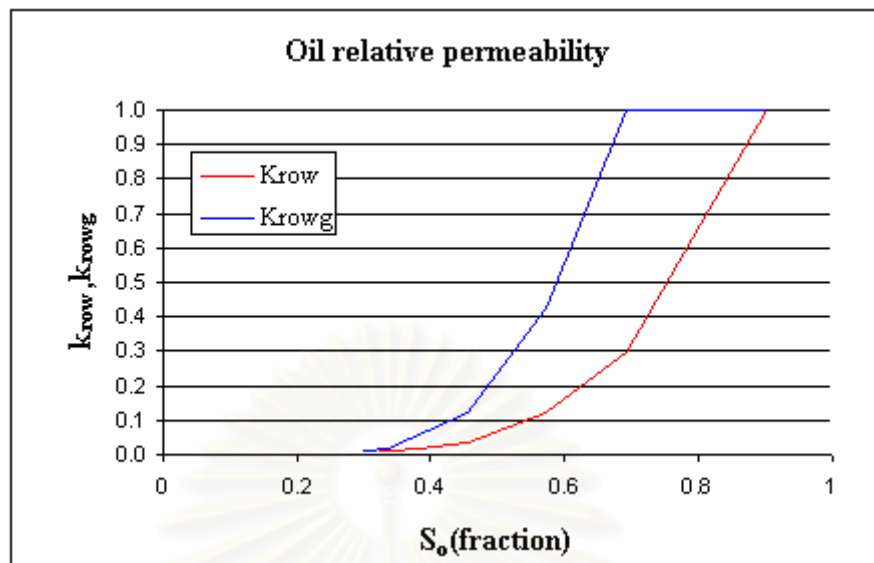
Figure 4.18: Oil relative permeability.

From Fig. 4.16 and Fig. 4.17, the end point saturations are estimated as follows:

Minimum water saturation	=	0.11
Maximum water saturation	=	1.00
Minimum gas saturation	=	0.00
Maximum gas saturation	=	0.89
Critical gas saturation	=	0.30
Critical water saturation	=	0.313

▪ **Initial water saturation adjustment concept**

Initially, GWC or the equivalent GWC (in case that the exact GWC is not available) and the capillary pressure model p_c1 were used for all reservoirs. The adjustment of GWC and capillary pressure model was performed in case that S_w (model) at the well block differs from the value of S_w obtained from well log. The adjustment can be divided into 2 cases.

Case 1 : S_w (model) at well block is lower than S_w obtained from well log. In this case, the capillary curve was shifted to the upper right side of the original capillary pressure model. The shifting was performed until S_w (model) at well block is well matched with S_w obtained from well log. The

new capillary models that provide a good match on S_w were organized into two models which are p_c4 and p_c5 as shown in Fig. 4.19.

Case 2 : S_w (model) at well block is higher than S_w obtained from well log. In this case, we moved the capillary curve to the lower left side of the original capillary pressure model. The shifting was performed until S_w (model) at well block is well matched with S_w obtained from well log or the capillary model reaches the capillary pressure model p_c3. The capillary pressure model p_c3, as shown in Fig. 4.19, is the lowest capillary pressure curve that can be fitted to the data points. If necessary, equivalent GWC was adjusted until S_w model is successfully calibrated within 10% error. The new capillary models that provide a good match on S_w were organized into two models which are p_c2 and p_c3 as shown in Fig. 4.19.

The appropriate GWC and capillary pressure model can be summarized in Table 4.3.
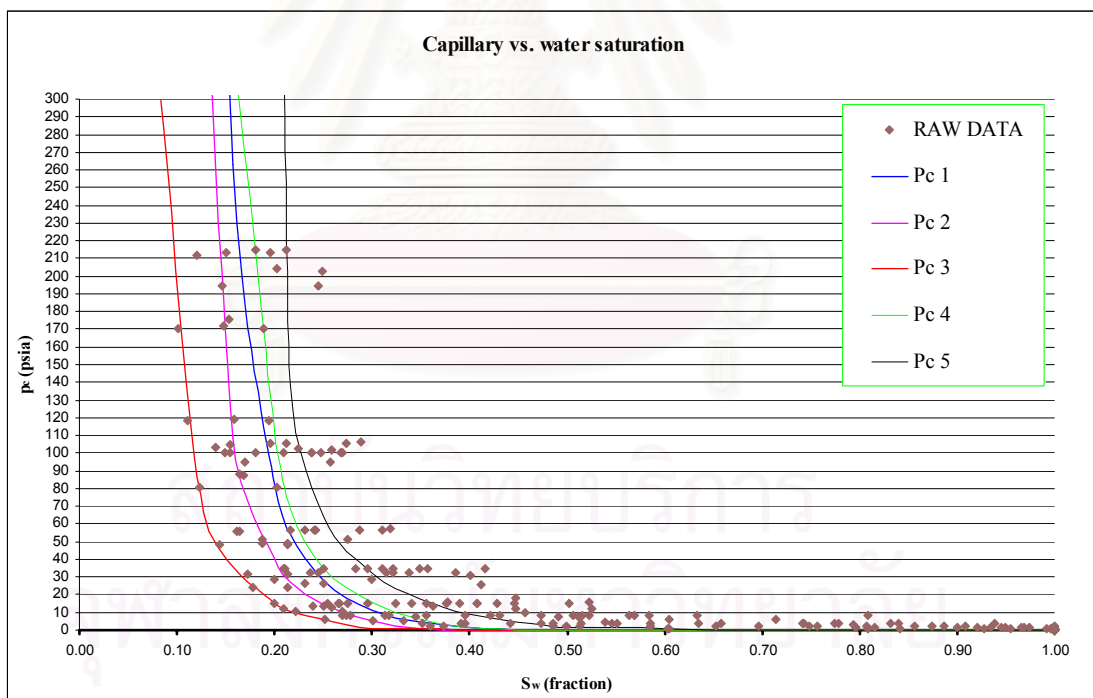
Figure 4.19: Capillary pressure model adjustment.

Table 4.3: GWC and p_c model for each reservoir.

Reservoir Name	GWC (m)	p_c Model
355	1390	3
405	1440	3
440	1468	3
475	1514	2
480	1520	2
495	1541	2
515	1550	3
525	1564	3
535	1578	3
560	1609	1
570	1609	3
585	1627	3
605	1660	1
620	1653	3
625	1661	3
685	1713	3
700	1724	4
710	1730	3
740	1773	3
760	1800	3
830	1904	1
840	1875	5

After GWC and capillary pressure model were adjusted, S_w(model) at the well block and S_w obtained from well log indicates a good agreement as shown in Fig. 4.20. Initial water saturation model is shown in Fig. 4.21.
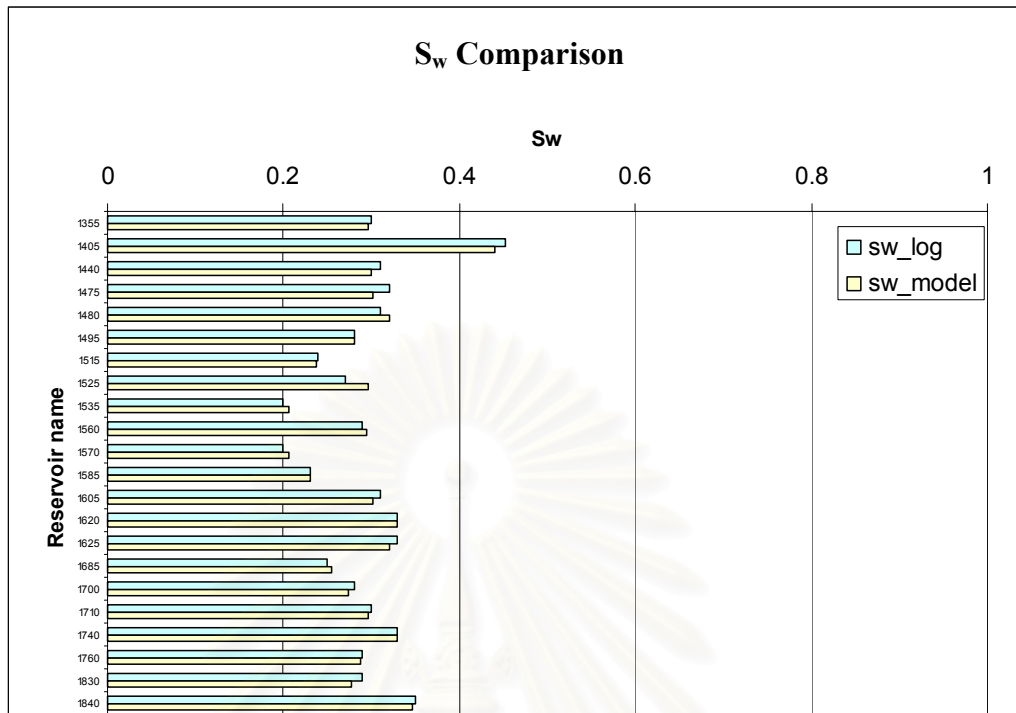
Figure 4.20: S_w model at well block vs. S_w obtained from well log.
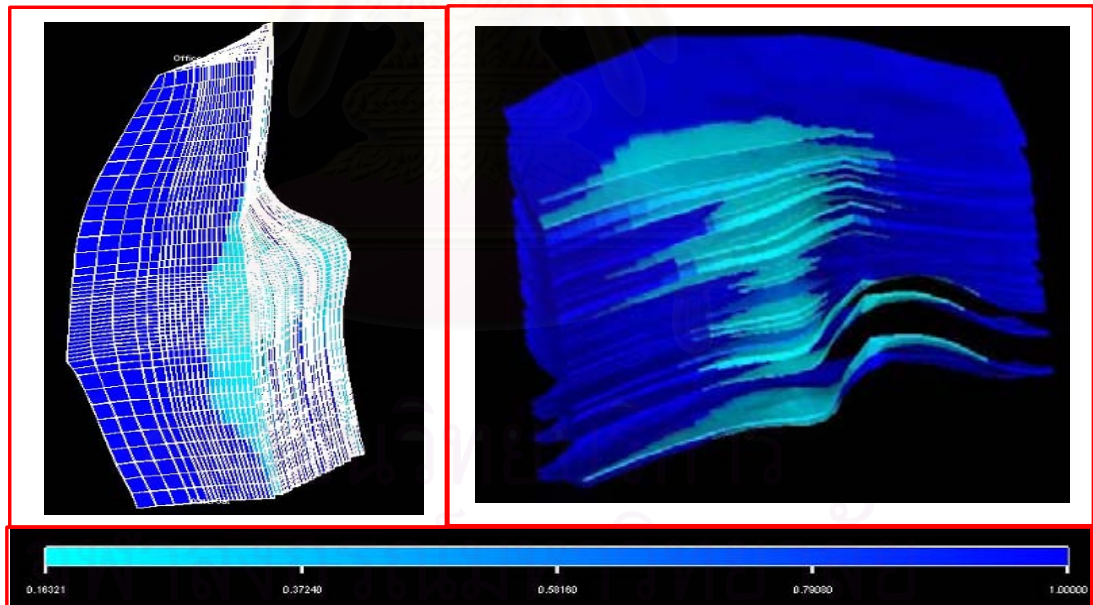
Figure 4.21: Initial water saturation model.

♦ **Initial reservoir pressure**

The initial reservoir pressure data are taken from wells A2, A3, A6, A8, A12, and A13 which are located near well MN-1 as shown in Fig. 4.4. The pressure gradient of

these wells is shown in Fig. 4.22. From the graph, the relationship of pressure as a function of depth can be fitted by the equation:

$$Pressure(psia) = 1.378*TVDSS(M) + 14.7 \qquad (4.1)$$

where TVDSS(M) = true vertical depth at the middle of reservoir (m.)
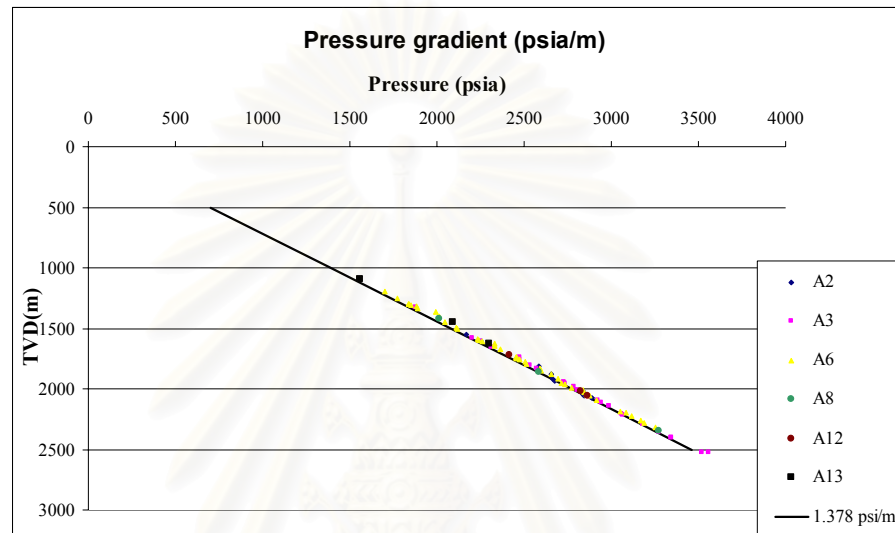
Figure 4.22: Reservoir pressure gradient.

♦ **Initial reservoir temperature**

The temperature record of well MN-1 during logging while drilling (LWD) is 128 ^{o}C at 1958 m TVD-MSL. So, the reservoir temperature as a function of depth can be described by the equation.

$$Temperature (^oC) = 0.05*TVDSS(M) + 30 \qquad (4.2)$$

♦ **PVT**

The compartment MN is a wet gas reservoir. As mentioned in Chapter 1 that this study involves mercury contaminated slurry injection, PVT properties of four fluids (gas, oil, water, and slurry) are needed to be entered into the reservoir simulation model.

▪ **Production fluids**

As mentioned before, PVT analysis was not performed for the compartment MN. The MN-1 production test data were averaged and used in various

correlations to determine production fluid properties. The following production test data were used:

1. Gas gravity at surface conditions*   = 0.967
2. Condensate density at surface conditions* = 50.6 ^{o}API
3. Condensate-gas ratio at surface conditions* = 5.8 STB/MMSCF
4. Water-gas ratio at surface conditions* = 68 STB/MMSCF
5. Water salinity   = 2309 ppm

* The surface conditions are 60 ^{o}F and 14.7 psig.

The following correlations were used to obtain PVT properties:

1. Gas formation volume factor : Katz correlation.
2. *Gas viscosity : Lee et. al.*
3. Water formation volume factor : Meehan
4. Water viscosity : Meehan
5. Oil formation volume factor : GasO
6. Oil viscosity : Beal *et. al.*
7. Condensate-gas ratio : Petroleum Experts

Gas properties

Gas density at surface conditions (60 ^{o}F and 14.7 psia) is 0.0604 lb/ft^3. The gas properties calculated from Katz, Lee *et. al.*, and Petroleum Expert correlations are given in Table 4.4 and Fig. 4.23

Table 4.4: Wet gas PVT properties.

p_g (psia)	CGR (stb /Mscf)	FVF (rcf /scf)	Visc (cp)
16	0.300	0.962	0.010
359	0.070	0.042	0.011
704	0.020	0.021	0.012
1048	0.015	0.014	0.014
1393	0.012	0.010	0.015
1737	0.011	0.009	0.017
2082	0.010	0.008	0.018
2426	0.009	0.007	0.020
2771	0.008	0.007	0.021
3115	0.007	0.006	0.023
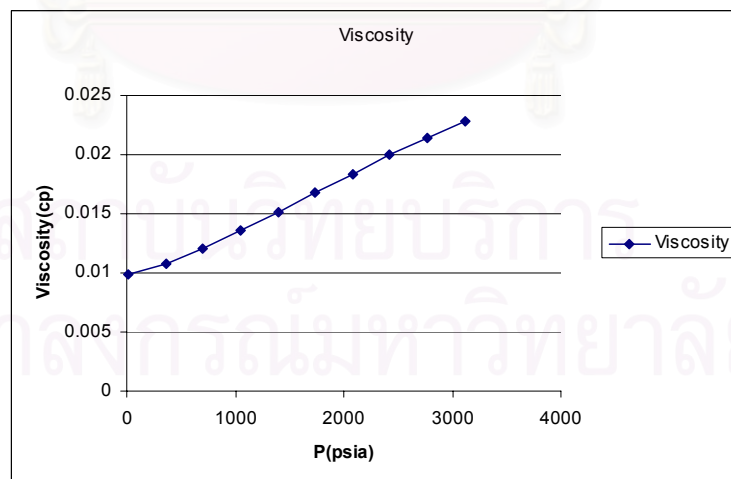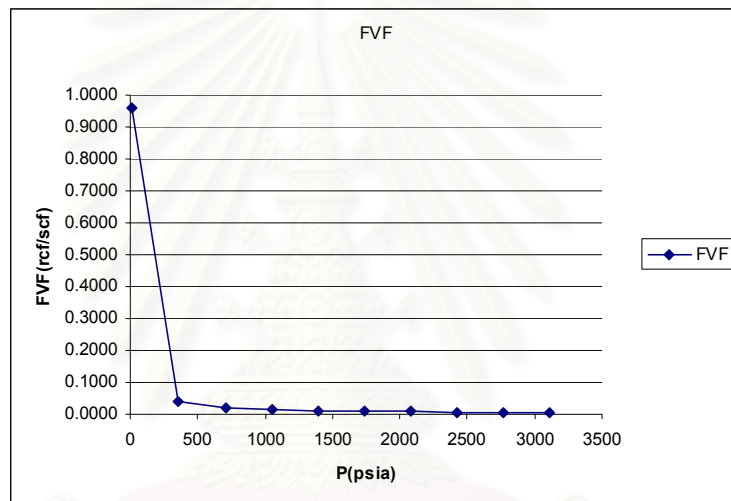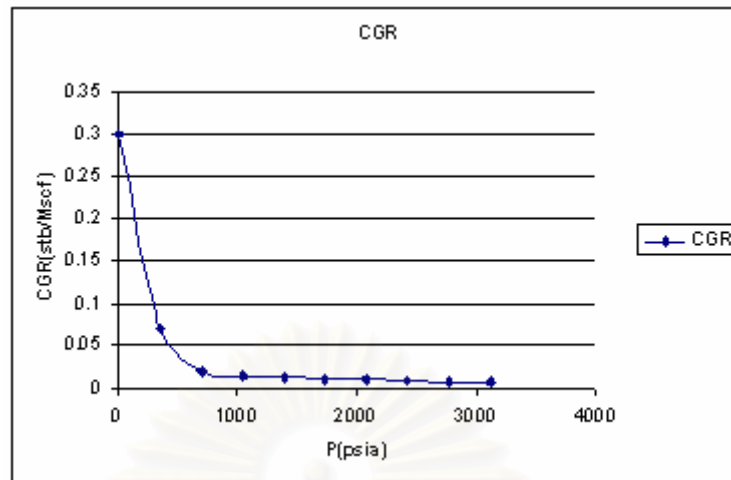
Figure 4.23: Wet gas PVT properties.

Water properties

Water density at surface conditions (60 ^{o}F and 14.7 psia) is 62.43 lb/ft^3. The water properties at a reference pressure of 2,292 psia calculated from Meehan correlations are given as follows:

Water FVF	1.0346	rb/STB
Water compressibility	3.365 x 10^{-6}	psi^{-1}
Water viscosity at the reference pressure	0.2505	cp

Oil properties

Oil density at surface conditions (60 ^{o}F and 14.7 psia) is 48.46 lb/ft^3 . The oil properties at a reference pressure of 449.7 psia calculated from GasO and Beal *et. al*. correlations are given as follows:

Oil FVF	1.1414	rb/STB
Oil compressibility	2 x 10^{-5}	psi^{-1}
Oil viscosity at the reference pressure	0.2998	cp

- **Injection fluid (slurry)**

Although ECLIPSE 100 can handle only three phases of fluid which are gas, water, and oil, it can handle injection fluid which has different properties from the production fluid by considering it as brine water. Then, salt concentration and density of brine water can be specified in the simulator. In this study, the simulation was performed for six slurry properties which are combinations of three sludge concentrations (20, 30, and 40% by volume) and two viscosities (40 cp and 70 cp). The approximate mercury contaminated sludge density is 168.84 lb/ft^3. The density of injected slurry for varied sludge concentration can be computed as follows:

Sludge concentration of 20% by volume:

Slurry density $\quad = (0.2 \times 168.84$ lb/ft$^3) + (0.8 \times 62.4$ lb/ft$^3)$

$\qquad\qquad\qquad = 83.7$ lb/ft^3

6,000 ton of sludge $\quad = (6000$ ton $\times 2204.62$ lb/ton / 168.84 lb/ft^3) / 0.2

$\qquad\qquad\qquad = 391,723$ ft$^3 = 69,764$ bbl

Sludge concentration of 30% by volume:

Slurry density $= (0.3 \times 168.84 \text{ lb/ft}^3) + (0.7 \times 62.4 \text{ lb/ft}^3)$
                   $= 94.3 \text{ lb/ft}^3$

6,000 ton of sludge $= (6000 \text{ ton} \times 2204.62 \text{ lb/ton} / 168.84 \text{ lb/ft}^3) / 0.3$
                     $= 261,150 \text{ ft}^3 = 46,510 \text{ bbl}$

Sludge concentration of 40% by volume:

Slurry density $= (0.4 \times 168.84 \text{ lb/ft}^3) + (0.6 \times 62.4 \text{ lb/ft}^3)$
                   $= 104.9 \text{ lb/ft}^3$

6,000 ton of sludge $= (6000 \text{ ton} \times 2204.62 \text{ lb/ton} / 168.84 \text{ lb/ft}^3) / 0.4$
                     $= 195,861 \text{ ft}^3 = 34,880 \text{ bbl}$

The six slurry properties are summarized in Table 4.5.

Table 4.5 : Slurry properties.

Slurry	Density (lb/ft^3)	Viscosity (cp)
1	83.7	40
2	83.7	70
3	94.3	40
4	94.3	70
5	104.9	40
6	104.9	70

♦ **Rock properties**

Rock compressibility was defined using Newman correlation. Rock compressibility at the average reservoir pressure (2,292 psia) is 1.1767×10^{-6} psi^{-1}.

♦ **Aquifer**

Each reservoir has its own aquifer component. Aquifer is categorized into two types which are channel aquifer and bar aquifer. The type of aquifer below each reservoir can be defined from the sand map. In this study, numerical aquifers were used in the model as follows:

▪ Edge water drive from west to east.

- The initial aquifer sizes were averaged from sand map and categorized to two groups as channel aquifer and bar aquifer. The aquifers have a size of 3×10^9 ft^3 for channel aquifer and 2×10^9 ft^3 for bar aquifer. There are just initial values. They are needed to be adjusted later in the history matching process.
- The aquifers have the same initial pressure as the initial reservoir pressure.
- The aquifers have the same porosity and permeability as the average reservoir properties.
- The type of aquifer below each reservoir is shown in Table 4.6.

Table 4.6: Aquifer types

Reservoir Name	Aquifer Formation
405	Channel
475	Bar
480	Bar
495	Bar
515	Bar
525	Bar
535	Bar
560	Bar
570	Bar
685	Bar
740	Channel
760	Channel
830	Channel

♦ **Well completions**

The trajectories of wells MN-1 and MN-2 were mapped onto the simulation model by transferring to WELSPECS and COMPDAT keywords in ECLIPSE to locate the well and the block intersection. Fig. 4.24 and Fig. 4.25 show the well trajectory of wells MN-1 and MN-2, respectively.
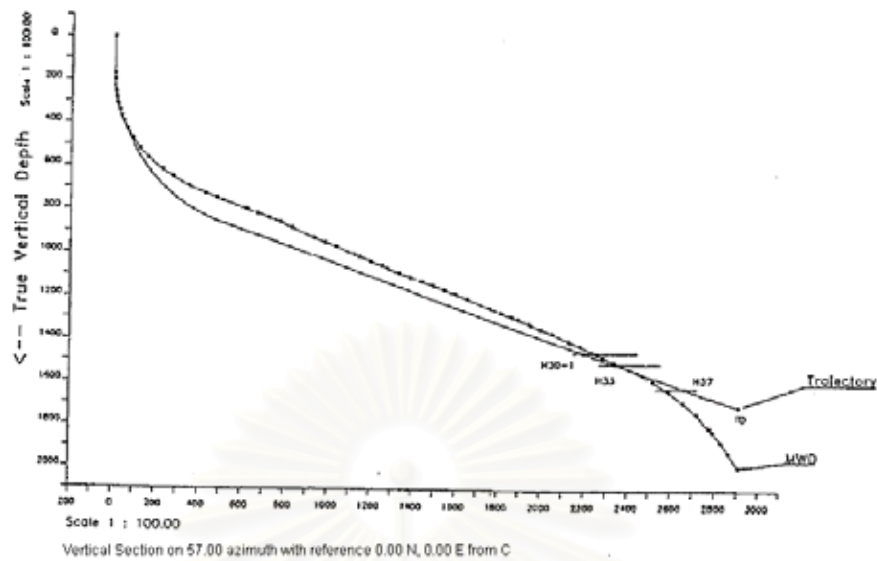
Figure 4.24: MN-1 well trajectory.
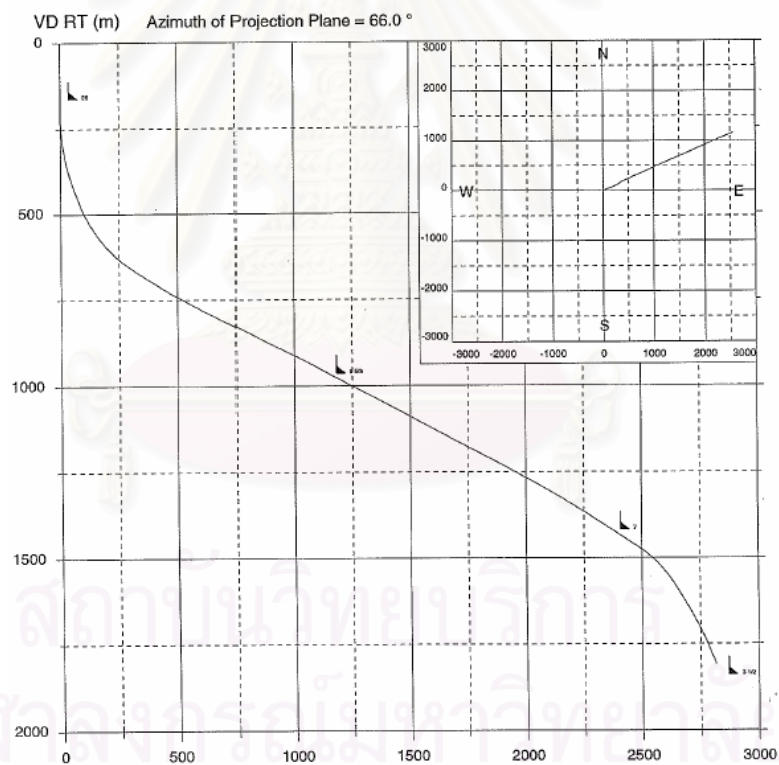
Figure 4.25: MN-2 well trajectory.

4.3 Original Gas In Place (OGIP)

The value of OGIP was determined from ECLIPSE using volumetric calculation. After inputting all necessary properties and performing model initialization, the

OGIP of the compartment was determined to be 13.13 BSCF. The OGIP of each reservoir is shown in Table 4.7.

Table 4.7: OGIP of compartment MN from model.

Reservoir name	OGIP (BSCF)
355	0.33
405	2.44
440	0.50
475	0.66
480	1.35
495	0.80
515	0.17
525	0.72
535	0.35
560	0.18
570	0.80
585	1.40
605	0.13
620	0.05
625	0.02
685	0.27
700	0.18
710	0.05
740	0.74
760	0.21
830	1.70
840	0.08
Compartment	**13.13**

In summary, to optimize hydrocarbon production and Hg waste injection, a reservoir simulation model for the MN compartment which is multi-layered gas reservoirs, was built using a 3D geological modeling software (PETREL). The workflow for reservoir model construction consists of fault modeling, gridding, surface making, zone making, well log up-scaling, grid block layering, facies modeling, petrophysical modeling, PETREL to ECLIPSE model transferring, and reservoir model initialization. The data required for model construction are structural depth map, well log data, and special core analysis data. To complete the model for simulation, initial reservoir pressure and temperature, reservoir fluid properties, rock properties, aquifers, and well trajectories must be entered into the reservoir simulation

model. Reservoir model initialization is then performed to determine the initial pressure and fluid saturation for each grid block.

CHAPTER V

HISTORY MATCHING

History matching is a process to fine tune the reservoir model by matching simulation production data with historical data. The data selected to be matched are production rates, cumulative productions, and reservoir pressure. In order to achieve a good match, adjustments need to be made to relative permeability, absolute permeability, aquifer size, and OGIP. The history matched model can be used as a representative reservoir.

5.1 Simulation Results

Production data of well MN-1 from the start of production in June 1996 until abandonment in October 2003 were used in the history matching process. The data selected to be matched is production rates, cumulative productions, and average reservoir pressure as shown in Fig. 5.1 to Fig. 5.7. Open and shut-in periods were included into the schedule, and the production condition was controlled by the tubing head pressure (THP).
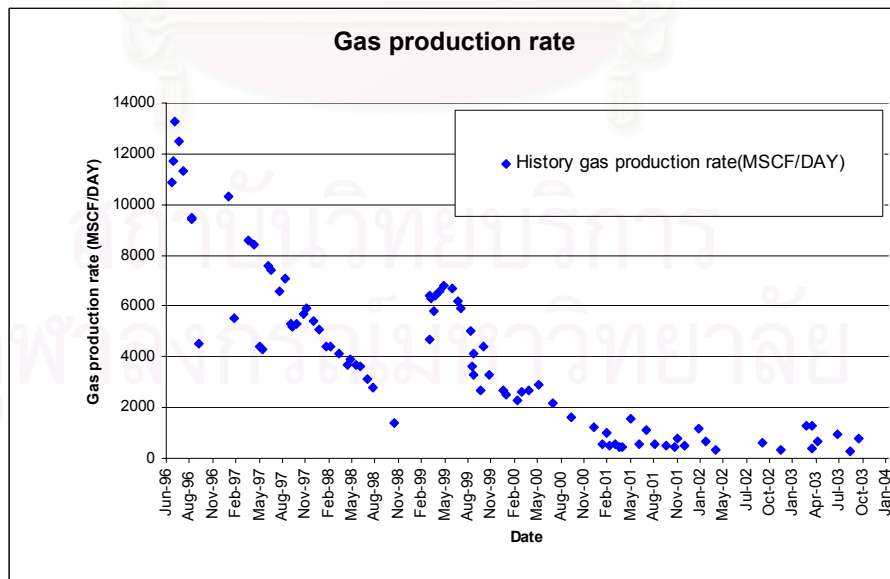
Figure 5.1: Historical data of gas production rate.
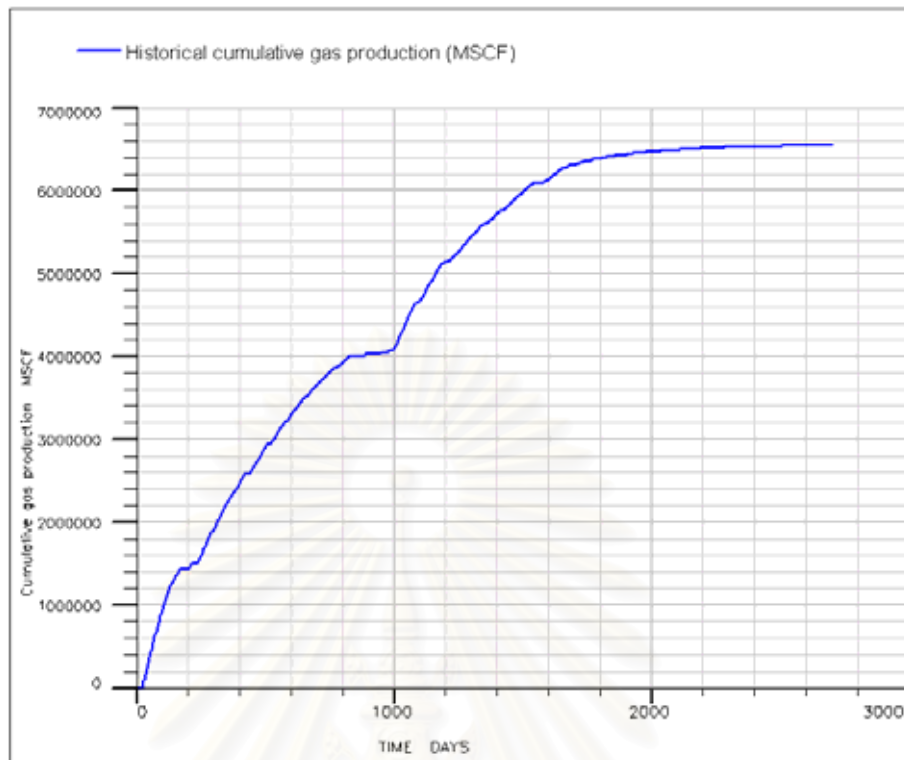
Figure 5.2: Historical data of cumulative gas production.
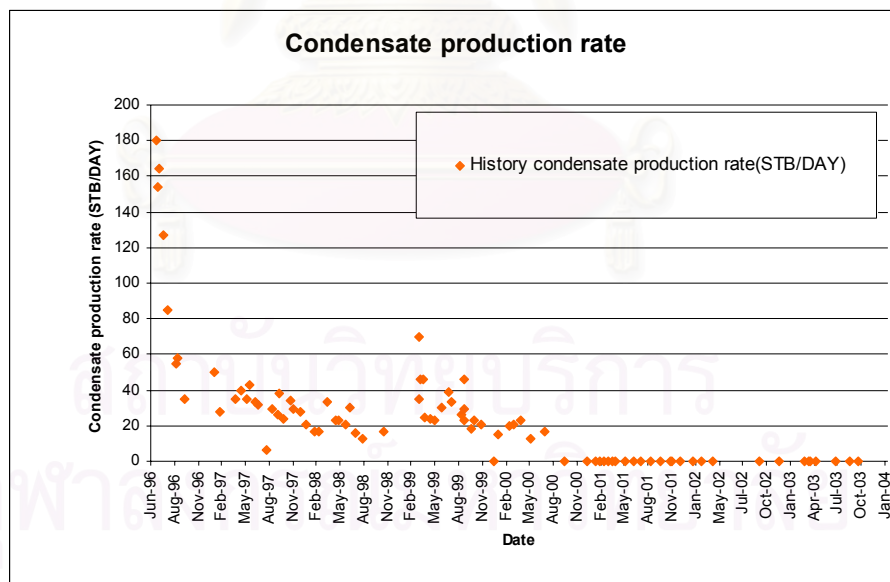
Figure 5.3: Historical data of condensate production rate.
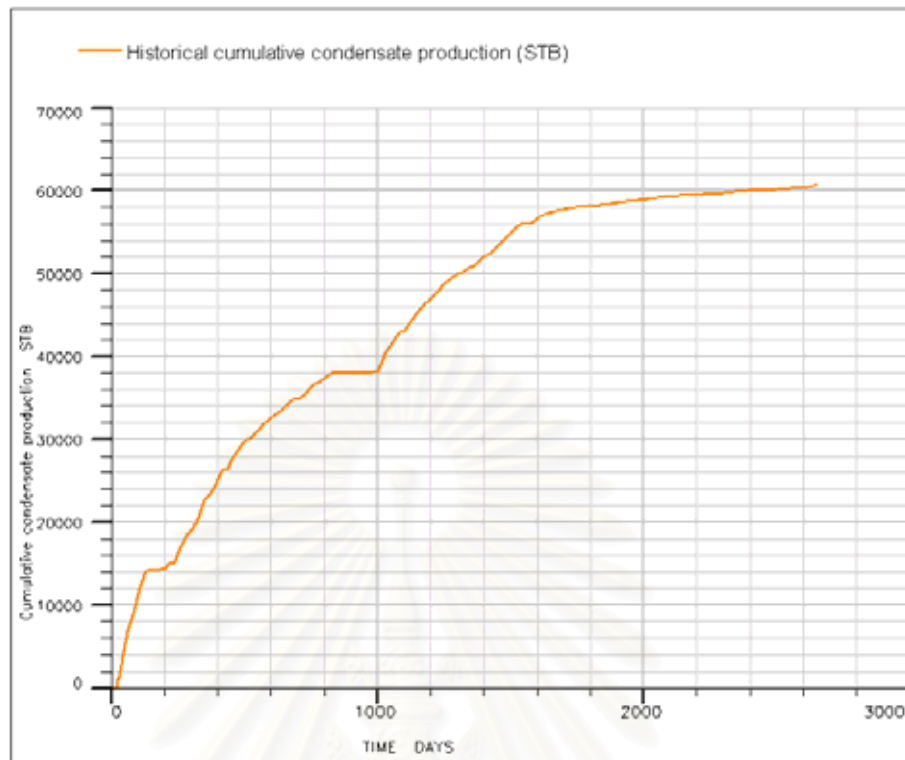
Figure 5.4: Historical data of cumulative condensate production.
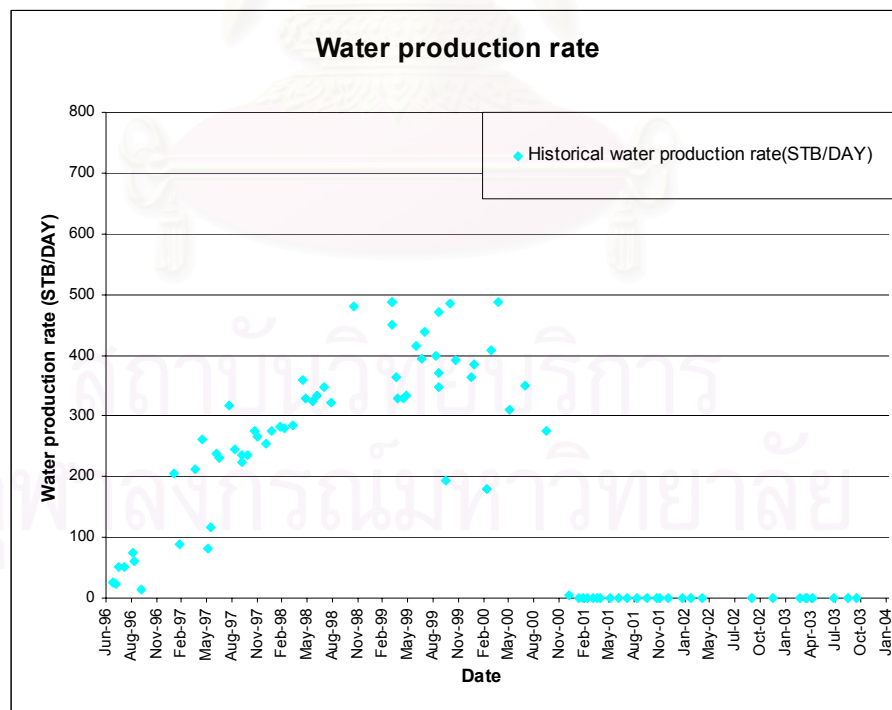
Figure 5.5: Historical data of water production rate.
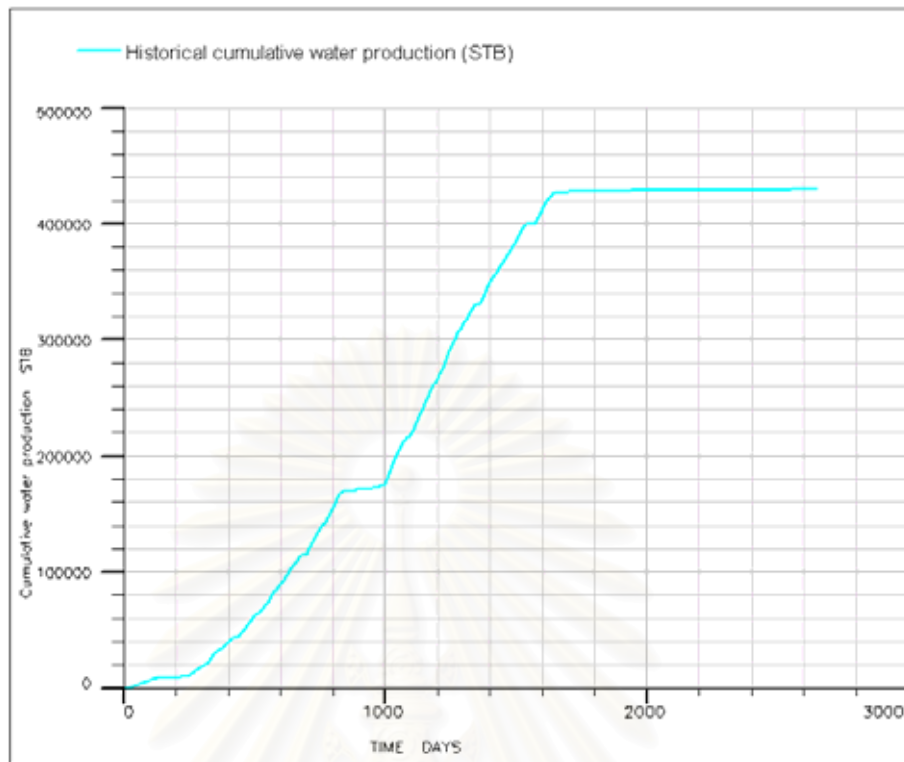
Figure 5.6: Historical data of cumulative water production.
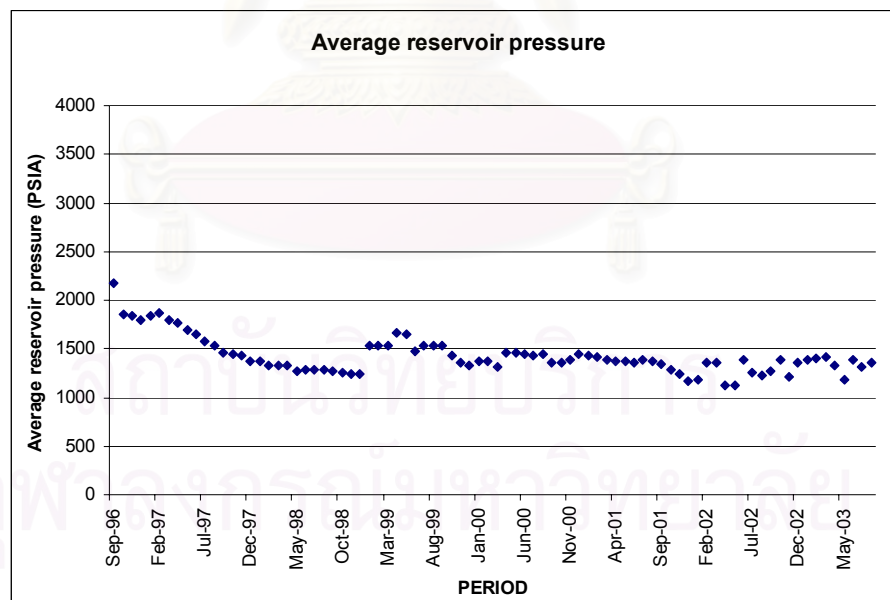
Figure 5.7: Historical data of average reservoir pressure.

Pressure survey has not been performed for the compartment MN, so the average reservoir pressure was determined from well head shut-in pressure (WHSIP)

added by the gas hydrostatic pressure. Actually, fluid in the wellbore should be both gas and liquid but the height of the liquid column is not known. Therefore, only gas column was then taken into account.

The Vertical Lift Performance Table (VFP Table) for the simulation was created using Prosper software introduced by Petroleum Experts. The program can export the results in a format required by ECLIPSE. In this study, the VFP table of well MN-1 and well MN-2 were created using the following information:

- PVT properties from average production test data of well MN-1

- Well MN-1 deviation profile (TVD 1997.3 m. vs. MD 3,755 m.) and well MN-2 deviation profile (TVD 1815.6 m. vs. MD 2,065.4 m.)

- Tubing size of 3.5 inches OD (2.991 inches ID)

o VFP graphs for gas production were constructed for the following conditions:

- gas production rate of 1 to 100 MMSCFD

- tubing head pressure of 314.7 to 614.7 psia

- water-gas ratio of 2 to 600 STB/MMSCF

- condensate gas ratio of 0 to 25 STB/MMSCF

o VFP graphs for slurry injection were constructed for the following conditions:

- slurry injection rate of 10 to 20,000 STBD

- tubing head pressure of 73 to 5,802 psia

The VFP graphs consist of a lot of lines and cannot be shown in details. A sample VFP curve for production was then constructed from well MN-1 data and shown in Fig. 5.8. Each curve is identified by a set of numbers. The first number represents the tubing head pressure, the second number represents the water-gas ratio, and the last number represents the condensate-gas ratio. From the figure, increasing of tubing head pressure, water-gas ratio and condensate-gas ratio requires more bottom hole pressure (BHP) to lift the fluid to the surface.

As mentioned in Chapter 4, there are three injection slurry densities which are 83.7, 94.3, and 104.9 lb/ft^3. VFP graphs for the injector, well MN-2, were constructed

for each slurry density. The VFP graph constructed using slurry density 104.9 lb/ft^3 is shown in Fig. 5.9 as an example. From the graph, we can observe that increasing of bottom hole pressure requires more tubing head injection pressure to inject the slurry. Using same tubing head injection pressure, lower bottom hole pressure allows for higher injection rate.
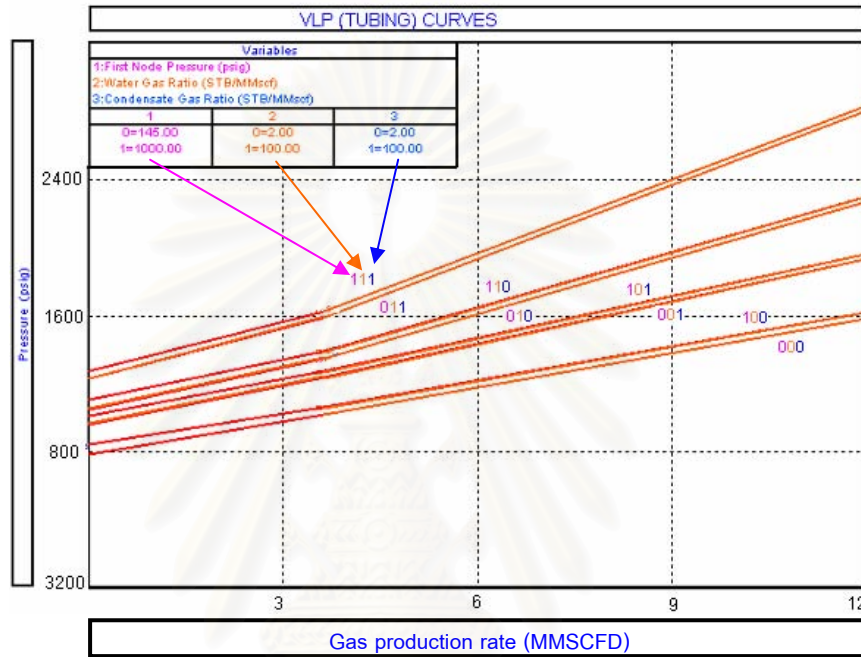
Figure 5.8: Sample VFP curve for producer (well MN-1).
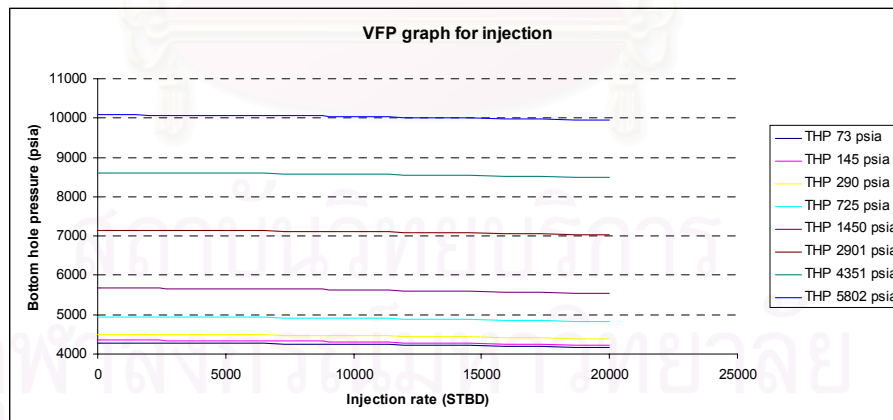
Figure 5.9: Sample VFP curve for injector (well MN-2).

In first initial run, the reservoir and well performance was simulated using initial reservoir characteristics as mentioned in Chapter IV. The initial results are shown in Fig. 5.10 to Fig. 5.16

Fig. 5.10 and Fig. 5.11 compare simulation results and actual gas production of well MN-1. The production period was divided to two stages. The first stage of production is from the first perforation batch. Eighteen gas reservoirs (480 to 840) were perforated and put on production in June 1996. The second stage is from the second perforation batch. Three additional gas reservoirs (355, 440 and, 475) were perforated and put on production in November 1998.

As seen in Fig. 5.10, the initial gas production rate during the first stage from the simulation is slightly higher than the actual production rate. The cumulative gas production from the simulation is higher than the actual cumulative data during this stage. During the second stage, the gas production rate from the simulation is lower than the actual production rate. At the end of production in October 2003, the cumulative gas production from the simulation is 7.5 % lower than the actual cumulative production.
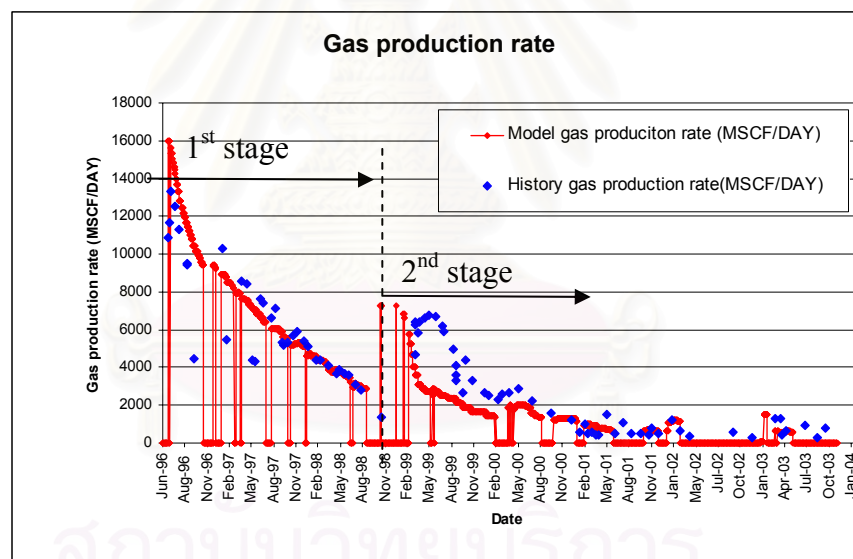
Figure 5.10: History matching on gas production rate (original model).
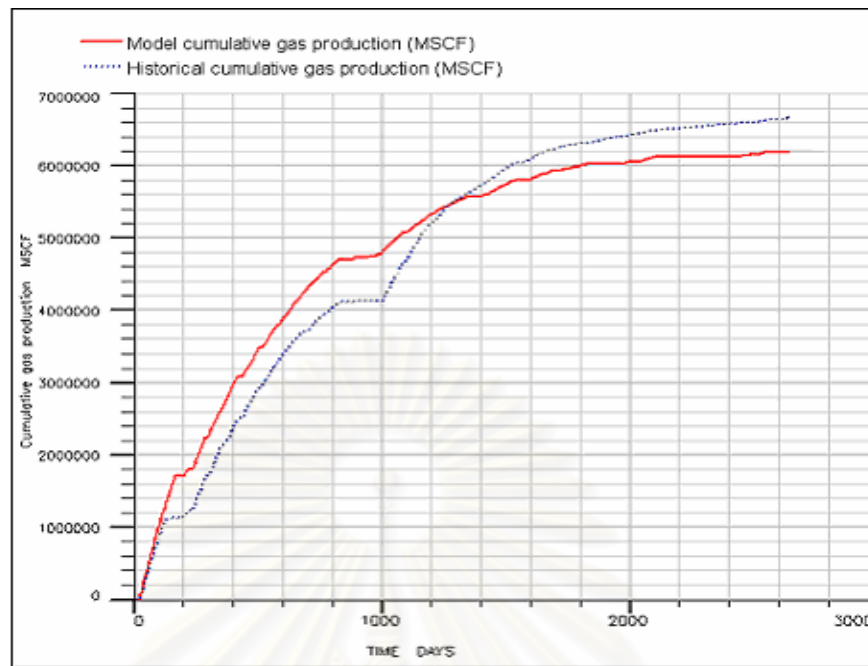
Figure 5.11: History matching on cumulative gas production (original model).

Fig. 5.12 and Fig. 5.13 show a comparison between simulation result and condensate production data of well MN-1. As seen in Fig. 5.12, the initial condensate production rate during the first stage from the simulation is slightly higher than the actual condensate production rate. The cumulative condensate production from the simulation is higher than the actual cumulative condensate data during this stage. During the second stage, the condensate production rate from the simulation is lower than the actual condensate production rate. At the end of production in October 2003, the cumulative condensate production from the simulation is 3.3% lower than the actual cumulative condensate production.
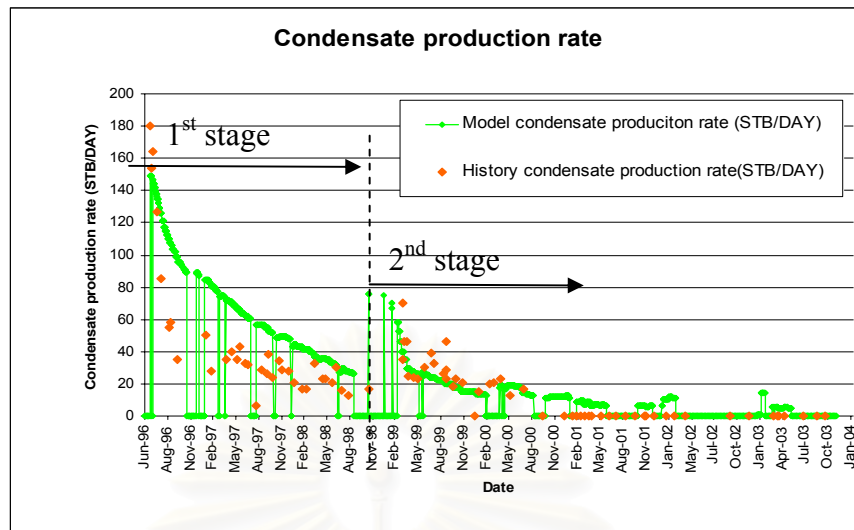
Figure 5.12: History matching on condensate production rate (original model).
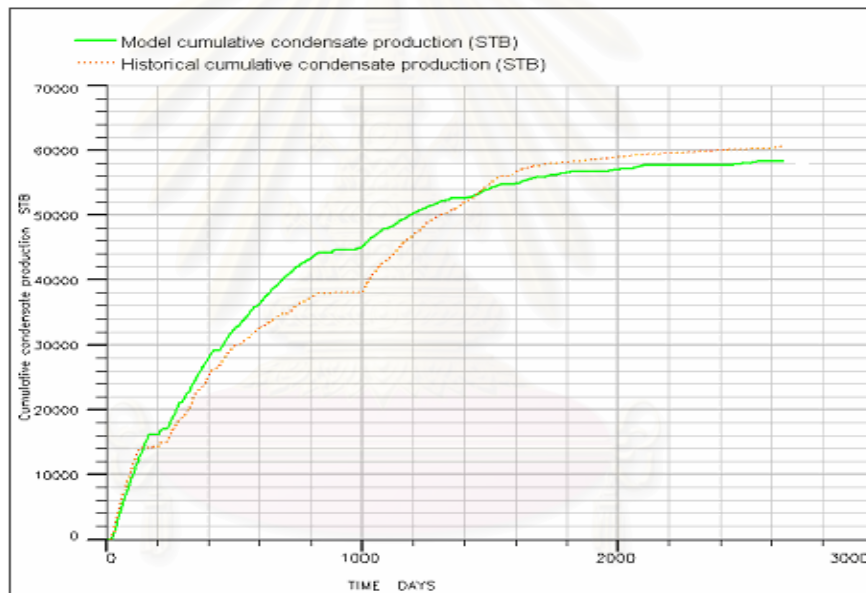
Figure 5.13: History matching on cumulative condensate production (original model).

Fig. 5.14 and Fig. 5.15 show a comparison between simulation and water production data of well MN-1. As seen in Fig. 5.14, in the first 7 months of production during the first stage, water production rate obtained from the simulation matches quite well with the actual water production rate. After that, water production rate from the simulation is significantly lower than the actual history. During the second stage, water production rate from the simulation is significantly lower than the actual production rate. From the history, it can be observed that the water production stopped at the end of year 2000, which may be due to water loading effect. At the end

of production in October 2003, the cumulative water production from the simulation is 35 % lower than the actual cumulative water production.
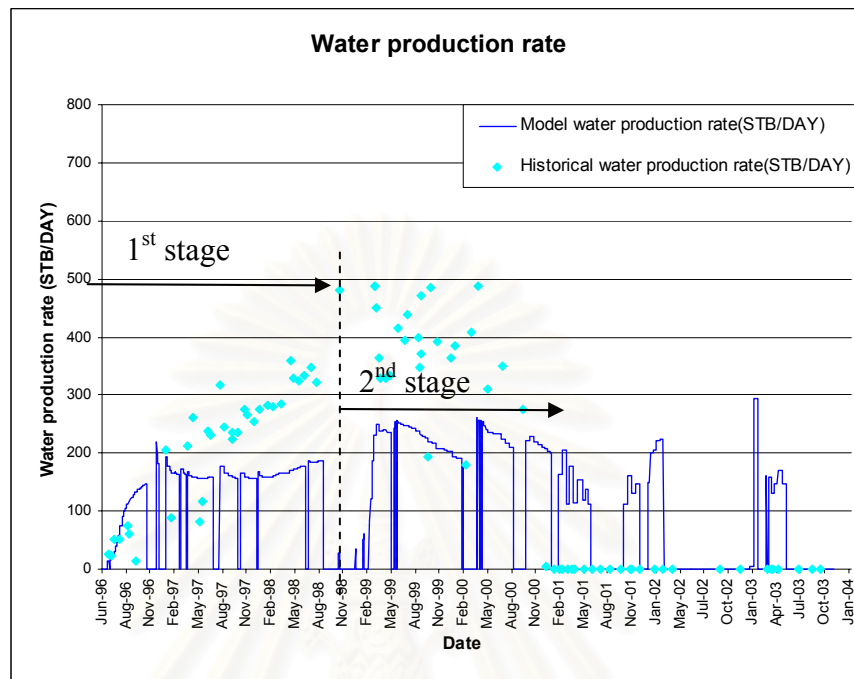
Figure 5.14: History matching on water production rate (original model).
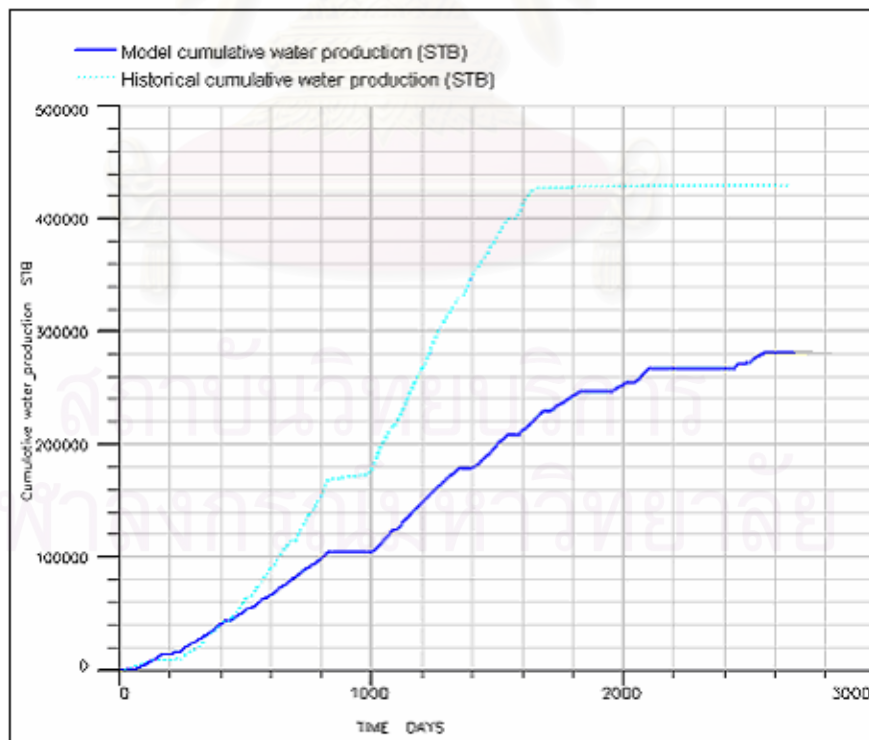
Figure 5.15: History matching on cumulative water production (original model).

Pressure survey has not been performed for the compartment MN, so the average reservoir pressure from the model was compared with the average reservoir pressure determined from well head shut-in pressure (WHSIP) added by the fluid hydrostatic pressure. As seen in Fig. 5.16 the initial average reservoir pressure during the first stage from the simulation provides a good match with the actual pressure obtained from WHSIP. During the second stage, the average reservoir pressure from the simulation is significantly lower than the actual pressure. At the end of production in October 2003, the average reservoir pressure from the simulation is 26 % lower than the actual average reservoir pressure.
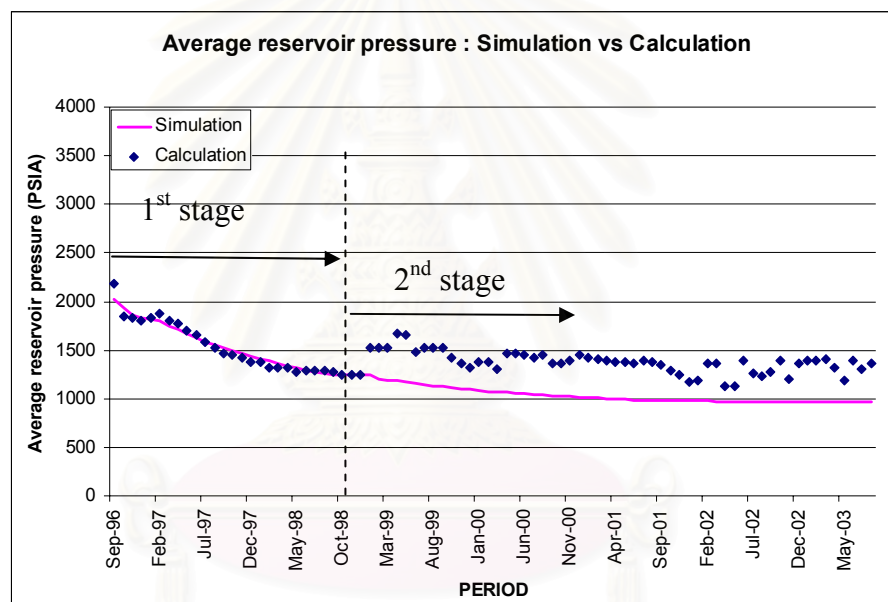
Figure 5.16: History matching on average reservoir pressure (original model).

5.2 Model Adjustment

5.2.1 Matching gas production

As seen in Fig. 5.10, at the start of production in the first stage, the gas production rate from the simulation is higher than the actual production data. This implies that the ability of gas flow in the early stage was too high. After taking a closer look at the simulation output, it was found that the initial gas saturation at the well block was 60-80%. To reduce gas production rate in the early stage of

production, the relative permeability curve *Krg1* was adjusted to *Krg2* by reducing the gas relative permeability value when the gas saturation is in the range of initial gas saturation ($S_g \approx 60 - 80\%$) as shown in Fig. 5.17. The relative permeability curve *Krg2* is the lowest relative permeability curve that can be fitted to the data points. This gas relative permeability was applied for the first 18 perforated reservoirs (the first batch of perforation). The gas relative permeability for each reservoir is summarized in Table 5.1.
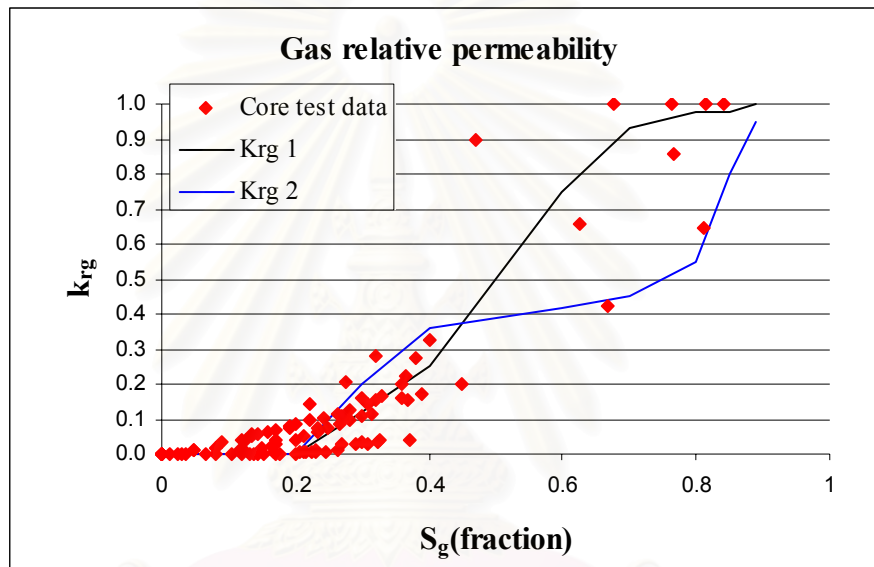
Figure 5.17: Gas relative permeability.

Table 5.1: Gas relative permeability by reservoir.

Reservoir Name	Krg Curve
355	Krg 1
440	Krg 1
475	Krg 1
480	Krg 2
495	Krg 2
515	Krg 2
525	Krg 2
535	Krg 2
560	Krg 2
570	Krg 2
585	Krg 2
605	Krg 2
620	Krg 2
625	Krg 2
685	Krg 2
700	Krg 2
710	Krg 2
740	Krg 2
760	Krg 2
830	Krg 2
840	Krg 2

After adjusting the gas relative permeability curve, the matching result is better but not perfect. The gas rate at the early stage of production from the simulation is still higher than the actual gas rate. The next parameter to be adjusted is the absolute permeability. Although the reduction of absolute permeabilities also affects the water production rate that is still lower than the historical data, we still need to reduce the absolute permeabilities to match the gas production profile. Later on, we can make an adjustment on aquifer volume in order to match the water production. Normally, the permeability in the formation can be 60% lower than the value obtained from a core test due to the effect of overburden pressure. To reduce gas production rate in the early stage of production, the permeabilities of all reservoirs were reduced to 80% (medium value between 60% and 100%) of the original permeabilities. The average absolute permeabilities after the adjustment are summarized in Table 5.2. After adjusting the absolute permeabilities, the gas production rate from the simulation has a good match with the historical data. The final match between the

simulation and the actual history is deferred to Section 5.3.1 since we still need to adjust other parameters.

Table 5.2: Absolute permeability adjusted for gas production during the first stage.

Reservoir Name	Average Permeability (md)		
	Original	Multiplier	Final
355	74	0.8	59
405	96	0.8	76
440	10	0.8	8
475	30	0.8	24
480	1	0.8	1
495	4	0.8	3
515	34	0.8	27
525	8	0.8	6
535	64	0.8	51
560	6	0.8	5
570	110	0.8	88
585	108	0.8	86
605	2	0.8	2
620	2	0.8	2
625	2	0.8	1
685	3	0.8	2
700	30	0.8	24
710	143	0.8	115
740	3	0.8	3
760	9	0.8	7
830	4	0.8	3
840	8	0.8	7

During the second stage of production, the gas production from the simulation is lower than the historical data. The expected main gas contribution zones are reservoirs 355, 440, and 475 which are newly perforated reservoirs. In an attempt to increase gas production from the simulation, the permeabilities of these reservoirs were adjusted. After observing the permeability-porosity correlation plot in Fig. 4.12, there are many data points that are far away from the correlation lines. Due to uncertainty of the correlation, the absolute permeability could be increased up to fifteen times of the original value. After trying to perform history matching using different values of permeability, the most appropriate permeabilities were obtained as shown in Table 5.3. These values gave a good match for gas production rate in the first 9 months of the second stage but after that, the production depleted faster than

the historical data. The cumulative production was still significant lower than the historical data.

Table 5.3: Absolute permeability adjusted for gas production during the second stage.

Reservoir Name	Average Permeability (md)		
	Original	Multiplier	Final
355	74	1.6	118
440	10	12.8	127
475	30	3.2	97

After examining several possibilities, we found that low gas production from the simulation in the second stage was due to underestimation of OGIP. Three bottom reservoirs (760, 830, and 840) have connections with the compartment F (located north of the compartment MN). These reservoirs in the compartment F have not been perforated. So, the OGIP of the mentioned reservoirs in this compartment should be added into the OGIP of the compartment MN. In ECLIPSE, the OGIP can be adjusted by applying pore volume multiplier. In this case, pore volume multiplier for each reservoir was obtained as follows:

$$\frac{Original\ OGIP\ in\ compartment\ MN + Additional\ OGIP\ from\ compartment\ F}{Original\ OGIP\ in\ compartment\ MN}$$

The OGIP adjustment was done for reservoirs 760, 830, and 840 as summarized in Table 5.4. Since these reservoirs have low average permeability (3 to 7 md), there is only small effect to the gas production performance in the first and second production stages. After the adjustment, the cumulative gas production in the second stage was still significant lower than the production data.

As mentioned earlier, the major gas production zones are reservoirs 355, 440, and 475. The total OGIP of these reservoirs is 1.49 BSCF. Fig. 5.11 shows that the cumulative production during the second stage was 2.5 BSCF which is significantly higher than the OGIP of the mentioned reservoirs. So, OGIP adjustment was done in these reservoirs until a good match in gas production rate was obtained. The OGIP were adjusted by applying pore volume multiplier as summarized in Table 5.4.

Table 5.4: OGIP adjustment.

Reservoir Name	OGIP (Bscf)		
	Original	Multiplier	Final
355	0.33	2.5	0.82
440	0.50	2.0	1.00
475	0.66	2.0	1.32
760*	0.21	4.1	0.87
830*	1.70	1.6	2.63
840*	0.08	5.1	0.39

* Additional GIP from nearby compartment

5.2.2 Matching condensate production

Condensate production is directly related to gas production. From the initial simulation results, condensate production has a good correlation with gas production. After performing gas production adjustment, we also obtained a good match on condensate production. The final result of the matching is deferred to Section 5.3.2 since we still need to adjust other parameters which have effects on the results.

5.2.3 Matching water production

As seen in Fig. 5.14, the water production rate from the simulation is significantly lower than the actual history. The first parameter that should be considered is aquifer volume since it has the highest uncertainty. The low water production from the simulation implies that the actual aquifer is larger than the model aquifer. To increase the water production rate, the aquifer volumes were adjusted by trial and error until the most appropriate value was obtained. The aquifer volume were increased from 3×10^9 to 5×10^9 ft^3 for channel sand and from 2×10^9 to 4×10^9 ft^3 for bar sand. Using volumes higher than these values causes only a small effect on water production rate. After increasing the aquifer size, the water production rate from the simulation significantly increases but is still lower than the actual history. This implies that the ability of water flow is still too low.

The next parameter that was considered is water relative permeability. From simulation, the water was produced from all reservoirs except reservoirs 560 and 605. To increase the water production rate, water relative permeability curves in water producing layers (reservoirs 355, 440, 475, 480, 495, 515, 525, 535, 570, 585, 620, 625, 685, 700, 710, 740, 760, 830, and 840) were shifted upward from *Krw1* until the

improvement of water production rate was observed. At first, the increase of water production in reservoirs 710 and 830 was observed when a relative permeability curve was shifted to *Krw2* as shown in Fig. 5.18. Further shifting of the relative permeability curve for both reservoirs causes the initial water production rate to be higher than the historical data. After shifting the relative permeability curve to *Krw2*, most reservoirs except reservoirs 710 and 830 had small changes in water production rate.

Then, the relative permeability of these remaining reservoirs was shifted further from *Krw2* to *Krw3*. *Krw3*, as shown in Fig. 5.18, is the highest water relative permeability curve that can be fitted to the data points. The water relative permeability curve for each reservoir is summarized in Table 5.5. After adjusting the water relative permeability, water production from the model was significant better but still lower than the historical data. Therefore, the absolute permeabilities of main water contributing reservoirs, which are reservoirs 495, 525, and 740, were increased as shown in Table 5.6. The absolute permeabilities of these reservoirs were adjusted until water production from the simulation has a good match with the historical data. However, the absolute permeability adjustment also affects gas and condensate production. So, change in gas production was also closely monitored. For reservoirs 495 and 740, after trying in several values of absolute permeabilities, we found that the permeabilities could be increased to 4 times of the original values without a significant effect on gas production of the whole compartment. For reservoir 525, the absolute permeability could be increased only 2.4 times of the original value.
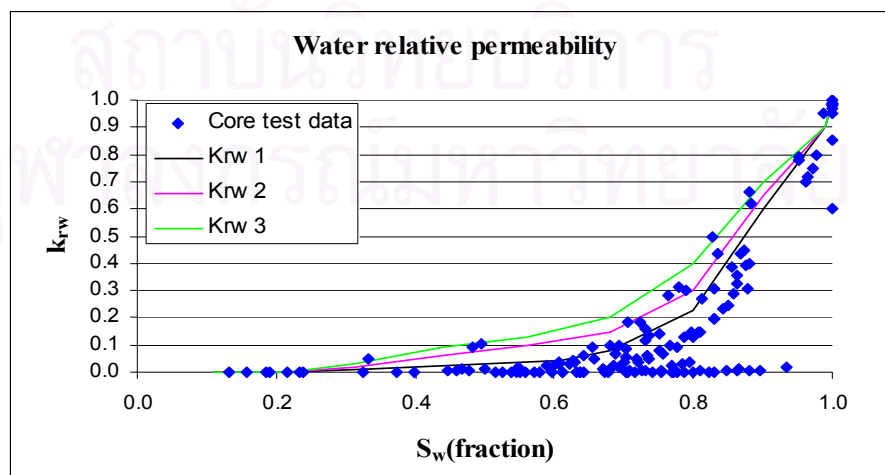
Figure 5.18: Water relative permeability.

Table 5.5: Water relative permeability by reservoirs.

Reservoir Name	Krw Curve
355	Krw 3
440	Krw 3
475	Krw 3
480	Krw 3
495	Krw 3
515	Krw 3
525	Krw 3
535	Krw 3
560	Krw 1
570	Krw 3
585	Krw 3
605	Krw 1
620	Krw 3
625	Krw 3
685	Krw 3
700	Krw 3
710	Krw 2
740	Krw 3
760	Krw 3
830	Krw 2
840	Krw 3

Table 5.6: Absolute permeability adjustment.

Reservoir Name	Average Permeability (md)		
	Original	Multiplier	Final
495	4	4.0	16
525	8	2.4	19
740	3	4.0	14

The historical data indicate that water loading occurred at the end of year 2000. This phenomenon was simulated by turning off all reservoirs except reservoir 355 on December 10, 2000 in the simulation schedule.

After applying all the adjustments, the water production rate from the simulation has a good match with the historical data. The final match between the simulation and the actual history is deferred to Section 5.3.3.

5.2.4 Matching average reservoir pressure

Initial matching result between the average reservoir pressure from the model and the average reservoir pressure determined from the well head shut-in pressure added by the fluid hydrostatic pressure was good during the first stage of production. During the second stage, the average reservoir pressure from the simulation is significantly lower than the actual pressure data. After adjusting the production data, we found that the average reservoir pressure from simulation has a good agreement with the historical data. The final result of the matching is deferred to Section 5.3.4.

5.3 History Matching Result

After finishing all necessary adjustments, production rates, cumulative productions and average reservoir pressure from the simulation were reasonably matched with the historical data.

5.3.1 Gas production

Fig. 5.19 and Fig. 5.20 show the comparison between the simulation results and the gas production data of well MN-1. There is a good match between the simulation results and the historical production rate and cumulative production. At the end of production in October 2003, the cumulative gas production from the simulation is only 1.8% lower than the historical data.
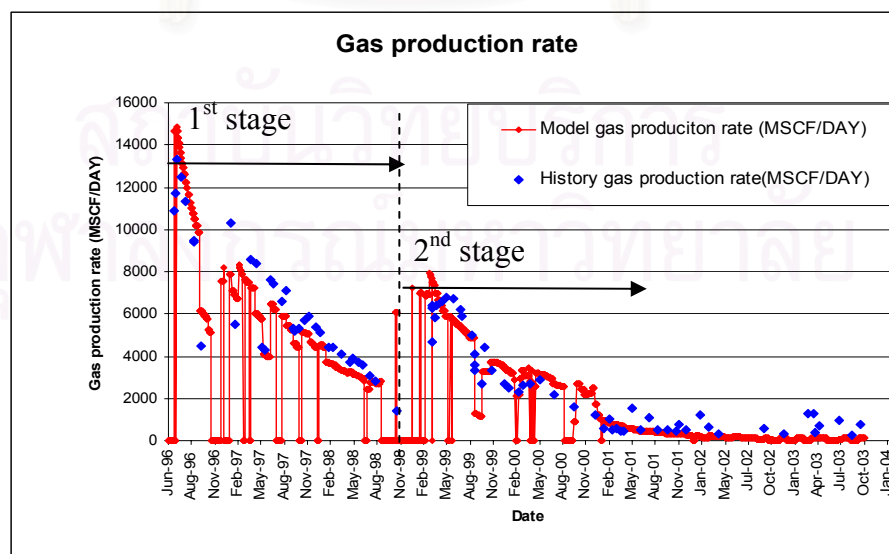
Figure 5.19: History matching on gas production rate (adjusted model).
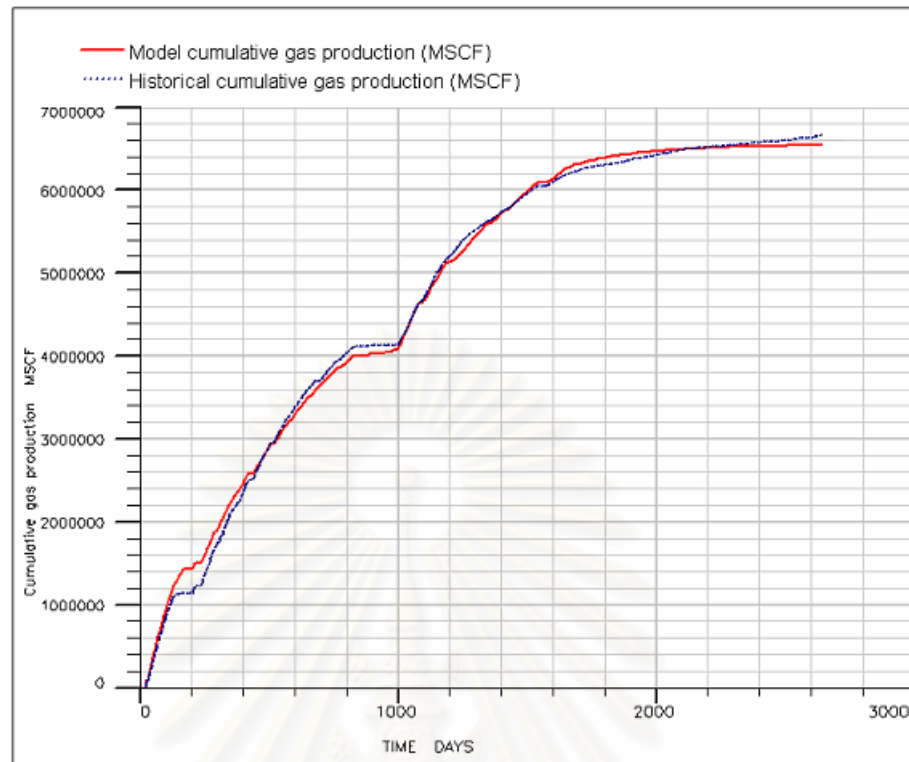
Figure 5.20: History matching on cumulative gas production (adjusted model).

5.3.2 Condensate production

Fig. 5.21 and Fig. 5.22 show the comparison between the simulation results and the historical oil production data of well MN-1. The condensate production rate obtained from the simulation model is slightly higher than the historical data. It is not significant to adjust condensate production since the cumulative condensate production is only 60.6 MSTB which is small comparing with 6.67 BSCF cumulative gas production and the cumulative condensate production from the simulation is only 3.3% different from the historical data.
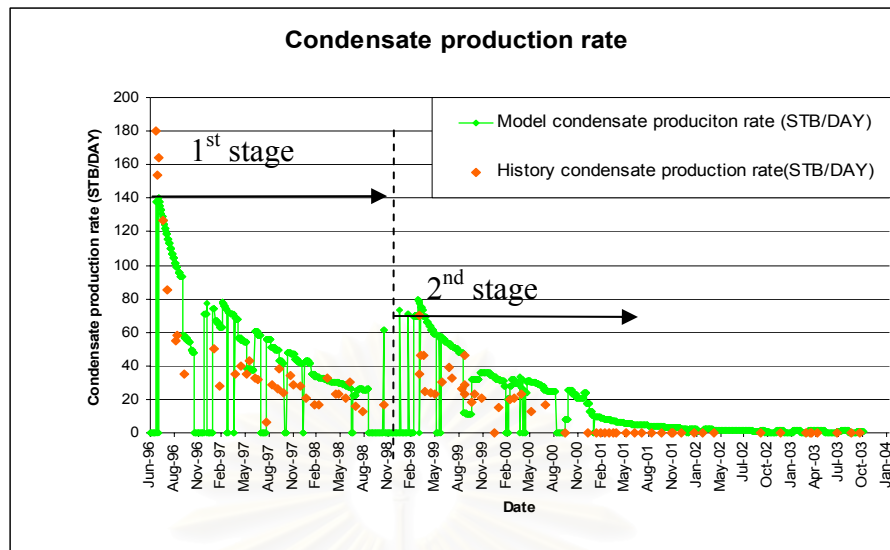
Figure 5.21: History matching on condensate production rate (adjusted model).
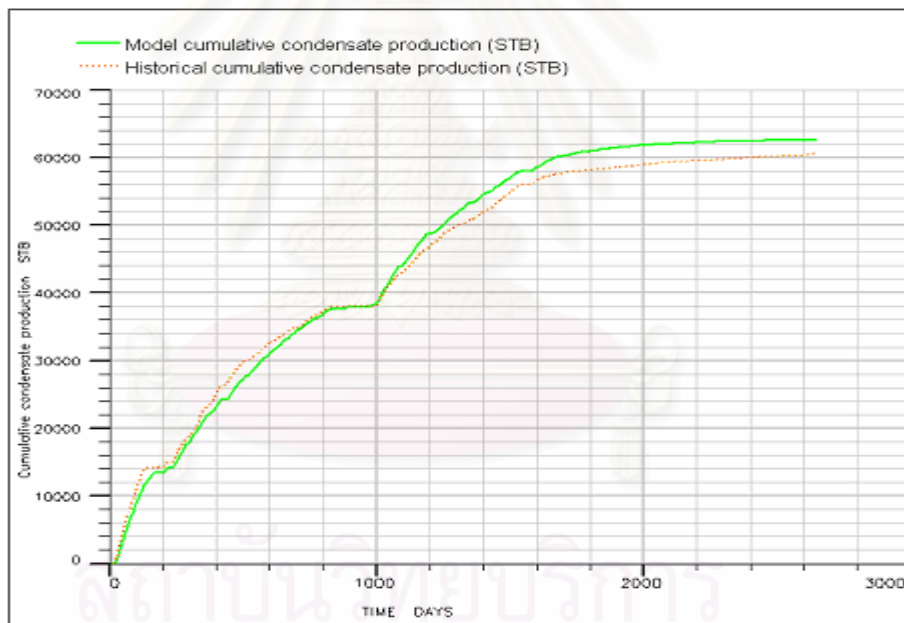
Figure 5.22: History matching on cumulative condensate production (adjusted model).

5.3.3 Water production

Fig. 5.23 and Fig. 5.24 show a comparison between the simulation results and the historical water production data of well MN-1. There is a good match between the simulation results and the historical production rate and cumulative production. At the

end of production in October 2003, the cumulative water production from the simulation is merely 4.9% higher than the historical data.
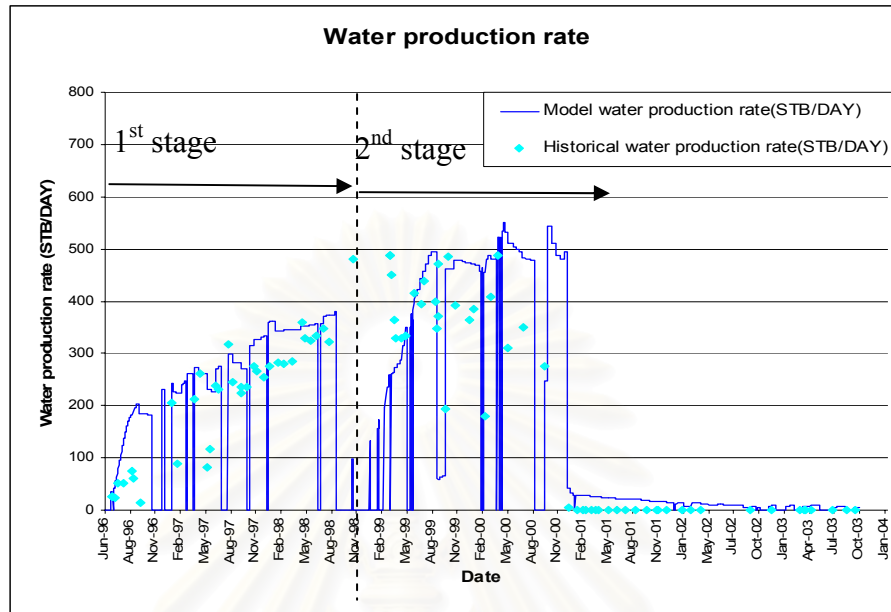
Figure 5.23: History matching on water production rate (adjusted model).
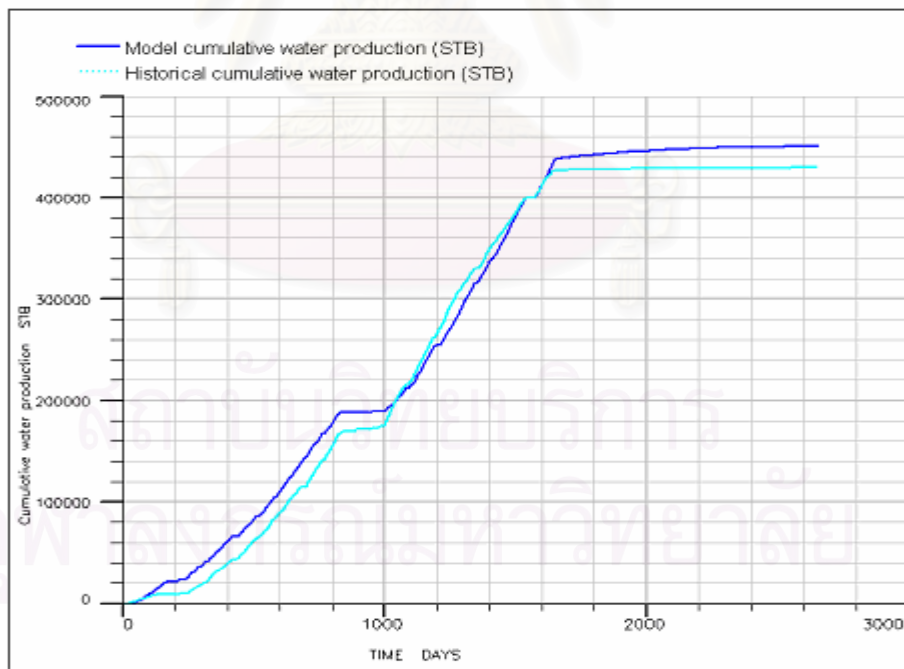
Figure 5.24: History matching on cumulative water production (adjusted model).

5.3.4 Average reservoir pressure

As mentioned earlier, pressure survey has not been performed for the compartment MN. So, the average reservoir pressure from the model was compared with the average reservoir pressure determined from wellhead shut-in pressure added by the fluid hydrostatic pressure. The historical average reservoir pressure shown in Fig. 5.25 considers only gas in the wellbore. Actually, fluids in the wellbore could be both gas and liquid. If the water column was taken into account, the calculated pressure would increase and provide a better match with the average reservoir pressure. After the second batch of perforation was performed, the pressure was expected to shift up. However, the pressure obtained from the simulation continues to decline. After reviewing reservoir details, only three reservoirs were perforated in the second perforation batch and the total pore volume of these reservoirs is significantly lower than pore volume of those in the initial perforation batch. The contribution of the second perforation batch is not enough to remarkably change the trend of the pressure. In addition, there was only one data point per month. Fig. 5.25 shows the comparison between simulation results and historical reservoir pressures. There is a good agreement between the simulation results and historical data with an average of only 3.0 % error and a maximum of less than 20 % error.
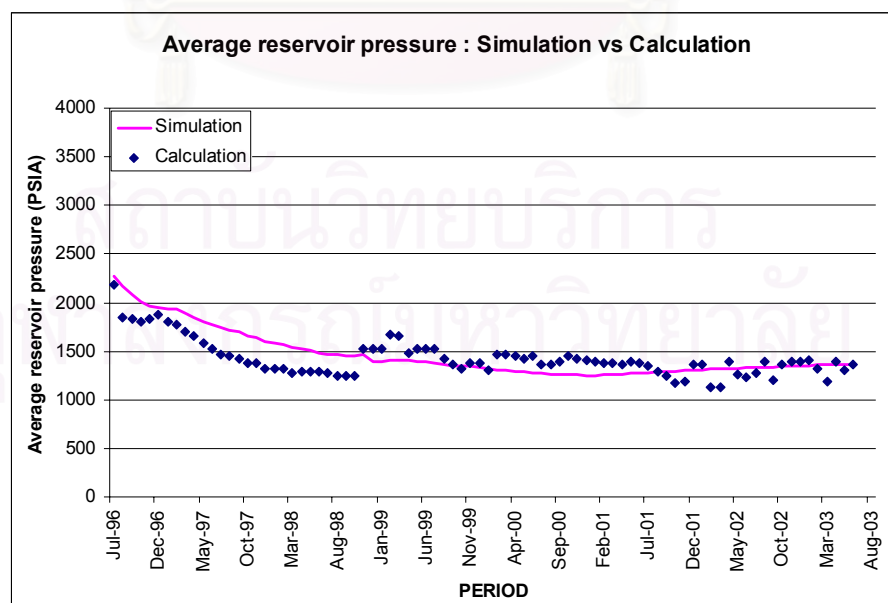
Figure 5.25: History matching on average reservoir pressure (adjusted model).

In summary, history matching is a process to fine tune the reservoir model. The history matched model can be used as a reservoir representation. In this study, the data selected to be matched are production rates, cumulative productions, and reservoir pressure. Production data of well MN-1 from the start of production in June 1996 until abandonment in October 2003 were used in the history matching. In an attempt to match gas production rate, the relative permeability and absolute permeability were adjusted in all the reservoirs while OGIP adjustment was done in some reservoirs. After adjusting these parameters, we also obtained a good match on condensate production. In an attempt to match water production rate, aquifer volume, water relative permeability, and absolute permeability of main water contribution reservoirs were adjusted. The average reservoir pressure from the model was compared with the average reservoir pressure that was determined from WHSIP added by the fluid hydrostatic pressure. After finishing all necessary adjustments, the results from simulation have good agreements with the historical data. The cumulative gas production is only 1.8% lower than historical data, and the cumulative condensate production is only 3.3% higher than historical data. The cumulative water production is 4.9% higher than production data, and the maximum error of average reservoir pressure is less than 20%.

CHAPTER VI

OPTIMIZATION OF HYDROCARBON PRODUCTION AND MERCURY WASTE INJECTION

Reservoir simulation can be used to optimize hydrocarbon production and Hg-contaminated slurry injection by varying design variables which are perforation plan, gas production rate, sludge concentration, Hg-contaminated slurry viscosity, and injection rate.

Perforation is planned to be done in batches from the bottom up. Mechanical problem, highest recovery factor, and enough storage capacity were taken into consideration when optimizing hydrocarbon production and Hg waste disposal.

Sensitivity analysis was performed by varying the design variables. The best production scenario with the highest productivity is recommended. The optimized injection scenarios for varied Hg sludge quantity are also concluded.

6.1 Optimization of Hydrocarbon Production

As mentioned in Chapter 1 that the well MN-2 will be used for alternate production and injection. Then, the reservoir simulation will be performed in two stages; (1) to maximize the hydrocarbon production and (2) to optimize Hg-contaminated slurry injection. In this section discusses in the details of hydrocarbon production optimization. The influences of design variables which are perforation plan and the maximum gas production rate are studied. Then, the scenario of maximum cumulative hydrocarbon production is defined.

6.1.1 Perforation plan

Well MN-2 will be used for alternate production and injection until it is completely depleted and reaches injection capacity. The injector/producer well, MN-2, is a highly deviated well with a maximum angle of 70°. To prevent the tool from being stuck in the well, only two batches of perforation are planned. Hydrocarbon production in the first perforation batch will last for 2 years. Then, Hg-contaminated slurry will be

injected as much as possible without causing any fracture. As mentioned earlier that mercury is hazardous; thus, it should be disposed in a confined structure. Injection pressure should not be high enough to create any fracture in the reservoirs. After finishing the first injection batch, the zone will be plugged, and upper reservoirs will be perforated. To prevent communication between the contaminated injection zone and producible zone, a sixty-meter interval which is a safe distance between the two perforated batches is planned to be left.

Considering the above criteria, there are two possibilities for the perforation scenario.

- Perforation plan 1: The first perforation batch covers reservoirs 560 to 720 (8 reservoirs), and the second perforation batch covers reservoirs 405 to 485 (5 reservoirs) as shown in Fig. 6.1. The two batches of perforation are 69.5 meters apart.

COMPARTMENT: MN

Formation	Reservoir	MN-1			MN-2		
		Net Pay (m)	Perf.	Top (mTVDSS)	Net Pay (m)	Perf.	Top (mTVDSS)
2D	355	1.2	2	1387.7			
	380						
2C	405	11.6/ 4.0 /3.3	✗	1430.5	9.7		1422.0
	440	2.8	2	1465.1	2.0		1455.5
	475	1.0	2	1502.7	1.7		1491.9
	480	2.2	1	1506.9	1.7		1496.9
	485			1515.6	1.3		1504.0
	495	3.3	1	1523.1			
	515	2.8	▨	1542.6	1.6		1533.6
	525	0.6	1	1552.7		✗	1542.0
	535	2.3	1	1562.4	2.4		1552.7
	545				0.7		1560.3
	560	1.4	1	1581.7	0.7		1574.7
	570	5.8	1	1593.6	12.6		1584.6
	585	1.3	1	1612.1	0.8		1609.8
	600			1625.3			
	605	0.8	1	1634.4	0.8	✗	1631.0
	620	1.8	1	1650.3	2.3		1647.1
	625	0.6	1	1659.9	1.4	✗	1657.9
	660			1683.9	1.8		1682.1
	675	4.5	1	1703.9	5.5		1703.4
	700	2.0	1	1715.4			
	710	0.9	1	1727.8	3.8		1729.1
2B	720			1744.7	3.4		1748.5
	740	8.3	1	1761.4		✗	1764.0
	760	4.6	1	1790.8			
	830	4.7	1	1861.7			
	840	1.4	1	1874.0			

2nd batch

69.5 m.

1st batch

Not perforated ✗
March 1996 **1**
October 1998 **2**

2.0	Reservoir with only gas (2.0 m gas net pay)
11.0/ 1.0 /2.0	Reservoir with GOC and OWC (11.0 m net sand / 1.0 m oil net pay / 2.0 m gas net pay)
	Reservoir with only water
▨	Isolation#1 (i.e. CSG patch, Cement&Chemical Squeezing)

Figure 6.1: Perforation plan 1 for well MN-2.

- Perforation plan 2: The first perforation batch covers reservoirs 660 to 720 (4 reservoirs) and the second perforation batch covers reservoirs 405 to 585 (11 reservoirs) as shown in Fig. 6.2. The two batches of perforation are 71.5 meters apart.

COMPARTMENT: MN

Formation	Reservoir	MN-1			MN-2		
		Net Pay (m)	Perf.	Top (mTVDSS)	Net Pay (m)	Perf.	Top (mTVDSS)
2D	355	1.2	2	1387.7			
	380						
2C	405	11.6/ 4.0 /3.3	✗	1430.5	9.7		1422.0
	440	2.8	2	1465.1	2.0		1455.5
	475	1.0	2	1502.7	1.7		1491.9
	480	2.2	1	1506.9	1.7		1496.9
	485			1515.6	1.3		1504.0
	495	3.3	1	1523.1			
	515	2.8		1542.6	1.6		1533.6
	525	0.6	1	1552.7		✗	1542.0
	535	2.3	1	1562.4	2.4		1552.7
	545				0.7		1560.3
	560	1.4	1	1581.7	0.7		1574.7
	570	5.8	1	1593.6	12.6		1584.6
	585	1.3	1	1612.1	0.8		1609.8
	600			1625.3			
	605	0.8	1	1634.4	0.8	✗	1631.0
	620	1.8	1	1650.3	2.3		1647.1
	625	0.6	1	1659.9	1.4	✗	1657.9
	660			1683.9	1.8		1682.1
	675	4.5	1	1703.9	5.5		1703.4
	700	2.0	1	1715.4			
	710	0.9	1	1727.8	3.8		1729.1
2B	720			1744.7	3.4		1748.5
	740	8.3	1	1761.4		✗	1764.0
	760	4.6	1	1790.8			
	830	4.7	1	1861.7			
	840	1.4	1	1874.0			

2nd batch

71.5 m.

1st batch

Not perforated ✗
March 1996 **1**
October 1998 **2**

2.0	Reservoir with only gas (2.0 m gas net pay)
11.0/ 1.0 /2.0	Reservoir with GOC and OWC (11.0 m net sand / 1.0 m oil net pay / 2.0 m gas net pay)
	Reservoir with only water
	Isolation#1 (i.e. CSG patch, Cement&Chemical Squeezing)

Figure 6.2: Perforation plan 2 for well MN-2.

The compartment MN was produced by well MN-1 for 7 years and 5 months (from June 1996 to the end of October 2003). As shown in Table 6.1, the original gas in place (OGIP) of compartment MN is 16.90 BSCF. At the time of well MN-1 abandonment, the remaining gas in the compartment MN was 10.36 BSCF and the

total recovery factor from well MN-1 was 38.68%. Without water production effect, OGIP and permeability are the main factors controlling production ability of each reservoir. From the table, reservoirs 405, 485, 660, and 720 did not contribute gas. The reasons are that reservoir 405 was not perforated and that reservoirs 480, 660, and 720 are very tight zones with average permeability about 1 md. The main contributing reservoir is 585 which is a high permeability zone. An average permeability of this reservoir is 108 md., and the OGIP is 1.40 BSCF which is the highest OGIP among other perforated reservoirs except reservoir 830. Reservoir 830 has the OGIP of 2.63 BSCF, which is significantly higher than other perforated reservoir but it gave a slightly lower gas production than reservoir 585 since this reservoir has an average permeability of 4 md.

Table 6.1: Cumulative gas production, recovery factor, and gas in place of compartment MN as of October 2003.

Reservoir name	OGIP (BSCF)	Cumulative gas production (BSCF)	Recovery factor (%)	GIP @ Nov 2003 (BSCF)
355	0.82	0.67	80.73	0.16
405	2.44	0.00	0	2.44
440	1.00	0.48	47.97	0.52
475	1.32	0.63	48.04	0.68
480	1.35	0.40	29.87	0.95
485	0.03	0.00	0	0.03
495	0.80	0.55	69.03	0.25
515	0.17	0.06	37.88	0.10
525	0.72	0.46	64.10	0.26
535	0.35	0.29	82.74	0.06
560	0.18	0.10	53.40	0.09
570	0.80	0.52	65.36	0.28
585	1.40	0.76	54.24	0.64
605	0.13	0.05	36.96	0.08
620	0.05	0.02	43.58	0.03
625	0.02	0.01	49.00	0.01
660	0.04	0.00	0	0.04
685	0.27	0.15	56.16	0.12
700	0.18	0.10	56.42	0.08
710	0.05	0.01	27.72	0.04
720	0.14	0.00	0	0.14
740	0.74	0.32	43.54	0.42
760	0.87	0.03	3.01	0.85
830	2.63	0.75	28.62	1.88
840	0.39	0.16	41.57	0.23
Compartment	16.90	6.54	38.68	10.36

The production period is 2 years per batch due to the initial plan to dispose Hg-contaminated waste every 2 years. In case that perforated reservoirs are not depleted within 2 years, additional cases will be simulated until the well produces at an economic limit of 0.1 MMSCFD.

6.1.2 Maximum gas production rate

To maximize hydrocarbon production, the sensitivity analysis of maximum gas production rate was performed. In this study, the maximum gas production rate was varied in the range of 1 to 7 MMSCFD. The well head flowing pressure (WHFP) can be operated down to 10 bar with a support of booster compressor. Since hydrocarbon production will come from two different batches of perforation, we need to study the effect of maximum gas production rate for each batch separately.

a) The first perforation batch

For the first perforation batch, four cases with different maximum gas production rate were simulated. To avoid confusion when naming the case, the names 1.1A, 1.1B, 1.1C, and 1.1D are used for plan 1 and case names 2.1A, 2.1B, 2.1C, and 2.1D are used for perforation plan 2.

Case 1.1A and 2.1A: Maximum gas production rate at 4 MMSCFD.
Case 1.1B and 2.1B: Maximum gas production rate at 3 MMSCFD.
Case 1.1C and 2.1C: Maximum gas production rate at 2 MMSCFD.
Case 1.1D and 2.1D: Maximum gas production rate at 1 MMSCFD.

b) The second perforation batch

For the second perforation batch, seven cases with different maximum gas production rate were simulated. To avoid confusion when naming the cases, the names 1.2A, 1.2B, 1.2C, 1.2D, 1.2E, 1.2F, and 1.2G are used for plan 1 and case names 2.2A, 2.2B, 2.2C, 2.2D, 2.2E, 2.2F, and 2.2G are used for perforation plan 2.

Case 1.2A and 2.2A: Maximum gas production rate at 7 MMSCFD.
Case 1.2B and 2.2B: Maximum gas production rate at 6 MMSCFD.
Case 1.2C and 2.2C: Maximum gas production rate at 5 MMSCFD.

Case 1.2D and 2.2D: Maximum gas production rate at 4 MMSCFD.

Case 1.2E and 2.2E: Maximum gas production rate at 3 MMSCFD.

Case 1.2F and 2.2F: Maximum gas production rate at 2 MMSCFD.

Case 1.2G and 2.2G: Maximum gas production rate at 1 MMSCFD.

6.1.3 Production maximization result

The simulated cases for the first perforation batch of plan 1 are discussed in details but for the other perforation plans, only important points are discussed.

(i) Plan 1

a) The first perforation batch

There are four cases for this perforation plan which are cases 1.1A, 1.1B, 1.1C, and 1.1D as mentioned in Section 6.1.2. This batch starts production at the day 2,923, and the maximum production period is 2 years. The production performances of the simulated cases are shown in Fig. 6.3 to Fig. 6.8.
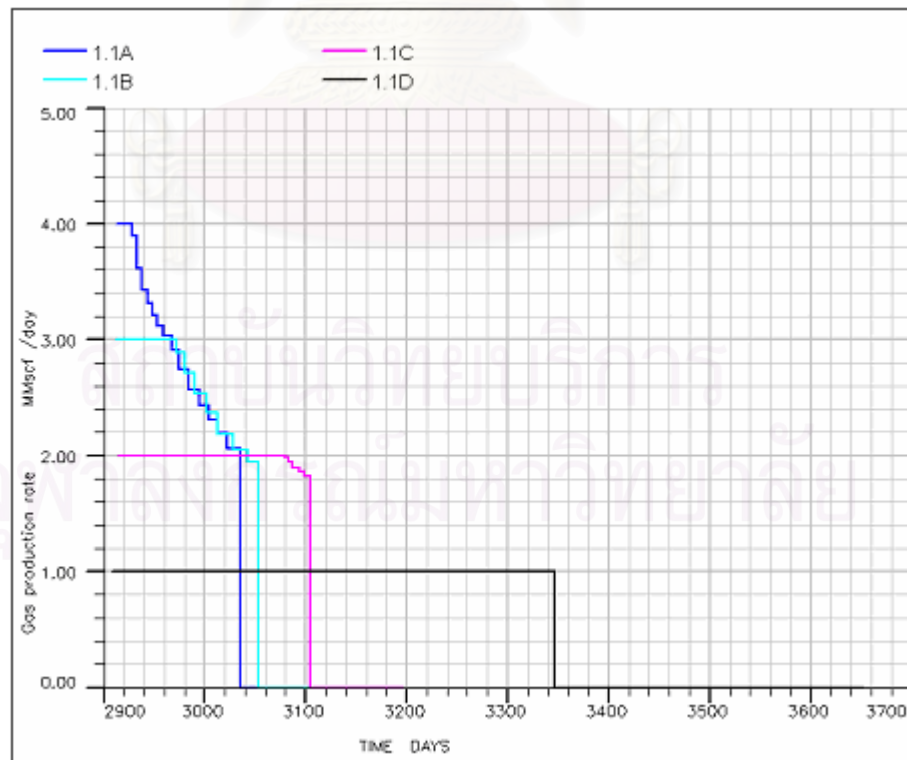
Figure 6.3: Gas production rate for the first batch of perforation plan 1.
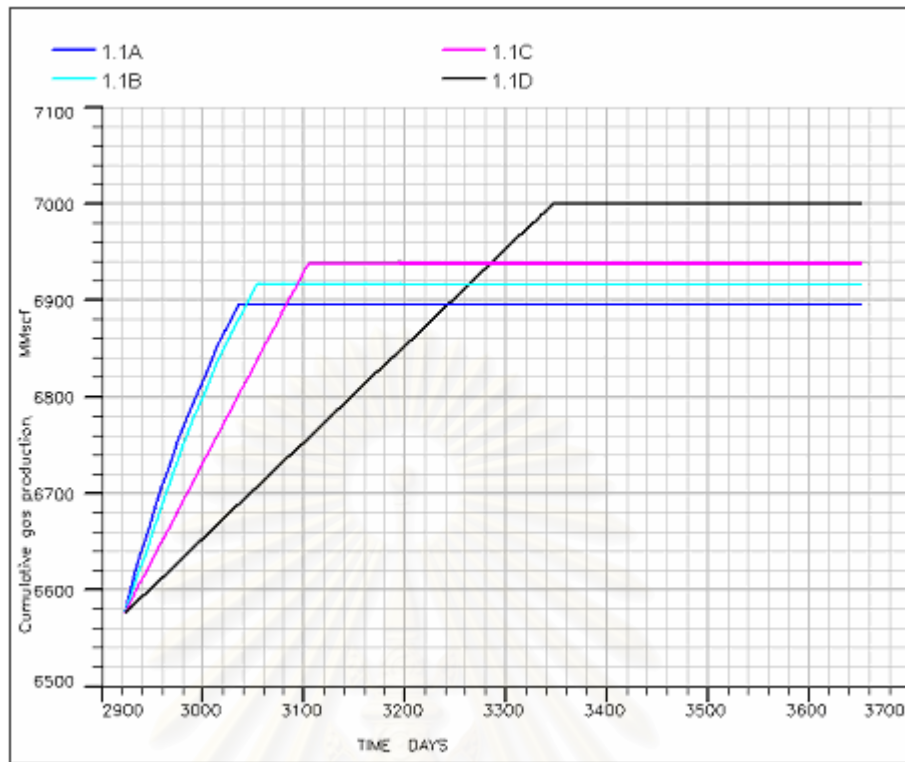
Figure 6.4: Cumulative gas production for the first batch of perforation plan 1.
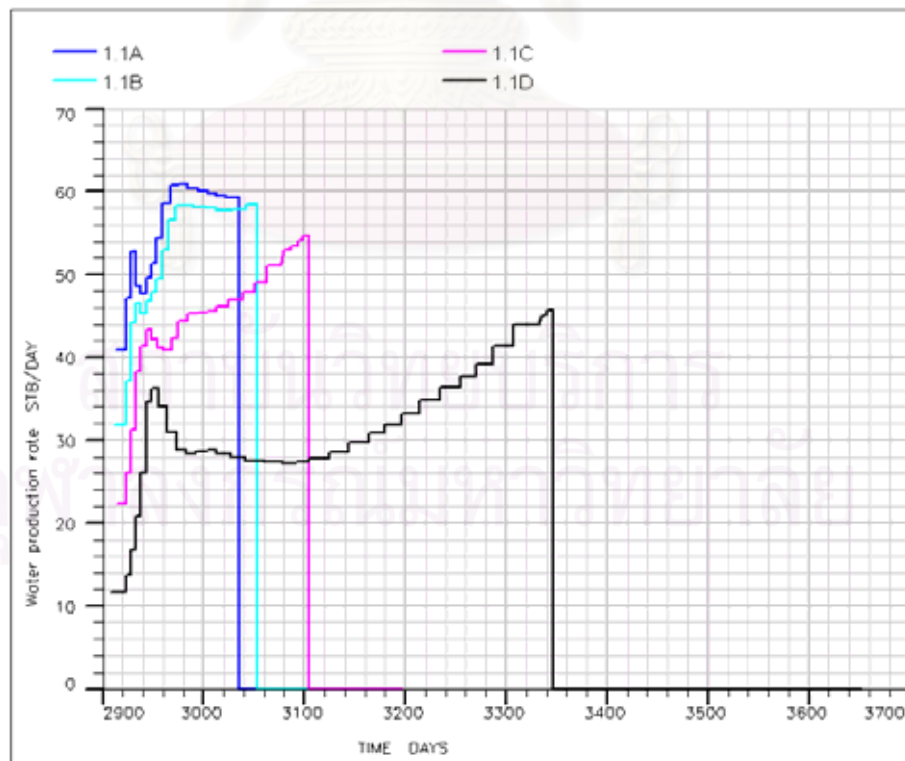
Figure 6.5: Water production rate for the first batch of perforation plan 1.
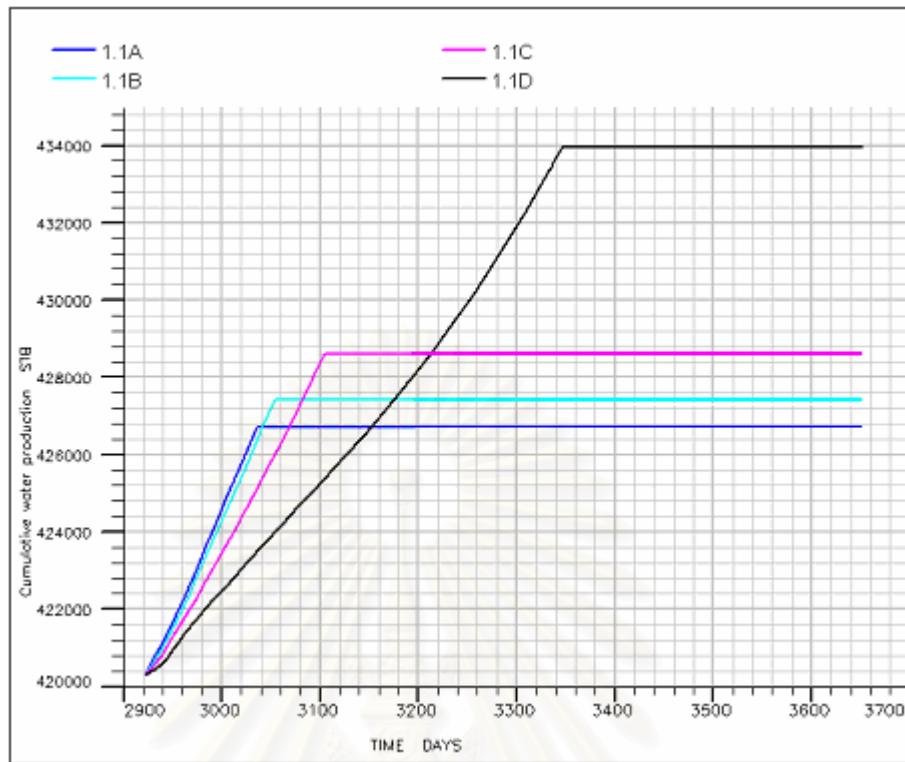
Figure 6.6: Cumulative water production for the first batch of perforation plan 1.
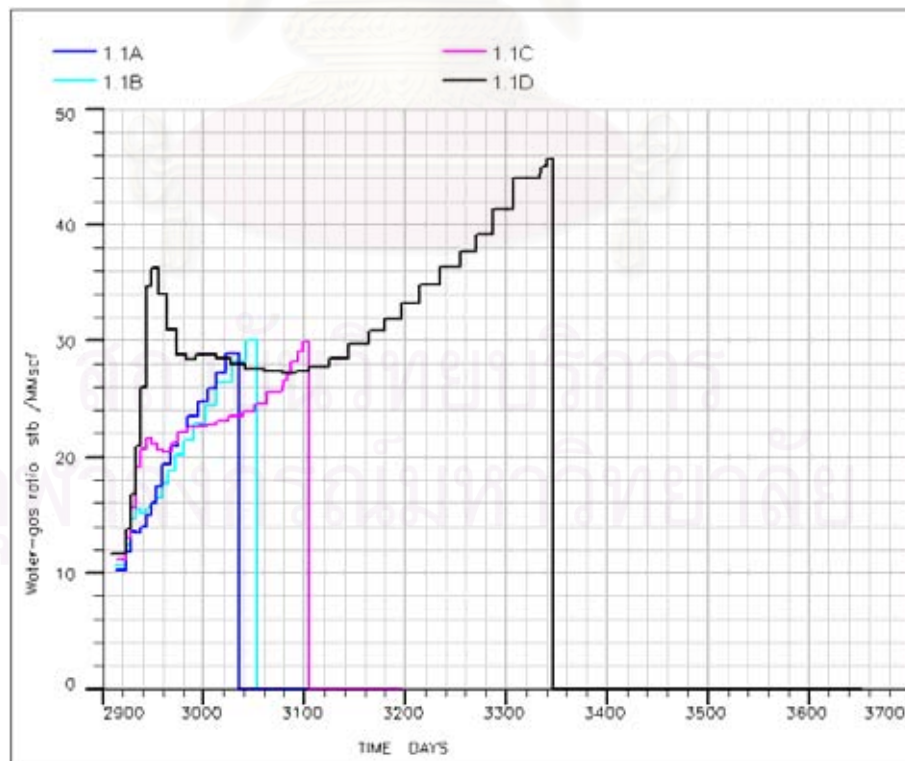
Figure 6.7: Water-gas ratio for the first batch of perforation plan 1.
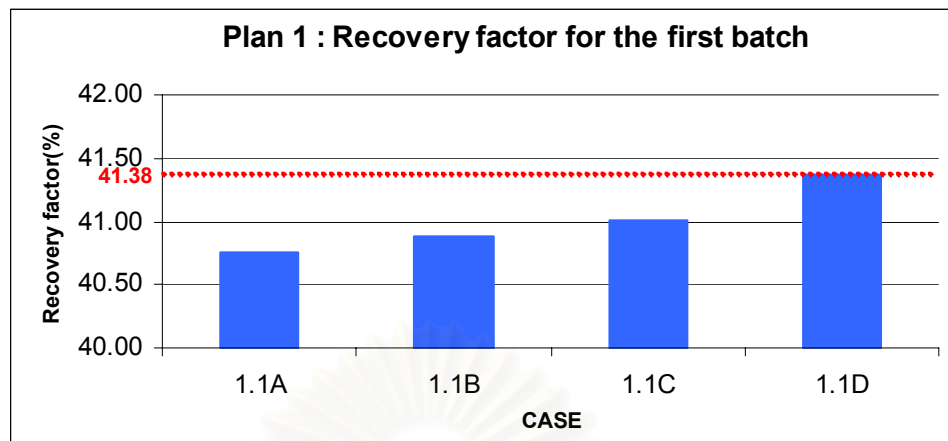
Figure 6.8: Recovery factor for the first batch of perforation plan 1.

In case 1.1A, in which the maximum gas production rate is 4 MMSCFD. Gas is produce with constant rate at 4 MMSCFD for 10 days before the production rate declines. The cumulative gas production from the first batch of well MN-2 is 0.34 BSCF. The gas recovery factor is 40.76%. In this case, the total production period is very short, only 112 days, due to high production rate in the early stage of production which causes the reservoir to be rapidly depleted.

In case 1.1B, in which the maximum gas production rate is 3 MMSCFD. Gas is produced with constant rate at 3 MMSCFD for 58 days before the production rate declines. The cumulative gas production from the first batch of well MN-2 is 0.36 BSCF. The gas recovery factor is 40.88%. In this case, the total production period is 131 days which is slightly longer than that in case 1.1A. Similar to case 1.1A, the high production rate in the early stage of production causes the reservoir to be rapidly depleted.

In case 1.1C, in which the maximum gas production rate is 2 MMSCFD. Gas is produced with constant rate at 2 MMSCFD for 160 days before the production rate declines. The cumulative gas production from the first batch of well MN-2 is 0.39 BSCF. The gas recovery factor is 41.0%. In this case, the total production period is 182 days.

In case 1.1D, in which the maximum gas production rate is 1 MMSCFD. Gas is produced with constant rate at 1 MMSCFD until the reservoirs completely depleted. The cumulative gas production from the first batch of well MN-2 is 0.45 BSCF. The

gas recovery factor is 41.38%. In this case, the total production period is 423 days which is significant higher than the other cases.

As seen in Fig. 6.5 to Fig. 6.7, the water production of all cases is moderate, being less than 62 STBD. The cumulative water production from the first batch of well MN-2 is less than 14,000 STB, and the water-gas ratio is less than 50 STB/MMSCF. Producing with higher gas production rate causes higher water production and the reservoir to be rapidly depleted. So, this perforation batch should be produced with a low production rate.

In summary, case 1.1A gives the lowest recovery factor which is 40.76%. Cases 1.1B and 1.1C give the recovery factor slightly higher than case 1.1A. the recovery factor of these cases are 40.88% and 41.0%, respectively. Case 1.1D gives the highest recovery factor which is 41.38%. Therefore, case 1.1D in which the maximum gas rate is 1 MMSCFD should be chosen as the maximum cumulative gas production scenario.

b) The second perforation batch

Scenario 1: Producing for two years

From the maximization of gas production during the first perforation batch, case 1.1D was selected to be the starting point for the second perforation batch. There are seven cases for this perforation plan which are cases 1.2A, 1.2B, 1.2C, 1.2D, 1.2E, 1.2F, and 1.2G as mentioned in Section 6.1.2. This batch starts production at the day 3,667, and the production period is 2 years. The production performances of the cases are shown in Fig. 6.9 to Fig. 6.11. Note that the cumulative gas production in Fig. 6.10 is the cumulative production from the two batches of perforation and the total recovery factor in Fig. 6.11 is the total recovery factor calculated from gas recovery during the two production periods.
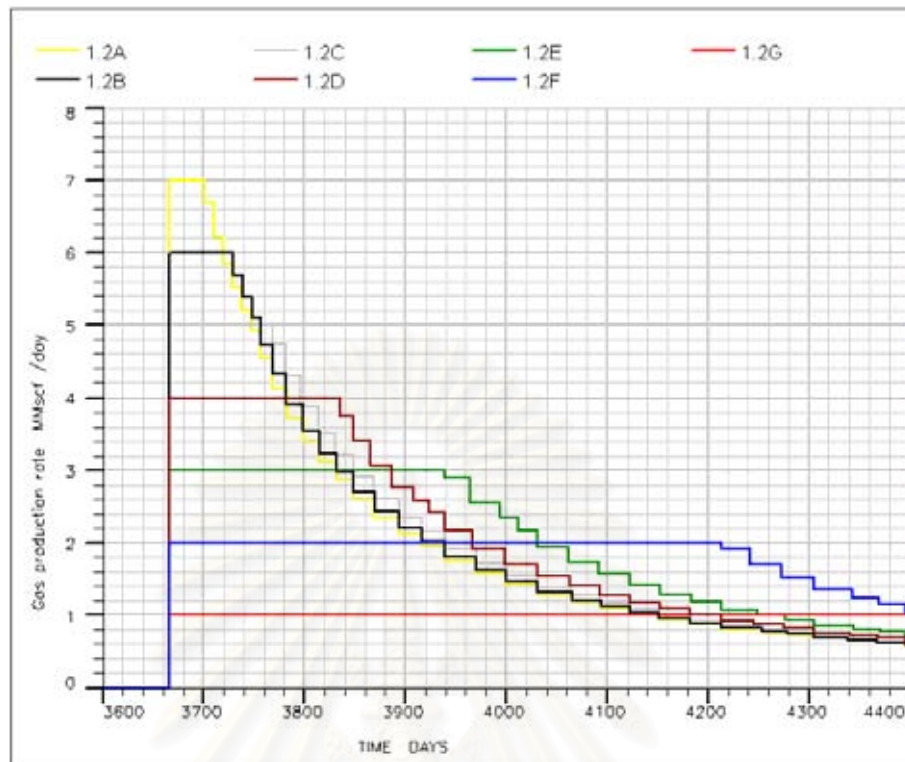
Figure 6.9: Gas production rate after the second batch of perforation plan 1 with
2-year production period.
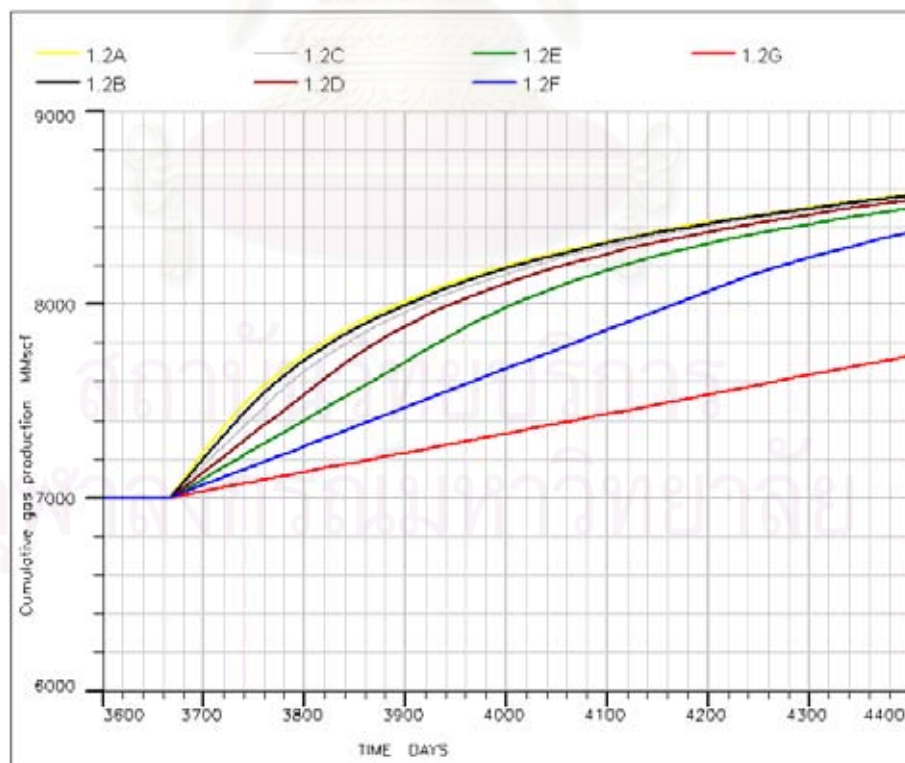
Figure 6.10: Cumulative gas production after the second batch of perforation plan 1
with 2-year production period.
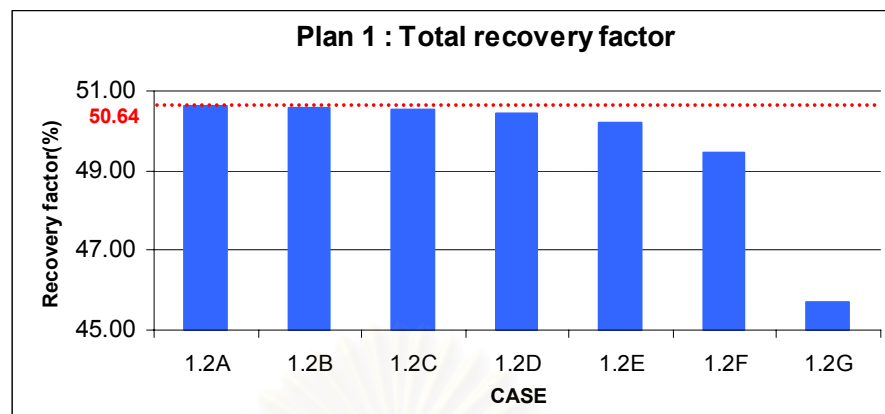
Figure 6.11: Total recovery factor after the second batch of perforation plan 1 with 2-year production period.

Fig. 6.10 shows that case 1.2A gives the highest total cumulative gas production which is 2.02 BSCF for well MN-2 or a total recovery factor of 50.64 %. Case 1.2B gives a total cumulative gas production of 2.01 BSCF (from the first and second batch combined) or a total recovery factor of 50.58%. Case 1.2C gives a total cumulative gas production of 2.00 BSCF or a total recovery factor of 50.55%. Case 1.2D gives a total cumulative gas production of 1.98 BSCF or a total recovery factor of 50.45%. Case 1.2E gives a total cumulative gas production of 1.94 BSCF or a total recovery factor of 50.22%. Case 1.2F gives a total cumulative gas production of 1.81 BSCF or a total recovery factor of 49.45%. Case 1.2G gives significant lower gas production rate than other cases which is a total cumulative gas production of 1.18 BSCF or a total recovery factor of 45.69%. Therefore, case 1.2A in which the maximum gas rate is 7 MMSCFD should be chosen as the maximum cumulative gas production scenario.

Water production rate for all simulation cases of the second perforation batch is less than 2 STBD which is very low comparing with the first perforation batch. Then, this batch can produce with highest production rate, 7 MMSCFD, without the effect from water production.

Scenario 2: Producing until reaching an economic limit of 0.1 MMSCFD

From the maximization of gas production for the second perforation batch, the reservoirs are not depleted within 2 years. To maximize the production without the

time limit, after producing with the simulation cases 1.2A, 1.2B, 1.2C, 1.2D, 1.2E, 1.2F, and 1.2G for 2 years, the well was allowed to flow until the production reaches the economic limit of 0.1 MMSCFD. The production performances of the simulated cases are shown in the Fig. 6.12 to Fig. 6.14. Note that the cumulative gas production in Fig. 6.13 is the cumulative production from the two batches of perforation and the total recovery factor in Fig. 6.14 is the total recovery factor calculation from gas recovery during the two production periods.
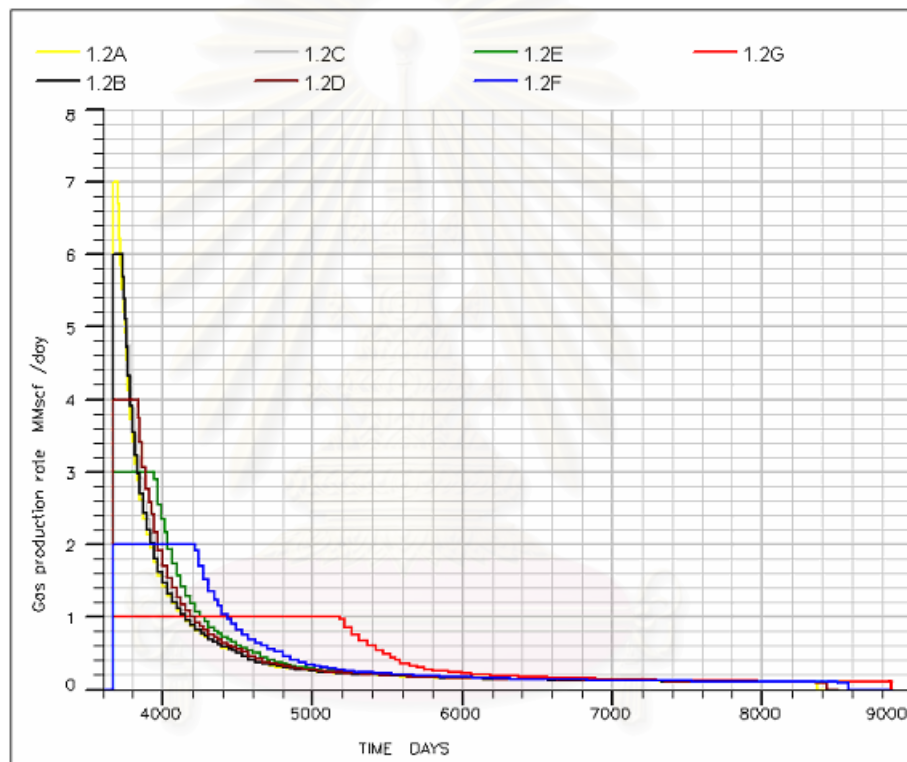
Figure 6.12: Gas production rate after the second batch of perforation plan 1 with an economic limit 0.1 MMSCFD.
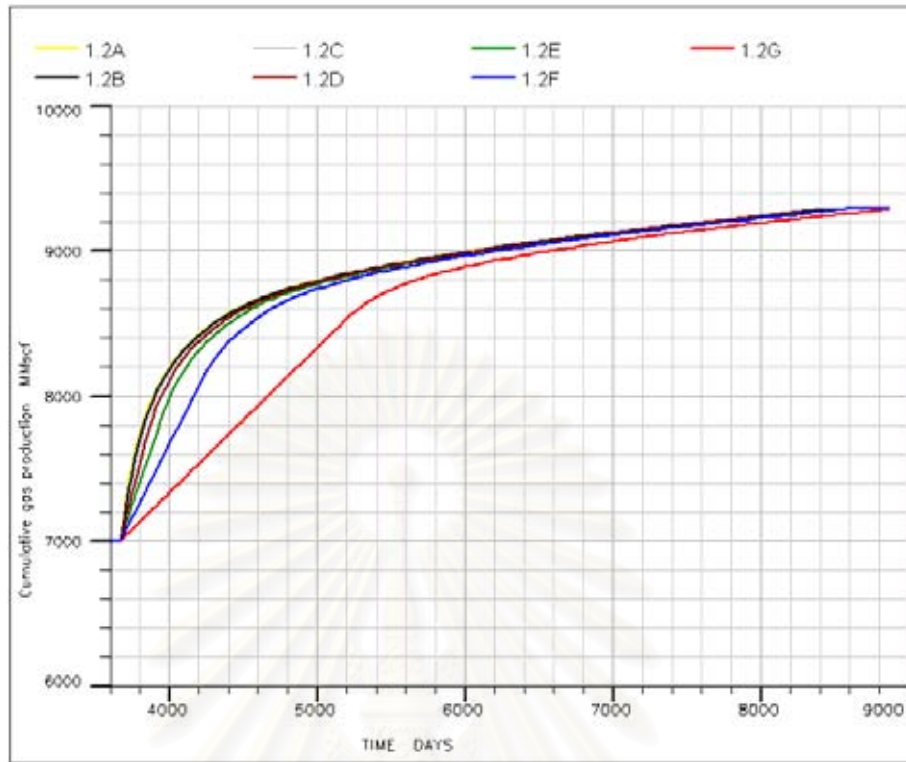
Figure 6.13: Cumulative gas production after the second batch of perforation plan 1 with an economic limit of 0.1 MMSCFD.
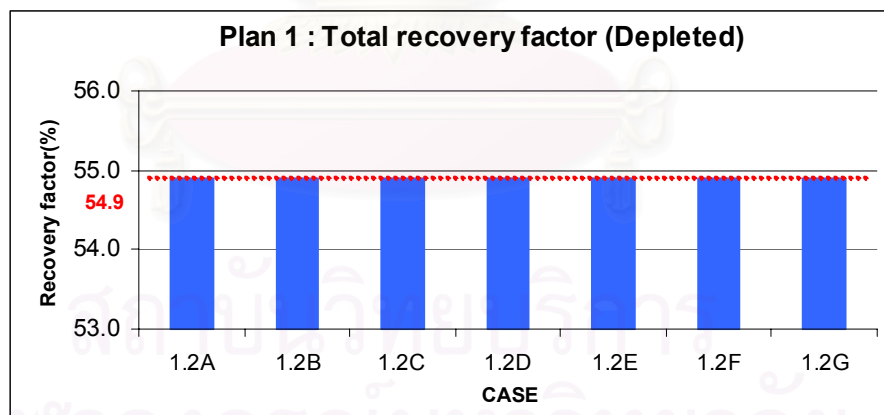
Figure 6.14: Total recovery factor after the second batch of perforation plan 1 with an economic limit of 0.1 MMSCFD.

Fig. 6.12 shows that case 1.2A, 1.2B, 1.2C, 1.2D, and 1.2E depletes at the same producing time of approximately 4,750 days (13 years after the second perforation). Case 1.2F depletes at the production time of 4,924 days (14 years 6 months after the second perforation). Case 1.2G depletes at the production time of

5,215 days (14 years 3 months after the second perforation). As seen in Fig. 6.13 and Fig. 6.14, all simulated cases give a similar value of total cumulative gas production which is 2.73 BSCF (from the first and second batch combined) or a total recovery factor of 54.90 %. Since case 1.2A required less production time, this case in which the maximum gas production rate is 7 MMSCFD should be chosen as the maximum cumulative gas production scenario.

(ii) Plan 2

a) The first perforation batch

There are four cases for this perforation plan which are cases 2.1A, 2.1B, 2.1C, and 2.1D as mentioned in section 6.1.2. The production performances of the simulated cases are shown in Fig. 6.15 to Fig. 6.17.
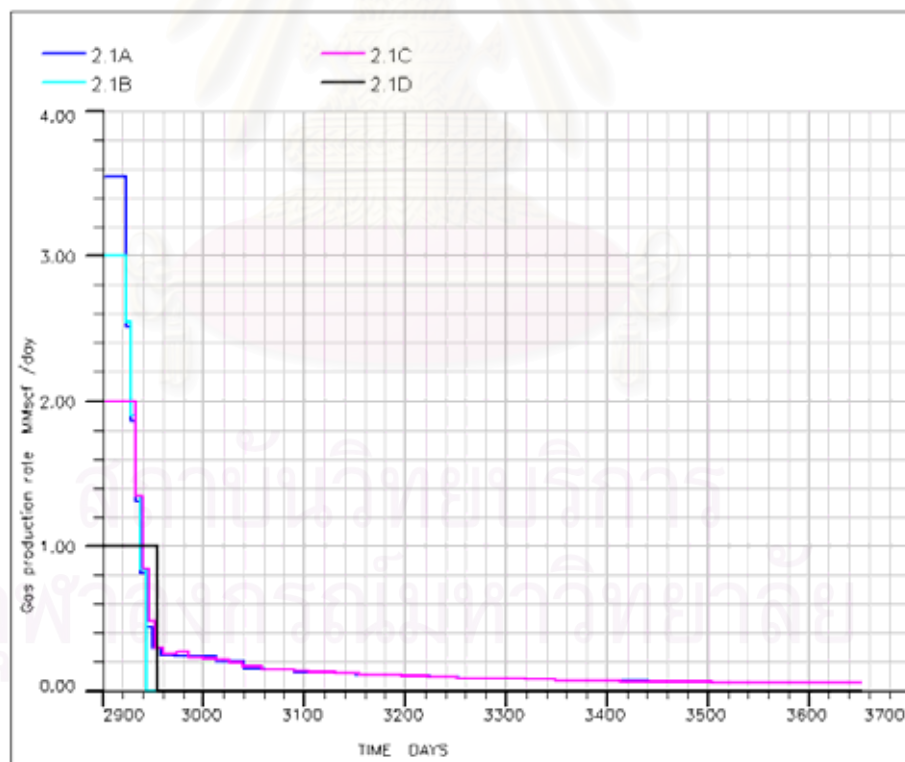
Figure 6.15: Gas production rate for the first batch of perforation plan 2.
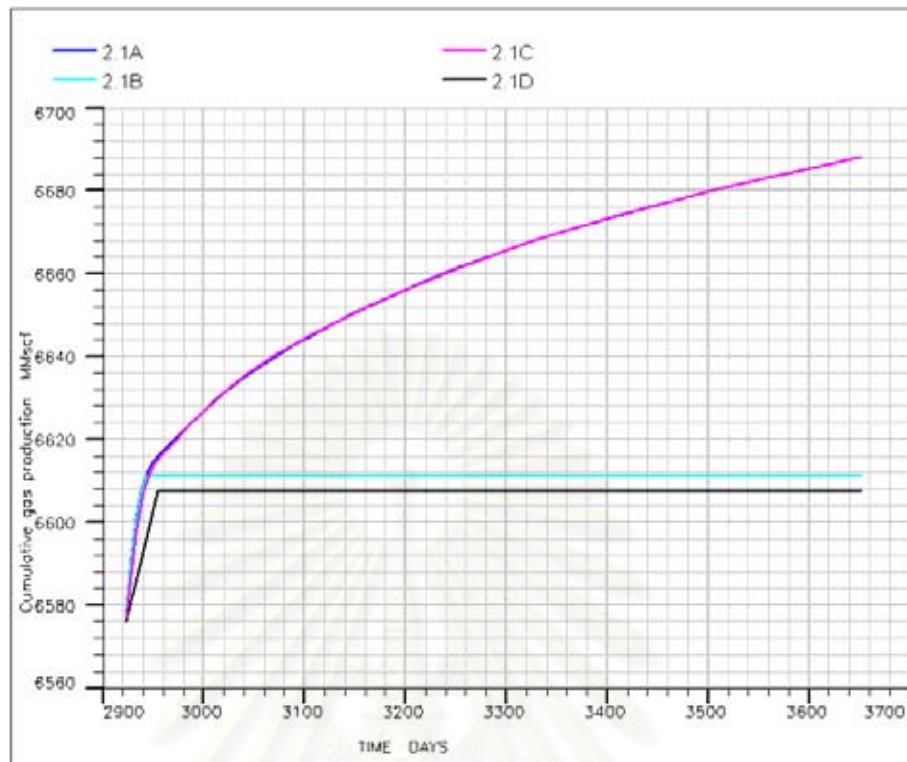
Figure 6.16: Cumulative gas production for the first batch of perforation plan 2.
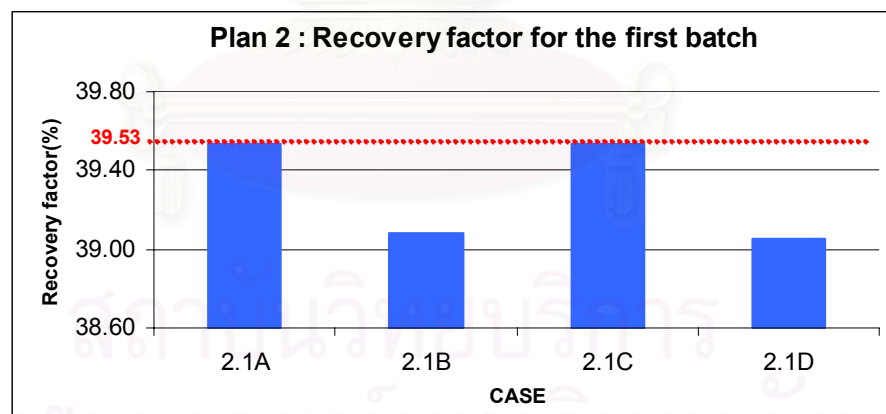
Figure 6.17: Recovery factor for the first batch of perforation plan 2.

Fig. 6.15 shows that the maximum production rate for the second perforation is less than 4 MMSCFD. Case 2.1A gives a maximum gas production rate of 3.55 MMSCFD. Fig. 6.16 shows that cases 2.1A and 2.1C give same gas production. Both cases give the highest total cumulative gas production from the first batch which is 0.14 BSCF or a total recovery factor of 39.53 %. Case 2.1B gives a total cumulative

gas production of 0.06 BSCF or a total recovery factor of 39.8 %. Case 2.1D gives the lowest total cumulative gas production which is 0.56 BSCF or a total recovery factor of 39.6%. Therefore, cases 2.1A and 2.1C in which the maximum gas production rate is 3.55 and 2 MMSCFD, respectively should be chosen as the maximum cumulative gas production scenarios.

The production rate for all simulated cases in this perforation plan rapidly declines because only 4 reservoirs (660, 685, 700, and 710) with a total OGIP of 0.5 BSCF are perforated. The remaining gas in place is only 0.34 BSCF before the production in this stage starts.

b) The second perforation batch with 2 years of production periods

Scenario 1: Producing for two years

From the maximization of gas production for the first perforation batch, case 2.1A was selected to be the starting points for the second perforation batch. There are seven cases for this perforation plan which are cases 2.2A, 2.2B, 2.2C, 2.2D, 2.2E, 2.2F, and 2.2G as mentioned in Section 6.1.2. The production performance of the cases are shown in Fig. 6.18 to Fig. 6.20. Note that the cumulative gas production in Fig. 6.19 is the cumulative production from the two batches of perforation and the total recovery factor in Fig. 6.20 is the total recovery factor calculated from gas recovery during the two production periods.
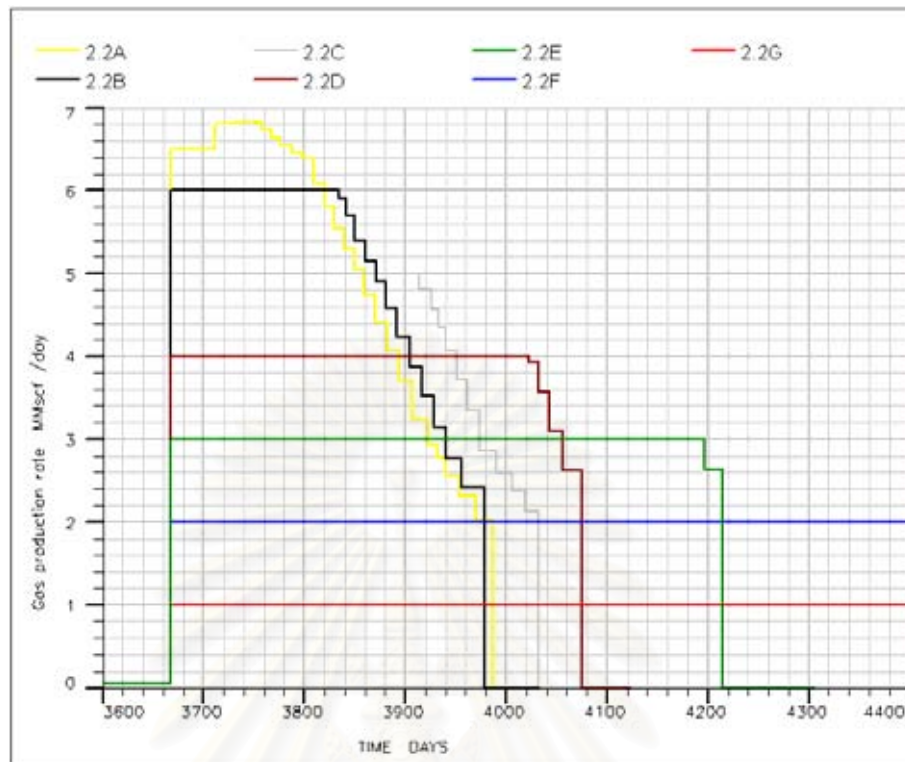
Figure 6.18: Gas production rate after the second batch of perforation plan 2
with 2-year production period.
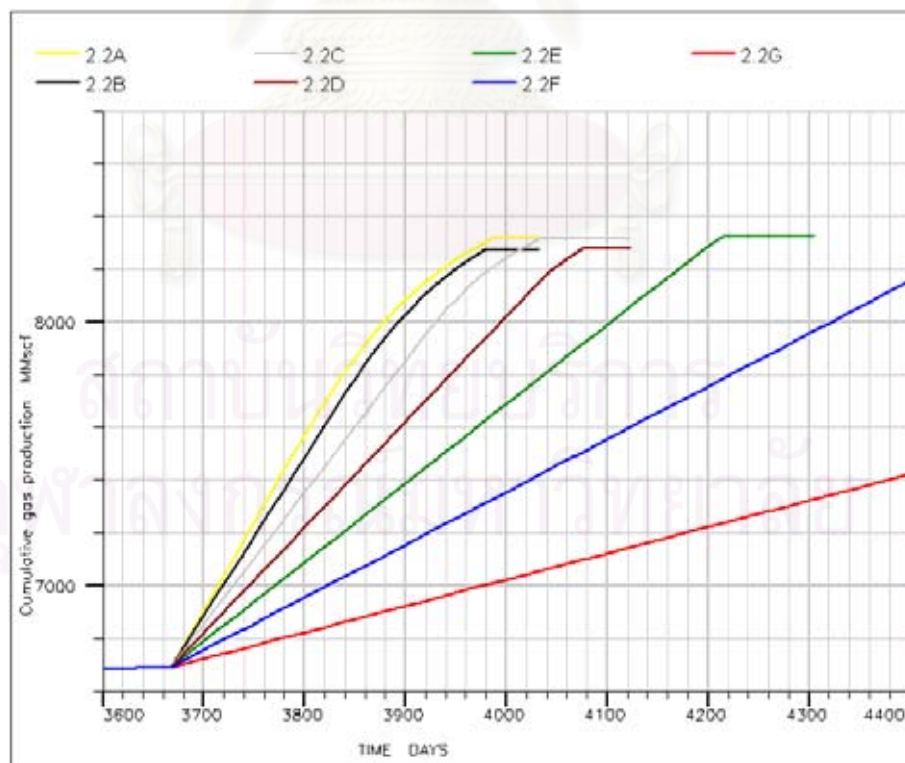
Figure 6.19: Cumulative gas production after the second batch of perforation plan 2
with 2-year production period.
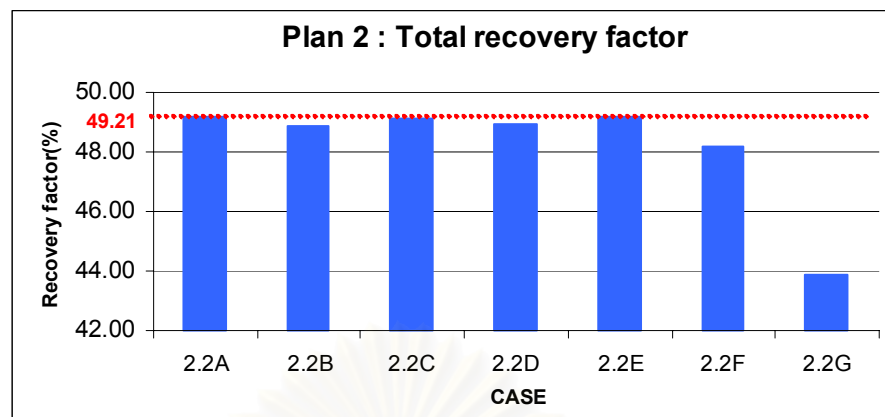
Figure 6.20: Total recovery factor after the second batch of perforation plan 2 with 2-year production period.

Fig. 6.18 shows that all simulated cases depletes within 2 years except cases 2.2F and 2.2G. As seen in Fig. 6.19 and Fig. 6.20, case 2.2E gives the highest total cumulative gas production which is 1.77 BSCF from well MN-2 (from the first and second batch combined) or a recovery factor of 49.20 %. Case 2.2A and 2.2C give the same total cumulative gas production of 1.76 BSCF or a total recovery factor of 49.15%. Cases 2.2B and 2.2D give the same total cumulative gas production of 1.72 BSCF or a total recovery factor of 48.90%. Case 2.2F gives a total gas production of 1.60 BSCF or a total recovery factor of 48.17%. Cases 2.2G gives the lowest total cumulative gas production which is 0.87 BSCF or a total recovery factor of 43.85%. Therefore, case 2.2E in which the maximum gas production rate is 3 MMSCFD should be chosen as the maximum cumulative gas production scenario.

Scenario 2: Producing until reaching an economic limit of 0.1 MMSCFD

From the maximization of gas production for the second perforation batch, all simulated cases depletes within 2 years except cases 2.2F and 2.2G. To maximize the production without the time limit, after producing with the simulation cases 2.2F and 2.2G for 2 years, the well is allowed to flow until the production reaches the economic limit of 0.1 MMSCFD. The production performances of the simulated cases are shown in the Fig. 6.21 to Fig. 6.26. Note that the cumulative gas production in Fig. 6.23 is the cumulative production from the two batches of perforation and the

total recovery factor in Fig. 6.26 is the total recovery factor calculated from gas recovery during the two production periods.
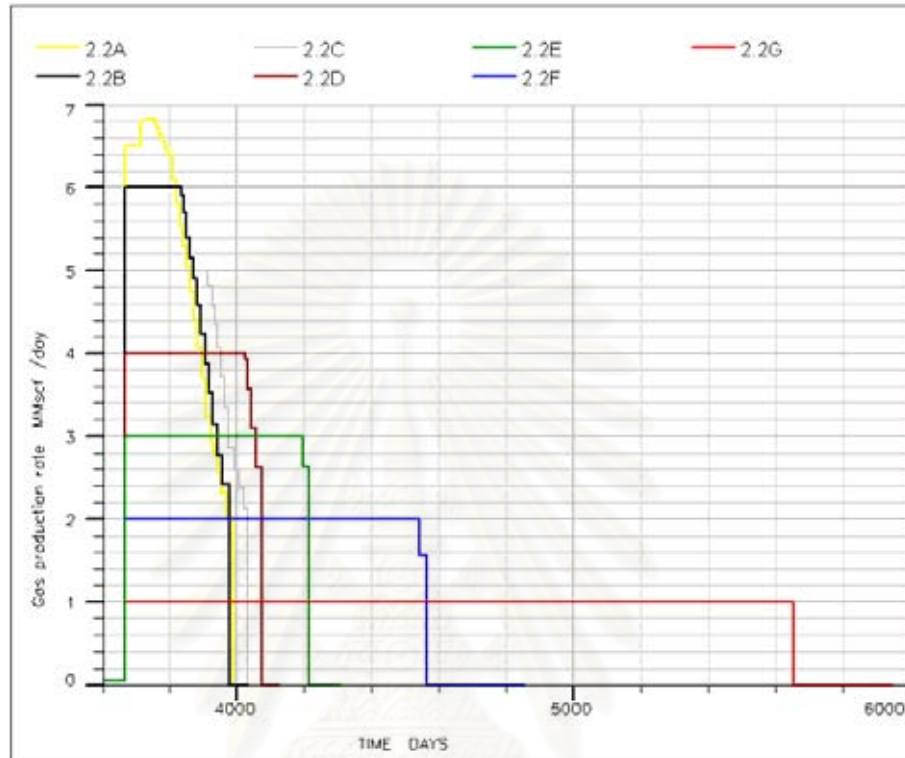
Figure 6.21: Gas production rate after the second batch of perforation plan 2 with an economic limit 0.1 MMSCFD.
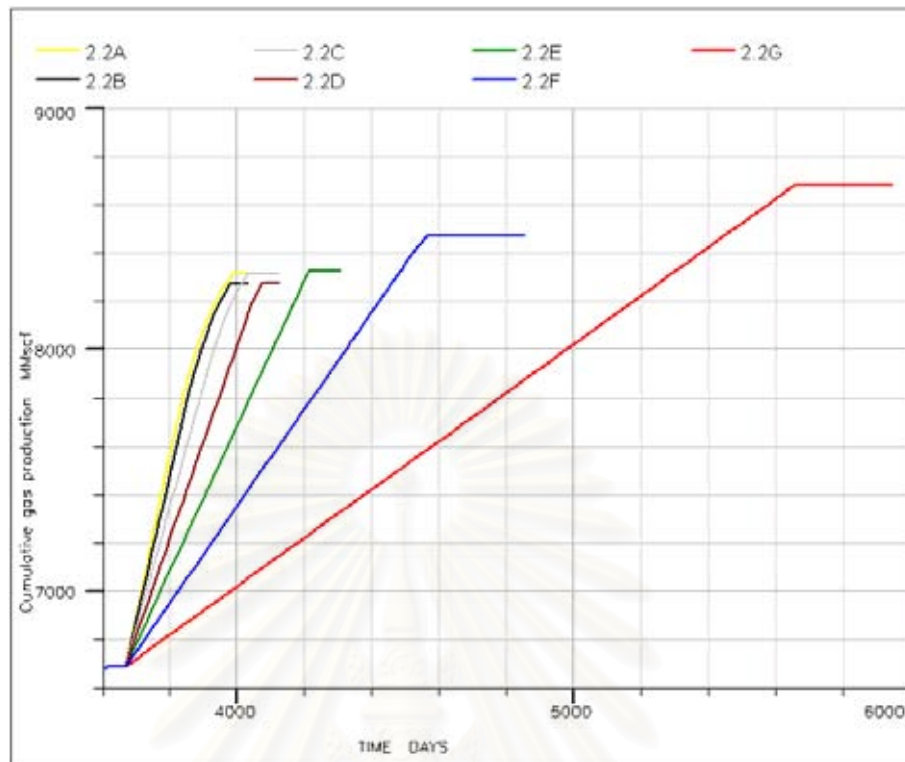
Figure 6.22: Cumulative gas production after the second batch of perforation plan 2 with an economic limit 0.1 MMSCFD.
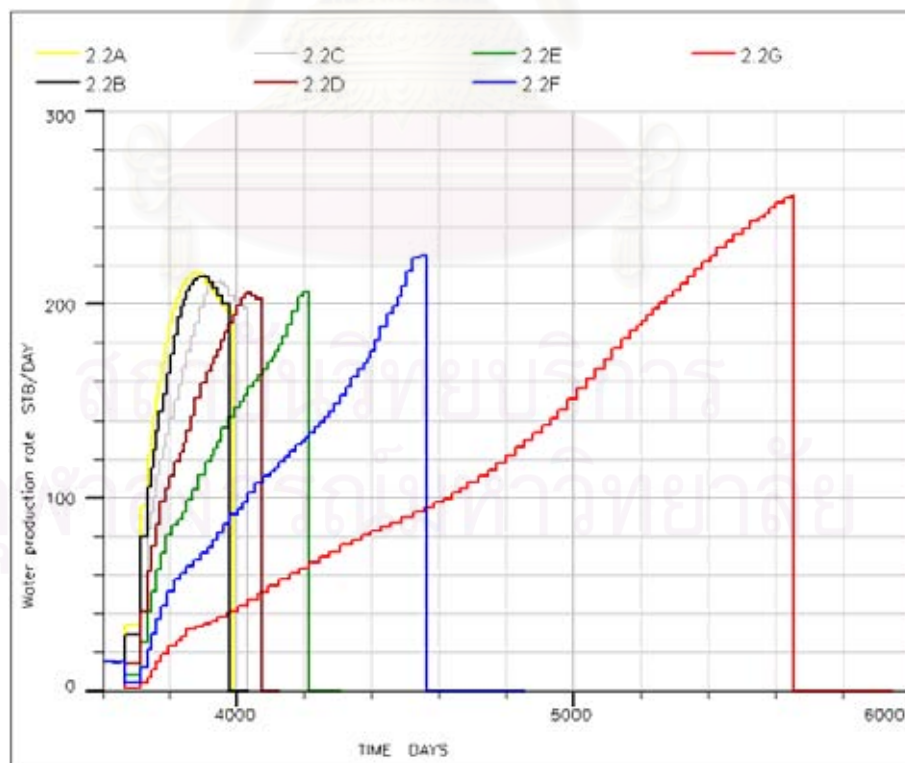
Figure 6.23: Water production rate after the second batch of perforation plan 2 with an economic limit 0.1 MMSCFD.
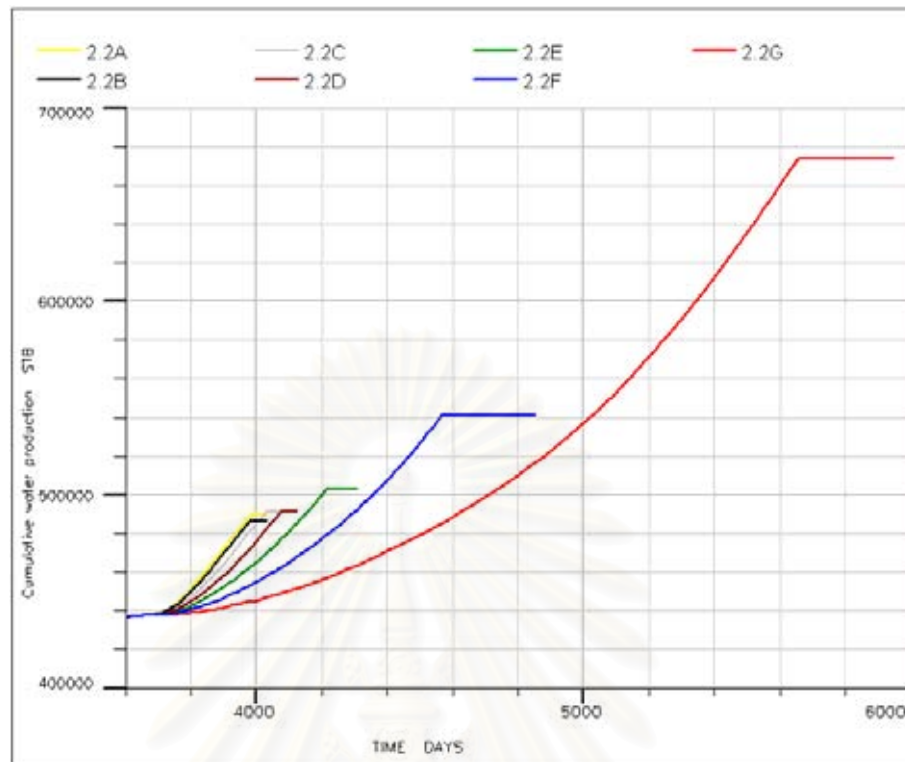
Figure 6.24: Cumulative water production after the second batch of perforation plan 2 with an economic limit 0.1 MMSCFD.
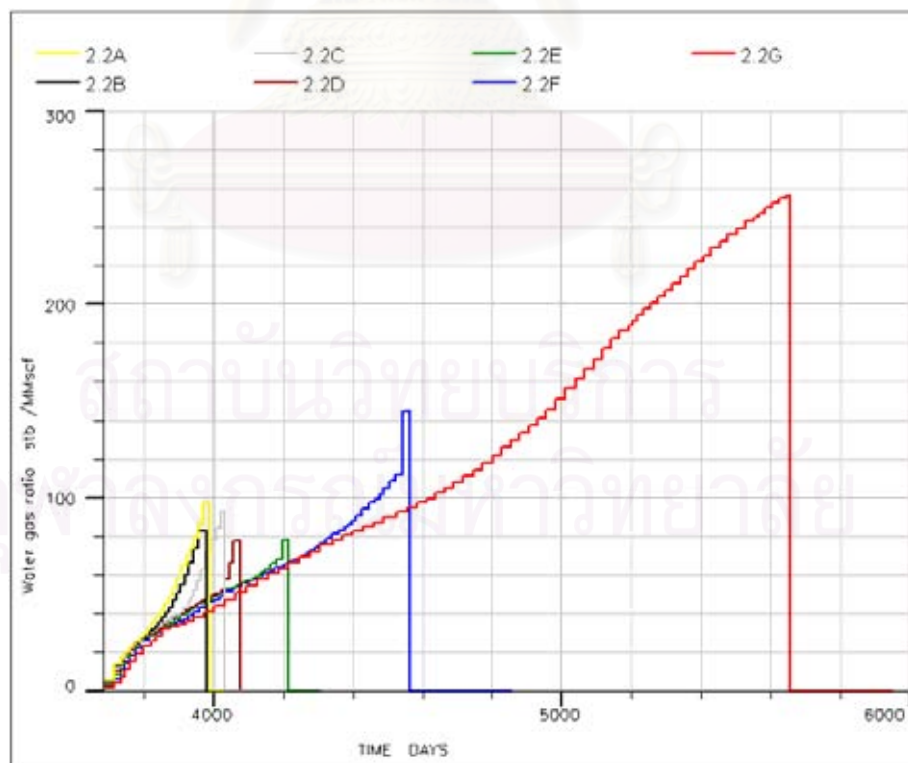
Figure 6.25: Water-gas ratio after the second batch of perforation plan 2 with an economic limit 0.1 MMSCFD.
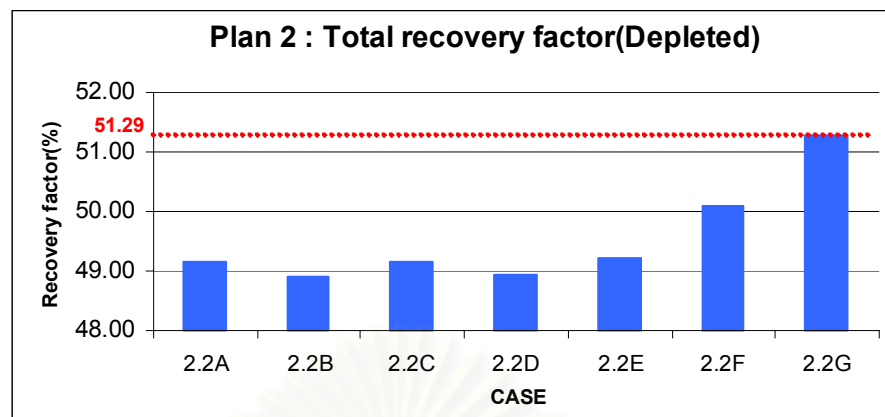
Figure 6.26: Total recovery factor after the second batch of perforation plan 2 with an economic limit 0.1 MMSCFD.

Fig. 6.21 shows that all simulated cases depletes within 2 years except cases 2.2F and 2.2G. Case 2.2F depletes at the production time of 4,564 days (2 years 6 months after the second perforation). Case 2.2G depletes at the production time of 2,003 days (5 years 6 months after the second perforation). As seen in Fig. 6.22 and Fig. 6.26, case 2.2F gives a total cumulative gas production of 1.92 BSCF (from the first and second batch combined) or a total recovery factor of 50.08%. Case 2.2G gives a total cumulative gas production of 2.13 BSCF or a total recovery factor of 51.29%. Therefore, case 2.2G in which the maximum gas production rate is 1 MMSCFD should be chosen as the maximum cumulative gas production scenario.

As seen in Fig. 6.23 to Fig. 6.25, the water production of all cases for the second perforation of plan 2 is high, being higher than 200 STBD. The cumulative water production is higher than 48,000 STB, and the water-gas ratio is higher than 70 STB/MMSCF. This high water production rate causes the reservoir to be rapidly depleted. The main contribution of water production in this second perforation is reservoir 535 which is not perforated in plan 1.

6.1.4 Production maximization summary

Table 6.2 shows the summary of production maximization scenarios. The best perforation plan is plan 1. The best production scenario is scenario 1.1D followed by scenario 1.2A for both two-year production period and without time limit. In case of

producing until the production reaches the economic of 0.1 MMSCFD, this scenario gives a total cumulative gas production of 2.73 BSCF or total recovery factor of 54.90 %. If the production period is fixed at 2 years per batch, this scenario gives a total gas production of 2.02 BSCF or total recovery factor of 50.64 %.

Table 6.2: Summary of production maximization scenarios.

Production period		Perforation plan	WHFP profile		Total recovery factor	Total cumulative gas production
1st batch	2 nd batch		1st batch	2 nd batch	(%)	(BSCF)
2 years	2 years	1	Case 1.1D	Case 1.2A	50.64	2.02
2 years	Until economic limit of 0.1 MMSCFD (Producing period :13 years)	1	Case 1.1D	Case 1.2A	54.90	2.73
2 years	2 years	2	Case 2.1A	Case 2.2E	49.2	1.77
2 years	Until economic limit of 0.1 MMSCFD (Producing period :5 years 6 month)	2	Case 2.1A	Case 2.2G	51.29	2.13

6.2 Optimization of Hg-contaminated Slurry Injection

After getting hydrocarbon production optimal scenario, reservoir simulation was performed to optimize mercury contaminated waste injection. The influences of design variables which are perforation plan, sludge concentration, Hg-contaminated slurry viscosity, and injection rate are studied. Then, the optimal scenario of injection is determined.

The mercury contaminated sludge consists of mercury, solid particles, condensate, and water. To dispose it, the sludge is ground into fine particles and mixed with seawater and viscosifier to form a slurry. Sludge concentration is the main factor that controls density and viscosity of the mixture. Density can be obtained from simple calculation. Viscosity is controlled by viscosifier, which should be added to the slurry until the particles are suspended. The particles should not segregate from the fluid before it flows to storage at the target location. The appropriate slurry viscosity, which can suspend the particles, can be obtained from laboratory test only and not available now. In this study, it is assumed that the suspended particles are fine enough to pass through formation without plugging or causing formation damage. The critical parameters that affect injection performance and were selected for sensitivity

simulation study are slurry density, injection rate, and slurry viscosity. For a specific sludge quantity, the optimal case is the case that requires a minimum injection time.

The injection optimization was performed based on the following conditions:

- Injection pressure is low enough to avoid any formation fracturing.
- Maximum Hg-sludge disposal quantity is 6000 ton. As mentioned in Chapter 1, the target disposal quantity is 600 ton. This quantity is too low to observe the effect of designed variables after performing sensitivity analysis. So, the maximum injection quantity is increased to 6,000 ton which is high enough for sensitivity study and can be used as a guideline in case of quantity of mercury contaminated waste required to be disposed increases.

The injection pressure should not be high enough to cause any fracture in the reservoirs. The formation fracturing pressure can be calculated using an available correlation for the M field as follows:

$$Fracturing\ pressure(bar) = \frac{FRAC.S.G. \times TVD}{10.2}$$

while

$$FRAC.S.G. = 1.22 + \left(TVD \times 1.6 \times 10^{-4}\right)$$

where $FRAC.S.G.$ = fracturing pressure gradient (bars/meter)

TVD = true vertical depth below rotary table (meters)

Using the above equation, the fracturing pressure for each reservoir can be computed as shown in Table 6.3 and Fig. 6.27

Table 6.3: Reservoir fracturing pressure.

Reservoir	Fracture pressure (psia)
405	3008
440	3088
475	3176
480	3188
485	3205
515	3278
535	3298
560	3324
570	3403
585	3465
620	4607
660	3558
685	3646
710	3764
720	3813
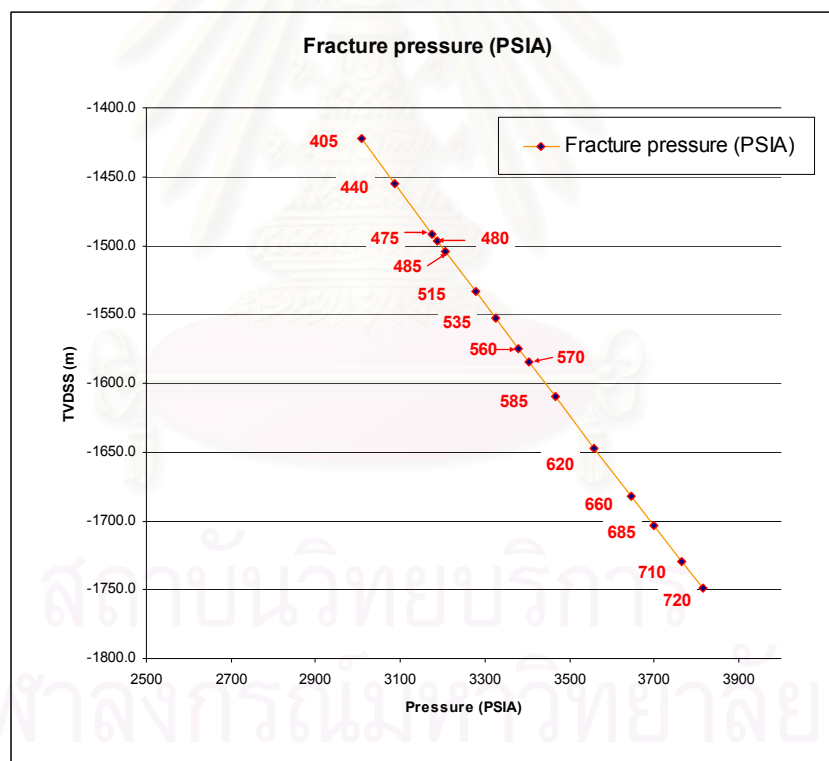
Figure 6.27: Fracture pressure gradient.

The sludge concentrations used in the simulation study are 20%, 30% and 40% by volume. The injection rates are 3, 4 and 5 STB/MIN. The slurry viscosity is a complex parameter that the actual value can be obtained by measuring the actual sample. The viscosity of slurry from previous works of Unocal Thailand, Ltd. [4]

which disposed Hg-waste originated from an area close to the M field is in the range between 40 and 70 cp. These viscosity values were used in this study.

By varying slurry density (sludge concentration), injection rate, and viscosity, the simulation can be organized into 18 cases as tabulated in Table 6.4.

Table 6.4: Injection simulation cases with varying sludge concentration, injection rate, and slurry viscosity.

Case	Sludge concentration (% by volume)	Injection rate (stb/min)	Slurry viscosity (cp)
A1	30	3	40
A2	30	3	70
A3	30	4	40
A4	30	4	70
A5	30	5	40
A6	30	5	70
A7	20	3	40
A8	20	3	70
A9	20	4	40
A10	20	4	70
A11	20	5	40
A12	20	5	70
A13	40	3	40
A14	40	3	70
A15	40	4	40
A16	40	4	70
A17	40	5	40
A18	40	5	70

From the optimization of gas production, the optimization scenario 1.1D followed by scenario 1.2A was selected to be the starting points for two batches of slurry injection. Recall that case 1.1D has a maximum gas production rate of 1 MMSCFD. Case 1.2A has a maximum gas production rate of 7 MMSCFD. The production period for case 1.1D is 2 years. Case 1.2A has two scenarios which are 2-years production period and producing until reservoir is completely depleted with an economic limit of 0.1 MMSCFD.

Since there are two batches of production and two injection periods (one after each batch of production), the injection schedule was designed as follows:

- Schedule 1: After the first batch of production (after finishing the production in the first phase)

- Schedule 2: After the second batch of production. Since there are two production periods in the second batch of production, the injection schedule was divided into two cases as follows:
  - o Schedule 2A: After the second batch of production which lasts 2 years.
  - o Schedule 2B: After the first batch of production which produces until the economic limit of 0.1 MMSCFD.

The 18 cases as listed in Table 6.4 were simulated for each schedule. A total of 54 cases were simulated in this study.

To optimize the slurry injection, the following steps were followed:

1) Run reservoir simulation using the following conditions:
   - Sludge concentration of 20% by volume (injection volume of 69,764 STB for 6000 ton of sludge)
   - Sludge concentration of 30% by volume (injection volume of 46,510 STB for 6000 ton of sludge)
   - Sludge concentration of 40% by volume (injection volume of 34,880 STB for 6000 ton of sludge)

2) Observe the evolution of sandface pressures of perforated reservoirs and determine the maximum injection volume before fracture occurs.

3) For a specific quantity of sludge to be disposed of, select the best case by considering two criteria: no formation fracture and minimum injection time.

6.2.1 The optimal case selection concept

This section presents a procedure to select the optimal case. Schedule 1 is selected as an example. The injection capabilities of different cases are compared. The optimal case is the case that has the least injection time without causing formation fracture.

a) Schedule 1: Injection after the first batch of production

All simulated cases start with an injection of Hg-contaminated slurry on June 1, 2004. Case A1 is used as an example. In this case, we used sludge concentration of 30%, injection rate of 3 STB/MIN, and slurry viscosity of 40 cp. The slurry volume that is

required to be disposed in this case is 46,510 STB (6000 tons of sludge). The sandface pressure evolution of perforated reservoirs with increasing injection volume is shown in Fig. 6.28. The injection pressures at reservoirs 560, 570, and 585 start to exceed the fracturing pressure after 242 hours of slurry injection. The maximum injection volume for this case before formation fracturing is 43,560 STB (5,619 ton of sludge). This volume is less than the required volume of 46,510 STB. Therefore, this case is not practical if we need to dispose 6,000 ton of sludge. The injection period of 242 hours is computed from injection volume divided by injection rate as follows:

$$\frac{43,560\,STB}{3\,STB/MIN} \times \frac{1\,HOUR}{60\,MIN} = 242\,HOURS$$
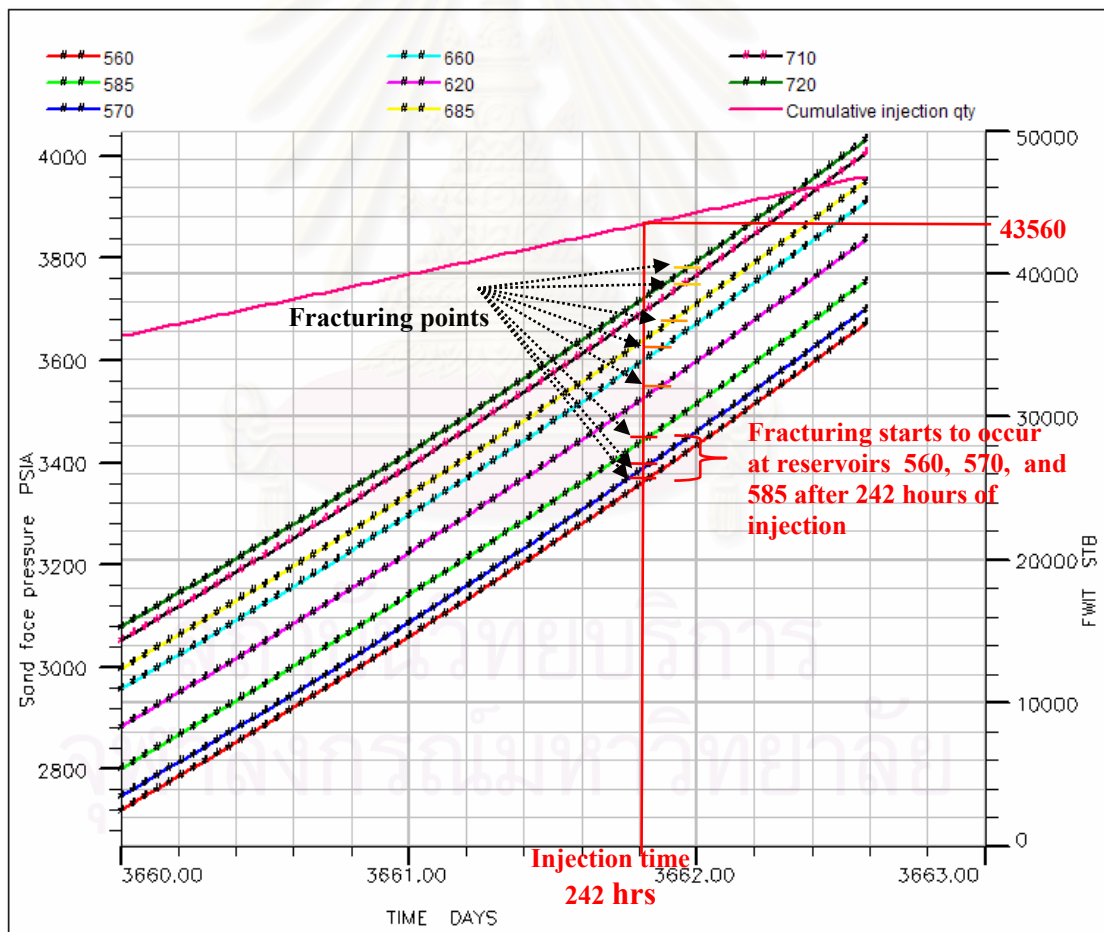
Figure 6.28: Sandface pressure evolution of case A1 during the first batch of injection.

After running simulation for all the 18 cases, we see that the evolution of sandface pressure in all the cases behave in the same manner. Furthermore, the first reservoir having pressure exceeding the fracturing pressure in all the 18 cases is the same. Fig. 6.29 compares the maximum amount of waste that can be injected in each simulated case. The results show that cases A13 and A14 have the highest injection capability, which is 6,000 ton of sludge (34,880 STB of slurry with sludge concentration 40 % by volume). Cases A11 and A12 have the minimum injection capability which is 1,486 ton of sludge (17,280 STB of slurry with sludge concentration 20 % by volume).
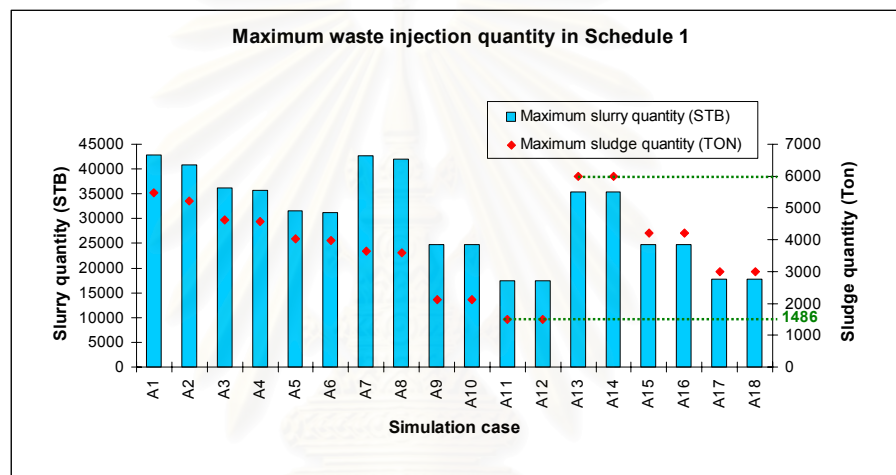
Figure 6.29: Comparison of maximum waste injection quantity for schedule 1.

For a specific quantity of sludge, all possible cases are selected and compared for the shortest injection time. The best case is the case that requires the minimum injection time. The optimal case is determined for each slurry viscosity. The actual slurry viscosity will be known at the time of injection. So, the proposed cases will be used as alternatives. A sludge quantity of 3,000 ton is selected as an example to demonstrate how the optimal case is obtained. There are 14 possible cases to dispose 3,000 ton of sludge without creating any fracture as shown in Table 6.5. The best case, requiring the minimum injection time, is A17 if the slurry viscosity is 40 cp and A18 when the slurry viscosity is 70 cp. To dispose 3,000 ton of sludge, both cases require 59 hours which is the minimum among the 14 possible cases. The most appropriate injection rate for both cases is 5 STB/MIN.

Table 6.5: Possible injection scenarios for disposing 3,000 ton of sludge.

Case	Sludge concentration (% volume)	Injection rate (STB/MIN)	Viscosity (cp)	Maximum disposal capability (TON)	Slurry volume for 3,000 ton of sludge (STB)	Disposal time for 3,000 ton of sludge (HOURS)
A1	30	3	40	5470	23255	129
A2	30	3	70	5217	23255	129
A3	30	4	40	4627	23255	97
A4	30	4	70	4566	23255	97
A5	30	5	40	4022	23255	78
A6	30	5	70	3984	23255	78
A7	20	3	40	3642	34882	194
A8	20	3	70	3581	34882	194
A13	40	3	40	6000	17440	97
A14	40	3	70	6000	17440	97
A15	40	4	40	4202	17440	73
A16	40	4	70	4202	17440	73
A17	**40**	**5**	**40**	**3009**	**17440**	**58**
A18	**40**	**5**	**70**	**3009**	**17440**	**58**

Table 6.6 shows the optimization injection scenario for varied quantity of sludge. For example, in a case that the required injection volume is less than 3,200 ton, the optimal case is A17 if the slurry viscosity is 40 cp and A18 when the slurry viscosity is 70 cp. Therefore, the sludge should be mixed such that the slurry concentration is 40% by volume. And, the injection rate should be 5 STB/MIN.

The most suitable sludge concentration is 40% by volume for all sludge quantities except for sludge quantity between 4,400 and 4,800 ton. For sludge quantity between 4,400 and 4,600 ton, the optimal sludge concentration is 30% by volume. For injection volume between 4,600 and 4,800 ton, the optimal concentrate is 40% by volume if the slurry viscosity is 70 cp and 30% by volume when the slurry viscosity is 40 cp. For quantity of sludge less than 3,200 ton, the optimal injection rate is 5 STB/MIN. When the sludge quantity increases, the suitable injection rate decreases. The injection time increases when the sludge quantity required to be disposed increases.

Table 6.6 : Optimized injection case of various sludge quantities in schedule 1.

Sludge quantity (TON)	Viscosity (cp)	Optimized case	Sludge concentration (% volume)	Injection rate (STB/MIN)	Injection time (HOURS)
600	40	A17	40	5	12
	70	A18	40	5	12
800	40	A17	40	5	16
	70	A18	40	5	16
1000	40	A17	40	5	20
	70	A18	40	5	20
1200	40	A17	40	5	24
	70	A18	40	5	24
1400	40	A17	40	5	28
	70	A18	40	5	28
1600	40	A17	40	5	31
	70	A18	40	5	31
1800	40	A17	40	5	35
	70	A18	40	5	35
2000	40	A17	40	5	39
	70	A18	40	5	39
2200	40	A17	40	5	43
	70	A18	40	5	43
2400	40	A17	40	5	47
	70	A18	40	5	47
2600	40	A17	40	5	51
	70	A18	40	5	51
2800	40	A17	40	5	55
	70	A18	40	5	55
3000	40	A17	40	5	59
	70	A18	40	5	59
3200	40	A15	40	4	79
	70	A16	40	4	79
3400	40	A15	40	4	83
	70	A16	40	4	83
3600	40	A15	40	4	88
	70	A16	40	4	88
3800	40	A15	40	4	93
	70	A16	40	4	93
4000	40	A15	40	4	98
	70	A16	40	4	98
4200	40	A15	40	4	103
	70	A16	40	4	103
4400	40	A3	30	4	144
	70	A4	30	4	144
4600	40	A3	30	4	150
	70	A14	40	3	150
4800	40	A13	40	3	157
	70	A14	40	3	157
5000	40	A13	40	3	164
	70	A14	40	3	164
5200	40	A13	40	3	170
	70	A14	40	3	170
5400	40	A13	40	3	177
	70	A14	40	3	177
5600	40	A13	40	3	183
	70	A14	40	3	183
5800	40	A13	40	3	190
	70	A14	40	3	190
6000	40	A13	40	3	196
	70	A14	40	3	196

b) Schedule 2A: Injection after the second batch of two-year production.

As mentioned earlier, the slurry volume in case A1 is 46,510 STB (6000 tons of sludge). The sandface pressure evolution of perforated reservoirs with increasing injection volume is shown in Fig. 6.30. The injection pressures at reservoirs 405 and 440 start to exceed the fracturing pressure after 127 hours of slurry injection. The maximum injection volume for this case before formation fracturing is 22,860 STB (2,949 ton of sludge).
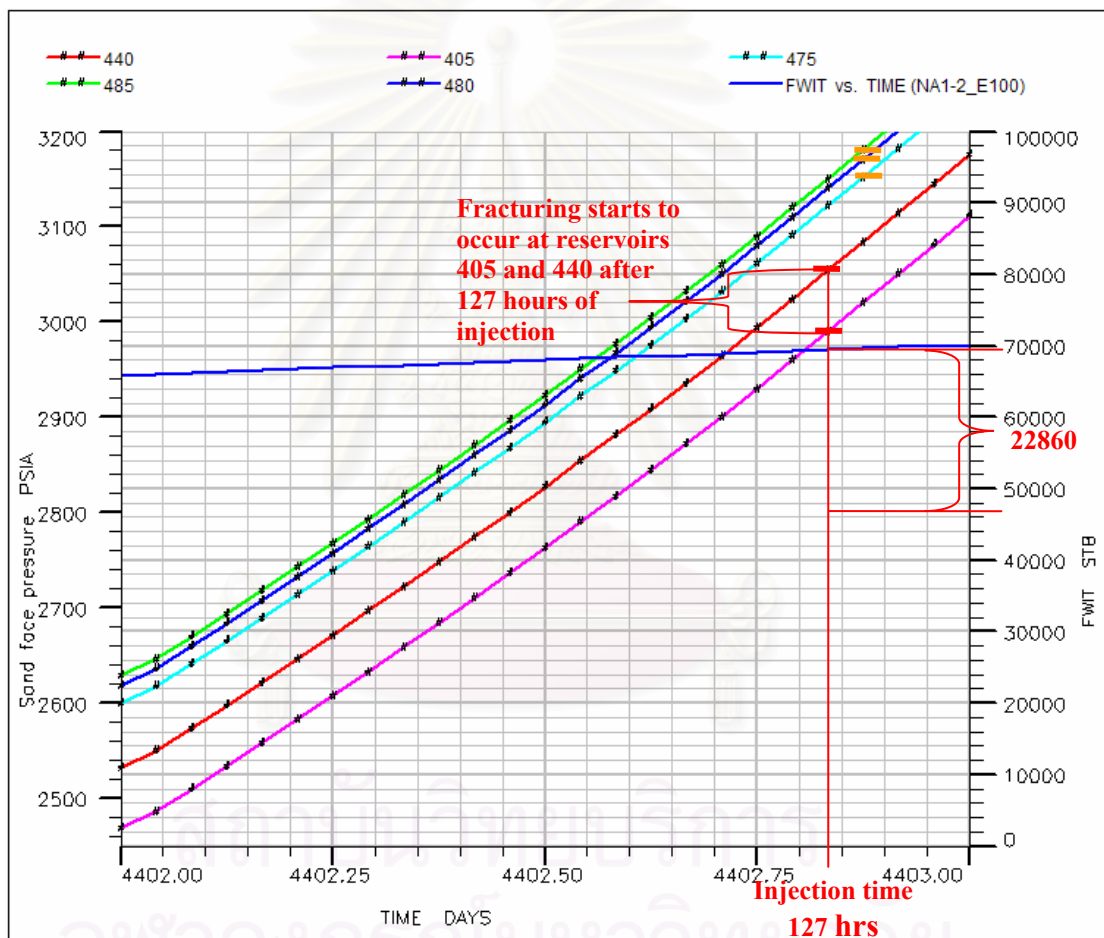
Figure 6.30: Sandface pressure evolution of simulation case A1 for injection schedule 2A.

After running simulation for all the 18 cases, we see that the evolution of sandface pressure in all the cases behave in a similar manner. Furthermore, the first reservoir having the pressure exceeding the fracturing pressure in all the 18 cases is the same. Fig. 6.31 compares the maximum amount of waste that can be injected in

each simulated case. The results show that cases A13 and A14 have the highest injection capability which is 3,121 ton of sludge (18,144 STB of slurry with sludge concentration 40 % by volume). Cases A9 and A10 have the minimum injection capability which is only 1,209 ton of sludge (14,060 STB of slurry with sludge concentration 20 % by volume).
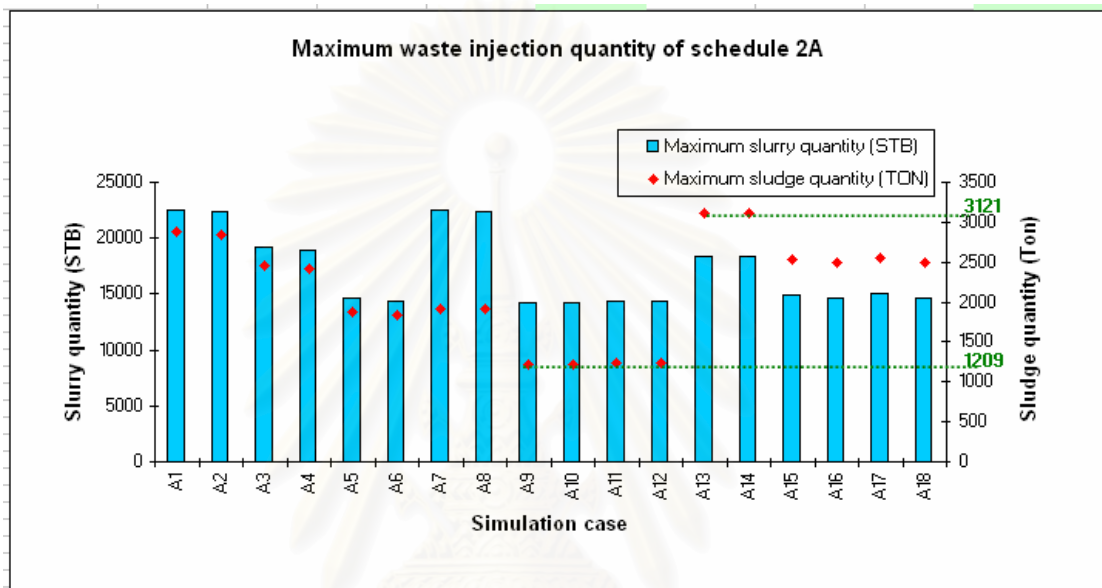
Figure 6.31: The comparison of maximum waste injection quantity for Schedule 2A.

Using the same procedure as described in schedule 1, the best injection scenarios for varied quantity of sludge were obtained and summarized in Table 6.7. The most suitable sludge concentration is 40% by volume for all sludge quantities. For quantity of sludge less than 2,600 ton, the optimal injection rate is 5 STB/MIN. When the sludge quantity increases, the suitable injection rate reduces to 3 STB/MIN. The injection time increases when the sludge quantity required to be disposed increases.

Table 6.7: Optimized injection case of varied sludge quantities in schedule 2A.

Sludge quantity (TON)	Viscosity (cp)	Optimized case	Sludge concentration (% volume)	Injection rate (STB/MIN)	Injection time (HOURS)
600	40	A17	40	5	11.8
	70	A18	40	5	11.8
800	40	A17	40	5	15.7
	70	A18	40	5	15.7
1000	40	A17	40	5	19.6
	70	A18	40	5	19.6
1200	40	A17	40	5	23.5
	70	A18	40	5	23.5
1400	40	A17	40	5	27.5
	70	A18	40	5	27.5
1600	40	A17	40	5	31.4
	70	A18	40	5	31.4
1800	40	A17	40	5	35.3
	70	A18	40	5	35.3
2000	40	A17	40	5	39.2
	70	A18	40	5	39.2
2200	40	A17	40	5	43.2
	70	A18	40	5	43.2
2400	40	A17	40	5	47.1
	70	A18	40	5	47.1
2600	40	A13	40	3	85.0
	70	A14	40	3	85.0
2800	40	A13	40	3	91.5
	70	A14	40	3	91.5
3000	40	A13	40	3	98.1
	70	A14	40	3	98.1

c) Schedule 2B: Injection after the second batch of production which is terminated at an economic limit of 0.1 MMSCFD.

For simulation case A1, after injecting 46,510 STB of slurry, the sandface pressure evolution of perforated reservoirs with increasing injection volume is shown in Fig. 6.32. The injection pressures at reservoir 405 and 440 start to exceed the fracturing pressure after 125 hours of slurry injection. The maximum injection volume for this case before formation fracturing is 22,500 STB (2,902 ton of sludge).
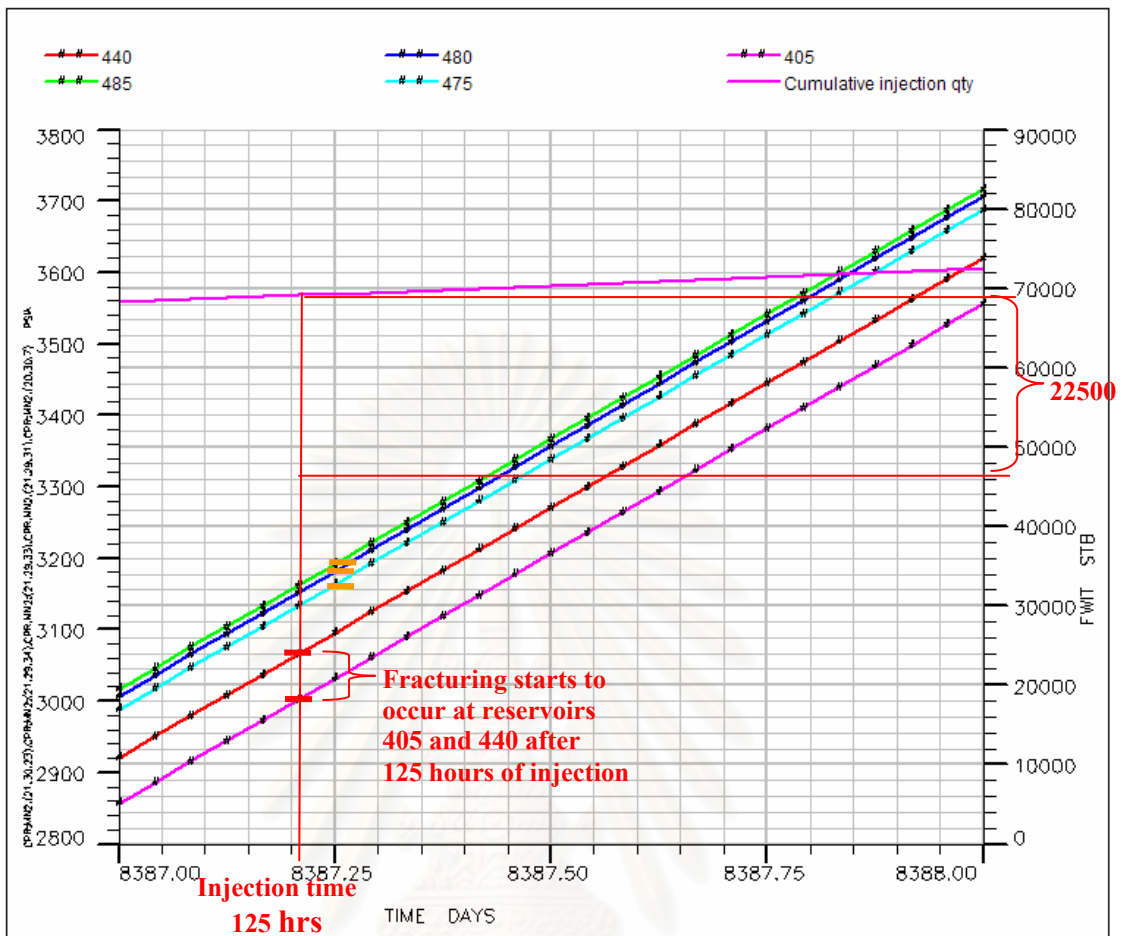
Figure 6.32: Sandface pressure evolution of simulation case A1 for injection schedule 2B.

After running simulation for all the 18 cases, we see that the evolution of sandface pressure in all the cases behave in the same manner. Furthermore, the first reservoir having pressure exceeding the fracturing pressure in all the 18 cases is the same. Fig. 6.33 compares the maximum amount of waste that can be injected in each simulated case. The results show that case A13 has the highest storage capability which is 3,824 ton of sludge (22,230 STB of slurry with sludge concentration 40 % by volume). Case A12 has the minimum storage capability which is only 1,383 ton of sludge (16,080 STB of slurry with sludge concentration 20 % by volume).
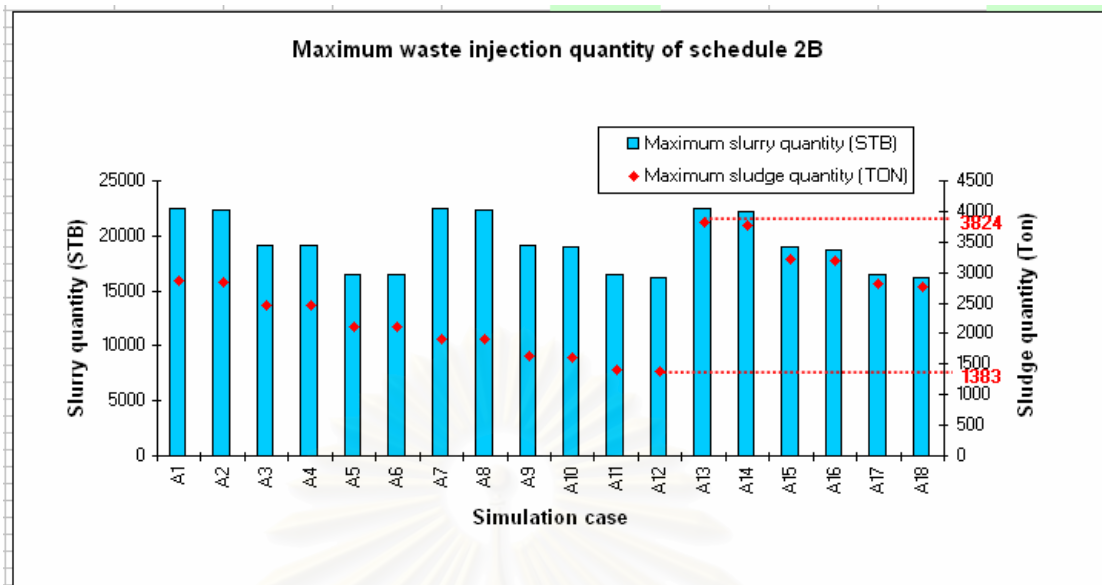
Figure 6.33: The comparison of maximum waste injection quantity for schedule 2B.

Using the same procedure as in schedule 1, the best injection scenarios for varied quantity of sludge were obtained and summarized in Table 6.8. The most suitable sludge concentration is 40% by volume for all sludge quantities. For quantity of sludge less than 2,800 ton, the optimal injection rate is 5 STB/MIN. When the sludge quantity increases, the suitable injection rate decreases. The injection time increases when the sludge quantity required to be disposed increases.

Table 6.8: Optimized injection case of varied sludge quantities in schedule 2B.

Sludge quantity (TON)	Viscosity (cp)	Optimized case	Sludge concentration (% volume)	Injection rate (STB/MIN)	Injection time (HOURS)
600	40	A17	40	5	11.8
	70	A18	40	5	11.8
800	40	A17	40	5	15.7
	70	A18	40	5	15.7
1000	40	A17	40	5	19.6
	70	A18	40	5	19.6
1200	40	A17	40	5	23.5
	70	A18	40	5	23.5
1400	40	A17	40	5	27.5
	70	A18	40	5	27.5
1600	40	A17	40	5	31.4
	70	A18	40	5	31.4
1800	40	A17	40	5	35.3
	70	A18	40	5	35.3
2000	40	A17	40	5	39.2
	70	A18	40	5	39.2
2200	40	A17	40	5	43.2
	70	A18	40	5	43.2
2400	40	A17	40	5	47.1
	70	A18	40	5	47.1
2600	40	A17	40	5	51.0
	70	A18	40	5	51.0
2800	40	A17	40	5	54.9
	70	A16	40	4	68.7
3000	40	A15	40	3	73.6
	70	A16	40	4	73.6
3200	40	A15	40	3	78.5
	70	A14	40	4	104.6
3400	40	A13	40	3	111.2
	70	A14	40	3	111.2
3600	40	A13	40	3	117.7
	70	A14	40	3	117.7
3800	40	A13	40	3	124.2

In summary, reservoir simulation was performed to maximize hydrocarbon production and optimize Hg-contaminated slurry injection by varying design variables which are perforation plan, maximum gas production rate, sludge concentration, Hg-contaminated slurry viscosity, and injection rate. Perforation is planned to be done in batches from the bottom up. Two scenarios were simulated in this study. In plan 1, the first perforation batch covers reservoirs 560 to 720 (8 reservoirs) and the second perforation batch covers reservoirs 405 to 485 (5 reservoirs). The two batches of perforation are 69.5 m. apart. For plan 2, the first perforation batch covers reservoirs 660 to 720 (4 reservoirs) and the second perforation batch covers reservoirs 405 to 585 (11 reservoir). The two batches of perforation are 71.5 m. apart. The optimal perforation plan is plan 1. The best production scenario is to produce gas at a

maximum rate of 1 MMSCFD after the first perforation batch and 7 MMSCFD after the second perforation batch.

For Hg-contaminated slurry injection optimization, the properties that affect injection performance and thus were selected for a sensitivity study are slurry density (20, 30, and 40% by volume), injection rate (3, 4, and 5 STB/MIN), and slurry viscosity (40 and 70 cp). The optimal sludge concentration for most of disposal quantities is 40% by volume. If the injection volume is small, a high injection rate is the most suitable. On the other hand, small injection rate is the most appropriate when the injection volume is high. Injecting with high injection rate causes a rapid increase of sandface pressure since there is not enough time for pressure to diffuse into the reservoirs. Injection with low injection rate results in a high injection capability because there is more time for pressure to disperse into the reservoirs, causing the sandface pressure to reach the fracturing pressure slower. If the injection volume increases, the injection rate should be reduced to avoid fracture initiation. The viscosity effect is very small. We obtain the same optimal injection scenario for slurry viscosity of 40 and 70 cp.

CHAPTER VII

CONCLUSIONS AND RECOMMENDATIONS

To dispose Hg-contaminated waste generated in the field selected for this study called the M field, the depleted reservoir disposal method was selected. After an integrated team of engineers and geologists had finished reviewing and studying the geological structure of the M field, the most suitable structure, the MN compartment, which is a confined reservoir and in the last stage of production, was chosen. There are 22 gas reservoirs located in the compartment and two highly deviated wells penetrating through these reservoirs. Since the selected reservoirs are not completely depleted, hydrocarbon should be produced before injecting mercury contaminated waste. This study thus focuses on the optimization of both hydrocarbon production and Hg-contaminated waste disposal strategy. The maximization of hydrocarbon production and Hg-contaminated waste disposal was performed using a 3-D reservoir simulator.

The conditions imposed in this study can be listed as follows:
1) Since there are several layers intersected by the well, the well will be perforated in two batches from the bottom up.
2) The well will be used for alternate production and injection until it is completely depleted and reaches injection capacity. After the first batch of perforation, the well will be on production for two years or until the gas rate reaches the economic limit. Then, Hg-contaminated slurry will be injected. Then, the zones will be plugged, and the second batch of reservoirs is perforated.
3) Hg-contaminated slurry will be injected every two years for a maximum injection period of two weeks.
4) The slurry is to be injected for a with maximum quantity 6,000 ton of sludge.

In order to optimize hydrocarbon production and mercury waste injection, four main steps were followed: (1) reservoir model construction, (2) history matching, (3) production optimization, and (4) injection optimization.

In the first step which is reservoir model construction, a 3D geological modeling software called PETREL, was used for geological modeling. The workflow for reservoir model construction consists of fault modeling, gridding, surface making, zone making, well log up-scaling, grid block layering, facies modeling, petrophysical modeling, PETREL to ECLIPSE model transferring, and reservoir model initialization. Porosity and permeability distributions were constructed using sequential Gaussian simulation. Then, necessary properties which are initial water saturation, fluid properties and aquifer and model initialization need to be incorporated into the model.

The next step is to fine tune the reservoir model by performing history matching. The history matched model can be used as a real reservoir representative. The data selected for the matching are production rate, cumulative production, and reservoir pressure. In order to achieve a good match, adjustment needs to be done on relative permeability, absolute permeability, aquifer size, and OGIP. After finishing all necessary adjustment, the results from simulation were reasonably matched with the historical data.

Then, reservoir simulation was performed to optimize hydrocarbon production by varying perforation plan and maximum gas rate. Perforation is planned in batches from the bottom up. Two plans were studied. Both plans have two perforation batches and a sixty meter interval between the two batches to prevent communication between the contaminated injection zone and producible zone. Several cases were investigated to determine the most appropriate maximum gas production rate. The production period was scheduled to be 2 years per batch. However, the reservoir is not completely depleted after 2 years of production in the second batch of perforation. Thus, additional cases which extend the production until the economic limit of 0.1 MMSCFD were simulated. The result from the simulation shows that the best perforation plan is to perforate reservoirs 560 to 720 (8 reservoirs) in the first batch and reservoirs 405 to 485 (5 reservoirs) in the second batch. The optimal production scenario is to produce at a maximum gas rate of 1 MMSCFD during the first batch of production and 7 MMSCFD during the second batch of production.

Next, reservoir simulation was performed to optimize Hg-contaminated slurry injection. The properties affecting injection performance selected for sensitivity study are slurry density, injection rate, and slurry viscosity. By varying these parameters, the simulation was organized into 18 cases. The maximum injection quantity is 6000 ton. The injection pressure should not be too high to create any fracture in the reservoirs. It is assumed that there is no particle filtration or formation damage effect.

There are two injection schedules for the simulation which are

- Schedule 1: After the first batch of production (after finishing the production in the first phase)
- Schedule 2: After the second batch of production. Since there are two production periods in the second batch of production, the injection schedule was divided into two cases as follows:
  - o Schedule 2A: After the second batch of production which lasts 2 years.
  - o Schedule 2B: After the first batch of production which produces until the economic limit of 0.1 MMSCFD.

From the injection optimization, it can be concluded that the most suitable sludge concentration is 40% by volume for most sludge quantities. The highest injection rate which is 5 STB/MIN is suitable for generally low injection volume. If the injection volume increases, the injection rate should be reduced to avoid fracture initiation. Difference of slurry viscosity gives very small effect to an injection capability. So, the same optimal injection scenario can be applied for viscosity in the range of 40 to 70 cp.

The following points are recommended for future study:
(1) Grinding sludge particles to be fine enough to pass through the formation without formation damage may be not economically feasible. Incorporating the particle effect into the simulator will give the prediction more realistic. In developing a filtration model, both internal and external filter cakes need to be accounted for.
(2) Without fracture being created, solid particles larger than 1/3 of pore diameter will bridge pore entrances at the formation face to form an external cake while

those with the sizes ranging between 1/3 of 1/7 of the pore diameter will invade into the formation and form an internal cake [13]. For a high injection volume, fractures are needed as storage space for the suspended solid in Hg-contaminated waste. So, the fracture model should be incorporated into the simulation to give the prediction more realistic for high disposal volume.

References

1. Mussig, S. and Rothmann, B. "Mercury in Natural Gas – Problems and Technical Solutions for its Removal," SPE 38088 presented at 1997 SPE Asia Pacific Oil and Gas Conference and Exhibition, Kuala Lumpur, Malaysia, April.

2. Wilhelm, S. and McArthur, A. "Removal and Treatment of Mercury Contamination at Gas Processing Facilities," SPE 29721 presented at 1995 SPE/EPA Exploration & Production Environmental Conference, Houston Texas, U.S.A., March.

3. Soponkanabhorn, T. and Killing, A. "Bongkot Floating Storage and Offloading Facility Mercury Contaminated Wastewater Treatment and Disposal," SPE 73958 presented at 2002 SPE International Conference on Health, Safety and Environment in Oil and Gas Exploration and Production, Kuala Lumpur, Malaysia, March.

4. Yod-In-Lom, W. and Doyle, A. "Deep Well Injection of Mercury Contaminated Sludge in the Gulf of Thailand," SPE 73964 presented at 2002 SPE International Conference on Health, Safety and Environment in Oil and Gas Exploration and Production, Kuala Lumpur, Malaysia, March.

5. Pongsiri, N. "Thailand's Initiatives on Mercury," SPE 38087 presented at 1997 SPE Asia Pacific Oil and Gas Conference and Exhibition, Kuala Lumpur, Malaysia, April.

6. Chaianansutcharit, T. "Well Selection Process for Hg-waste Subsurface Disposal in Bongkot Field," Technical paper presented at 2003 7th PTTEP Technical Forum, Bangkok, Thailand, August.

7. Dimitrakopoulos, R. "Geostatistical Modeling of Gridblock Permeabilities for 3D Reservoir Simulators," SPE 21520 accepted for publiction, September 1991.

8. Aly *et.al*. "Application of Geostatistical Modeling in an Integrated Reservoir Simulation Study of the Lower Bahariya Reservoir, Egypt," SPE 53118 presented at 1999 Middle East Oil Show and Conference, Bahrain, February.

9. Saleri, N. and Toronyi, R. "Engineering Control in Reservoir Simulation: Part I," SPE 18305 presented at 1988 Annual Technical Conference and Exhibition of the Society of Petroleum Engineers, Houston, October.

10. Thomas, G.W. "The Role of Reservoir Simulation in Optimal Reservoir Management," SPE 14129 presented at the SPE 1986 International Meeting on petroleum Engineering, Beijing, China, March.

11. Sanchez, N., Martinez, C. and Rattia, A. "Methodological Approach for Reservoir Simulation," SPE 23616 presented at the Second Latin American Petroleum Engineering Conference, II LAPEC, of the society, Caracas, Veneuala, March.

12. Williams, M. and Keating, J. "The Stratigraphic Method: A Structure Approach to History Matching Complex Simulation Models," SPE 38014 presented at the 1997 SPE Reservoir Simulation Symposium, Dallas, U.S.A., June.

13. Pautz, J. and Crocker, M. "Relating Water Quality and Formation Permeability to Loss of Injectivity," SPE 18888 presented at the SPE Production Operations Symposium, Oklahoma, Japan, March.

APPENDICES

APPENDIX A

MS.data

```
RUNSPEC
TITLE
title
START
 1 'JUN' 1996 /
FIELD
GAS
OIL
WATER
VAPOIL

NSTACK
 100 /

BRINE

MONITOR

RSSPEC

NOINSPEC

AQUDIMS
 13 13 2 0 0 0 /

DIMENS
 30 46 148 /

EQLDIMS
 26 100 20 1 20 /

REGDIMS
 26 1 0 0 /

TABDIMS
 26 1 20 20 26 20 20 1 /

VFPPDIMS
 10 10 10 10 1 3 /

WELLDIMS
 3 66 3 3 /

MESSAGES
9* 500 2* /


GRID

GRIDFILE
 0 1 /

INIT
```

```
INCLUDE
'MS_GGO.INC'  /

INCLUDE
'MS_GPRO.INC'  /

INCLUDE
'MS_GOTH.INC'  /

PROPS

INCLUDE
'MS_PVT.INC'  /

INCLUDE
'MS_SCAL.INC'  /

REGIONS

INCLUDE
'MS_REG.INC'  /

SOLUTION

INCLUDE
'MS_INIT.INC'  /

SUMMARY

INCLUDE
'MS_SUM.INC'  /

SCHEDULE

INCLUDE
'MS_SCH.INC'  /

END
```

MS_GGO.INC

```
MAPAXES
-- Grid Axes wrt Map Coordinates
      0    1000      0      0    1000      0 /
GRIDUNIT
-- Grid data units
'FEET' /
NOECHO
MAPUNITS
-- Units for MAPAXES Data
'FEET' /
-- Grid Block Coordinate Lines
COORD
2835200.5  2905916.5  4600.8784  2837364.2  2906887.8  6917.2104
. . .
/

ZCORN
4600.8784 4594.8442 4594.8442 4595.1226 4595.1226 4586.8281 4586.8281
. . .
/
```

MS_GPRO.INC

```
PERMX
0.16288995E+03   0.16288995E+03   0.16288995E+03   0.14411073E+03
. . .
/

PORO
0.11438000E-01   0.18619999E-01   0.18619999E-01   0.18619999E-01
. . .
/

BOX
 1 30 1 46 34 34 /
EQUALS
ACTNUM 1 /
/
ENDBOX

BOX
 1 30 1 46 1 148 /
EQUALS
ACTNUM 1 /
/
ENDBOX
```

MS_GOTH.INC

```
AQUCON
-- Numerical Aquifer Connections
1     2     2     1     46     7      21 'I-'    1*      1* 'NO'    1* /
2     2     2     1     46     96    105 'I-'    1*      1* 'NO'    1* /
3     2     2     1     46     113   117 'I-'    1*      1* 'NO'    1* /
4     2     2     1     46     136   136 'I-'    1*      1* 'NO'    1* /
5     2     2     1     46     33     33 'I-'    1*      1* 'NO'    1* /
6     2     2     1     46     36     36 'I-'    1*      1* 'NO'    1* /
7     2     2     1     46     39     39 'I-'    1*      1* 'NO'    1* /
8     2     2     1     46     41     41 'I-'    1*      1* 'NO'    1* /
9     2     2     1     46     42     42 'I-'    1*      1* 'NO'    1* /
10    2     2     1     46     44     44 'I-'    1*      1* 'NO'    1*/
11    2     2     1     46     49     54 'I-'    1*      1* 'NO'    1* /
12    2     2     1     46     71     76 'I-'    1*      1* 'NO'    1* /
13    2     2     1     46     31     31 'I-'    1*      1* 'NO'    1* /
/

AQUNUM
-- Numerical Aquifer Assignments
1     1     23     15     5000000     1000     0.3     70     1*      1* 1 2 /
/

AQUNUM
-- Numerical Aquifer Assignments
2     1     23     100    5000000     1000     0.3     70     1*  1*  1    19 /
/

AQUNUM
-- Numerical Aquifer Assignments
3     1     23     115    5000000     1000     0.3     70     1*  1*  1    20 /
/

AQUNUM
-- Numerical Aquifer Assignments
4     1     23     136    4000000     1000     0.3     70     1*  1*  1    21 /
/

AQUNUM
-- Numerical Aquifer Assignments
5     1     23     33     4000000     1000     0.3     70     1*  1*  1  5 /
/

AQUNUM
--
-- Numerical Aquifer Assignments
6     1     23     36     4000000     1000     0.3     70     1*   1*   1 6 /
/

AQUNUM
--
-- Numerical Aquifer Assignments
--
7     1     23     39     4000000     1000     0.3     70     1*  1*  1  7 /
/

AQUNUM
```

```
--
-- Numerical Aquifer Assignments
--
8    1    23    41   4000000    1000    0.3    70    1*   1*   1   8 /
/

AQUNUM
--
-- Numerical Aquifer Assignments
--
9    1    23    42   4000000    1000    0.3    70    1*   1*   1   9 /
/

AQUNUM
--
-- Numerical Aquifer Assignments
--
10   1    23    44   4000000    1000    0.3    70    1*   1*   1  10 /
/

AQUNUM
--
-- Numerical Aquifer Assignments
--
11   1    23    51   4000000    1000    0.3    70    1*   1*   1  11 /
/

AQUNUM
--
-- Numerical Aquifer Assignments
--
12   1    23    73   4000000    1000    0.3    70    1*   1*   1  16 /
/

AQUNUM
--
-- Numerical Aquifer Assignments
--
13   1    23    31   4000000    1000    0.3    70    1*   1*   1   4 /
/

ECHO
NOECHO
MS_PVT.inc
-- Brine Surface Density
BDENSITY
-- Brine Surface Density
     70
     75
     80
     85
     90
     95
/

PVTWSALT
-- Water PVT Functions with Salt Present
```

```
    2292    2309 /
    2309   1.034639  3.3654e-006  0.2504701  3.102996e-006
    5000   1.034639  3.3654e-006        70   0.00021 /
PVTG
-- Wet Gas PVT Properties (Vapourised Oil)
    16.08      0.3 171.393051661923  0.00982 /
   359.19     0.07 7.48052392164686  0.01082 /
   703.68     0.02 3.77588350330746   0.0121 /
  1048.16    0.015 2.54694028760833  0.01356 /
  1392.65    0.012 1.9591848366218   0.01514 /
  1737.14    0.011 1.62078018302349  0.01676 /
  2081.63     0.01 1.42486169936131  0.01838 /
  2426.12    0.009 1.28237552942518  0.01994 /
  2770.61    0.008 1.19332167321509  0.02144 /
  3115.09    0.007 1.12207858824703  0.02286
            0    1.122   0.0229 /
/

DENSITY
-- Fluid Densities at Surface Conditions
  48.4615507614816 62.4279737253144 0.060367850592379
/

PVCDO
-- Dead Oil PVT Properties
    449.7  1.1414  2e-005  0.2998      1*
/

ROCK
-- Rock Properties
    2292 1.1767330533933e-006
/



MS_SCAL.inc

-- Water Saturation Functions
--
SWFN
--
-- Water Saturation Functions
--
    0.11        0       250
    0.157       0        53
    0.216       0        13
    0.313     0.03        1
    0.44      0.09        0
    0.56      0.13        0
    0.68       0.2        0
    0.8        0.4        0
    0.9        0.7        0
      1        0.9        0
/
    0.11        0       250
    0.157       0        53
    0.216       0        13
    0.313     0.03        1
```

```
        0.44        0.09        0
        0.56        0.13        0
        0.68        0.2         0
        0.8         0.4         0
        0.9         0.7         0
        1           0.9         0
/
        0.11        0           250
        0.157       0           53
        0.216       0           13
        0.313       0.03        1
        0.44        0.09        0
        0.56        0.13        0
        0.68        0.2         0
        0.8         0.4         0
        0.9         0.7         0
        1           0.9         0
/
        0.11        0           1200
        0.157       0           300
        0.216       0           55
        0.313       0.03        10
        0.44        0.09        0
        0.56        0.13        0
        0.68        0.2         0
        0.8         0.4         0
        0.9         0.7         0
        1           0.9         0
/
        0.11        0           1200
        0.157       0           300
        0.216       0           55
        0.313       0.03        10
        0.44        0.09        0
        0.56        0.13        0
        0.68        0.2         0
        0.8         0.4         0
        0.9         0.7         0
        1           0.9         0
/
        0.11        0           1200
        0.157       0           300
        0.216       0           55
        0.313       0.03        10
        0.44        0.09        0
        0.56        0.13        0
        0.68        0.2         0
        0.8         0.4         0
        0.9         0.7         0
        1           0.9         0
/
        0.11        0           250
        0.157       0           53
        0.216       0           13
        0.313       0.03        1
        0.44        0.09        0
        0.56        0.13        0
        0.68        0.2         0
```

0.8	0.4	0
0.9	0.7	0
1	0.9	0

/

0.11	0	250
0.157	0	53
0.216	0	13
0.313	0.03	1
0.44	0.09	0
0.56	0.13	0
0.68	0.2	0
0.8	0.4	0
0.9	0.7	0
1	0.9	0

/

0.11	0	250
0.157	0	53
0.216	0	13
0.313	0.03	1
0.44	0.09	0
0.56	0.13	0
0.68	0.2	0
0.8	0.4	0
0.9	0.7	0
1	0.9	0

/

0.11	0	2000
0.2	0	1000
0.21	0	94.3
0.336	0.01	12.5
0.61	0.04	0.9
0.68	0.08	0.3
0.8	0.23	0.3
0.9	0.6	0
1	0.9	0

/

0.11	0	250
0.157	0	53
0.216	0	13
0.313	0.03	1
0.44	0.09	0
0.56	0.13	0
0.68	0.2	0
0.8	0.4	0
0.9	0.7	0
1	0.9	0

/

0.11	0	250
0.157	0	53
0.216	0	13
0.313	0.03	1
0.44	0.09	0
0.56	0.13	0
0.68	0.2	0
0.8	0.4	0
0.9	0.7	0
1	0.9	0

/

0.11	0	2000
0.2	0	1000
0.21	0	94.3
0.336	0.01	12.5
0.61	0.04	0.9
0.68	0.08	0.3
0.8	0.23	0.3
0.9	0.6	0
1	0.9	0

/

0.11	0	250
0.157	0	53
0.216	0	13
0.313	0.03	1
0.44	0.09	0
0.56	0.13	0
0.68	0.2	0
0.8	0.4	0
0.9	0.7	0
1	0.9	0

/

0.11	0	250
0.157	0	53
0.216	0	13
0.313	0.03	1
0.44	0.09	0
0.56	0.13	0
0.68	0.2	0
0.8	0.4	0
0.9	0.7	0
1	0.9	0

/

0.11	0	250
0.157	0	53
0.216	0	13
0.313	0.03	1
0.44	0.09	0
0.56	0.13	0
0.68	0.2	0
0.8	0.4	0
0.9	0.7	0
1	0.9	0

/

0.11	0	800
0.157	0	90
0.216	0	20
0.313	0.03	2
0.44	0.09	0
0.56	0.13	0
0.68	0.2	0
0.8	0.4	0
0.9	0.7	0
1	0.9	0

/

0.11	0	250
0.157	0	53
0.216	0	13

0.313	0.02	1
0.44	0.06	0
0.56	0.1	0
0.68	0.15	0
0.8	0.3	0
0.9	0.65	0
1	0.9	0

/

0.11	0	250
0.157	0	53
0.216	0	13
0.313	0.03	1
0.44	0.09	0
0.56	0.13	0
0.68	0.2	0
0.8	0.4	0
0.9	0.7	0
1	0.9	0

/

0.11	0	250
0.157	0	53
0.216	0	13
0.313	0.03	1
0.44	0.09	0
0.56	0.13	0
0.68	0.2	0
0.8	0.4	0
0.9	0.7	0
1	0.9	0

/

0.11	0	2000
0.2	0	1000
0.21	0	94.3
0.336	0.01	12.5
0.61	0.04	0.9
0.68	0.08	0.3
0.8	0.23	0.3
0.9	0.6	0
1	0.9	0

/

0.11	0	1100
0.157	0	200
0.216	0	45
0.313	0.03	7
0.44	0.09	0
0.56	0.13	0
0.68	0.2	0
0.8	0.4	0
0.9	0.7	0
1	0.9	0

/

0.11	0	299
0.379	0	121
0.426	0.001	69
0.497	0.03	38
0.555	0.06	22
0.611	0.12	12
0.68	0.3	2.5

```
        0.8      0.45          1
          1      0.6          0
/
SOF3
--
-- Oil Saturation Functions
--
        0.2        0          0
        0.32 0.0046296296    0.015625
        0.44 0.037037037       0.125
        0.56      0.125   0.421875
        0.68   0.2962963         1
        0.89         1          1
/
        0.2        0          0
        0.32 0.0046296296    0.015625
        0.44 0.037037037       0.125
        0.56      0.125   0.421875
        0.68   0.2962963         1
        0.89         1          1
/
        0.2        0          0
        0.32 0.0046296296    0.015625
        0.44 0.037037037       0.125
        0.56      0.125   0.421875
        0.68   0.2962963         1
        0.89         1          1
/
        0.2        0          0
        0.32 0.0046296296    0.015625
        0.44 0.037037037       0.125
        0.56      0.125   0.421875
        0.68   0.2962963         1
        0.89         1          1
/
        0.2        0          0
        0.32 0.0046296296    0.015625
        0.44 0.037037037       0.125
        0.56      0.125   0.421875
        0.68   0.2962963         1
        0.89         1          1
/
        0.2        0          0
        0.32 0.0046296296    0.015625
        0.44 0.037037037       0.125
        0.56      0.125   0.421875
        0.68   0.2962963         1
        0.89         1          1
/
        0.2        0          0
        0.32 0.0046296296    0.015625
        0.44 0.037037037       0.125
        0.56      0.125   0.421875
        0.68   0.2962963         1
        0.89         1          1
/
        0.2        0          0
        0.32 0.0046296296    0.015625
```

```
       0.44 0.037037037      0.125
       0.56     0.125   0.421875
       0.68   0.2962963        1
       0.89         1          1
/
        0.2        0          0
       0.32 0.0046296296   0.015625
       0.44 0.037037037      0.125
       0.56     0.125   0.421875
       0.68   0.2962963        1
       0.89         1          1
/
        0.2        0          0
       0.32 0.0046296296   0.015625
       0.44 0.037037037      0.125
       0.56     0.125   0.421875
       0.68   0.2962963        1
       0.89         1          1
/
        0.2        0          0
       0.32 0.0046296296   0.015625
       0.44 0.037037037      0.125
       0.56     0.125   0.421875
       0.68   0.2962963        1
       0.89         1          1
/
        0.2        0          0
       0.32 0.0046296296   0.015625
       0.44 0.037037037      0.125
       0.56     0.125   0.421875
       0.68   0.2962963        1
       0.89         1          1
/
        0.2        0          0
       0.32 0.0046296296   0.015625
       0.44 0.037037037      0.125
       0.56     0.125   0.421875
       0.68   0.2962963        1
       0.89         1          1
/
        0.2        0          0
       0.32 0.0046296296   0.015625
       0.44 0.037037037      0.125
       0.56     0.125   0.421875
       0.68   0.2962963        1
       0.89         1          1
/
        0.2        0          0
       0.32 0.0046296296   0.015625
       0.44 0.037037037      0.125
       0.56     0.125   0.421875
       0.68   0.2962963        1
       0.89         1          1
/
        0.2        0          0
       0.32 0.0046296296   0.015625
       0.44 0.037037037      0.125
       0.56     0.125   0.421875
```

```
        0.68   0.2962963        1
        0.89        1        1
/
         0.2        0        0
        0.32 0.0046296296   0.015625
        0.44 0.037037037      0.125
        0.56      0.125   0.421875
        0.68   0.2962963        1
        0.89        1        1
/
         0.2        0        0
        0.32 0.0046296296   0.015625
        0.44 0.037037037      0.125
        0.56      0.125   0.421875
        0.68   0.2962963        1
        0.89        1        1
/
         0.2        0        0
        0.32 0.0046296296   0.015625
        0.44 0.037037037      0.125
        0.56      0.125   0.421875
        0.68   0.2962963        1
        0.89        1        1
/
         0.2        0        0
        0.32 0.0046296296   0.015625
        0.44 0.037037037      0.125
        0.56      0.125   0.421875
        0.68   0.2962963        1
        0.89        1        1
/
         0.2        0        0
        0.32 0.0046296296   0.015625
        0.44 0.037037037      0.125
        0.56      0.125   0.421875
        0.68   0.2962963        1
        0.89        1        1
/
         0.2        0        0
        0.32 0.0046296296   0.015625
        0.44 0.037037037      0.125
        0.56      0.125   0.421875
        0.68   0.2962963        1
        0.89        1        1
/
          0        0        0
         0.2        0        0
        0.32 0.0046296296   0.015625
        0.44 0.037037037      0.125
        0.56      0.125   0.421875
         0.6   0.2962963        1
        0.89        1        1
/
         0.2        0        0
        0.32 0.0046296296   0.015625
        0.44 0.037037037      0.125
        0.56      0.125   0.421875
```

```
        0.68   0.2962963           1
        0.89          1           1
/
        0.2           0           0
        0.32 0.0046296296    0.015625
        0.44 0.037037037        0.125
        0.56      0.125    0.421875
        0.68   0.2962963           1
        0.89          1           1
/
        0.2           0           0
        0.32 0.0046296296    0.015625
        0.44 0.037037037        0.125
        0.56      0.125    0.421875
        0.68   0.2962963           1
        0.89          1           1
/

SGFN
--
-- Gas Saturation Functions
--
        0            0        1*
        0.2          0        1*
        0.3        0.12       1*
        0.4        0.25       1*
        0.6        0.75       1*
        0.7        0.93       1*
        0.8       0.975       1*
        0.85       0.98       1*
        0.89          1       1*
/
        0            0        1*
        0.2          0        1*
        0.3         0.2       1*
        0.4        0.38       1*
        0.6        0.42       1*
        0.7        0.45       1*
        0.8        0.55       1*
        0.85        0.8       1*
        0.89       0.95       1*
/
        0            0        1*
        0.2          0        1*
        0.3        0.12       1*
        0.4        0.25       1*
        0.6        0.75       1*
        0.7        0.93       1*
        0.8       0.975       1*
        0.85       0.98       1*
        0.89          1       1*
/
        0            0        1*
        0.2          0        1*
        0.3        0.12       1*
        0.4        0.25       1*
        0.6        0.75       1*
        0.7        0.93       1*
```

0.8	0.975	1*
0.85	0.98	1*
0.89	1	1*

/

0	0	1*
0.2	0	1*
0.3	0.2	1*
0.4	0.38	1*
0.6	0.42	1*
0.7	0.45	1*
0.8	0.55	1*
0.85	0.8	1*
0.89	0.95	1*

/

0	0	1*
0.2	0	1*
0.3	0.2	1*
0.4	0.38	1*
0.6	0.42	1*
0.7	0.45	1*
0.8	0.55	1*
0.85	0.8	1*
0.89	0.95	1*

/

0	0	1*
0.2	0	1*
0.3	0.2	1*
0.4	0.38	1*
0.6	0.42	1*
0.7	0.45	1*
0.8	0.55	1*
0.85	0.8	1*
0.89	0.95	1*

/

0	0	1*
0.2	0	1*
0.3	0.2	1*
0.4	0.38	1*
0.6	0.42	1*
0.7	0.45	1*
0.8	0.55	1*
0.85	0.8	1*
0.89	0.95	1*

/

0	0	1*
0.2	0	1*
0.3	0.2	1*
0.4	0.38	1*
0.6	0.42	1*
0.7	0.45	1*
0.8	0.55	1*
0.85	0.8	1*
0.89	0.95	1*

/

0	0	1*
0.2	0	1*
0.3	0.2	1*
0.4	0.38	1*

```
        0.6     0.42      1*
        0.7     0.45      1*
        0.8     0.55      1*
        0.85    0.8       1*
        0.89    0.95      1*
/
        0       0         1*
        0.2     0         1*
        0.3     0.2       1*
        0.4     0.38      1*
        0.6     0.42      1*
        0.7     0.45      1*
        0.8     0.55      1*
        0.85    0.8       1*
        0.89    0.95      1*
/
        0       0         1*
        0.2     0         1*
        0.3     0.2       1*
        0.4     0.38      1*
        0.6     0.42      1*
        0.7     0.45      1*
        0.8     0.55      1*
        0.85    0.8       1*
        0.89    0.95      1*
/
        0       0         1*
        0.2     0         1*
        0.3     0.2       1*
        0.4     0.38      1*
        0.6     0.42      1*
        0.7     0.45      1*
        0.8     0.55      1*
        0.85    0.8       1*
        0.89    0.95      1*
/
        0       0         1*
        0.2     0         1*
        0.3     0.2       1*
        0.4     0.38      1*
        0.6     0.42      1*
        0.7     0.45      1*
        0.8     0.55      1*
        0.85    0.8       1*
        0.89    0.95      1*
/
        0       0         1*
        0.2     0         1*
        0.3     0.2       1*
        0.4     0.38      1*
        0.6     0.42      1*
        0.7     0.45      1*
        0.8     0.55      1*
        0.85    0.8       1*
        0.89    0.95      1*
/
        0       0         1*
        0.2     0         1*
```

```
     0.3      0.2      1*
     0.4      0.38     1*
     0.6      0.42     1*
     0.7      0.45     1*
     0.8      0.55     1*
     0.85     0.8      1*
     0.89     0.95     1*
/
     0        0        1*
     0.2      0        1*
     0.3      0.2      1*
     0.4      0.38     1*
     0.6      0.42     1*
     0.7      0.45     1*
     0.8      0.55     1*
     0.85     0.8      1*
     0.89     0.95     1*
/
     0        0        1*
     0.2      0        1*
     0.3      0.2      1*
     0.4      0.38     1*
     0.6      0.42     1*
     0.7      0.45     1*
     0.8      0.55     1*
     0.85     0.8      1*
     0.89     0.95     1*
/
     0        0        1*
     0.2      0        1*
     0.3      0.2      1*
     0.4      0.38     1*
     0.6      0.42     1*
     0.7      0.45     1*
     0.8      0.55     1*
     0.85     0.8      1*
     0.89     0.95     1*
/
     0        0        1*
     0.2      0        1*
     0.3      0.2      1*
     0.4      0.38     1*
     0.6      0.42     1*
     0.7      0.45     1*
     0.8      0.55     1*
     0.85     0.8      1*
     0.89     0.95     1*
/
     0        0        1*
     0.2      0        1*
     0.3      0.2      1*
     0.4      0.38     1*
     0.6      0.42     1*
     0.7      0.45     1*
     0.8      0.55     1*
     0.85     0.8      1*
     0.89     0.95     1*
/
```

```
        0        0       1*
        0.2      0       1*
        0.3      0.2     1*
        0.4      0.38    1*
        0.6      0.42    1*
        0.7      0.45    1*
        0.8      0.55    1*
        0.85     0.8     1*
        0.89     0.95     1*
/
        0        0       1*
        0.1      0       1*
        0.2      0       1*
        0.3      0.2     1*
        0.4      0.4     1*
        0.6      0.85    1*
        0.7      0.9     1*
        0.8      0.92    1*
        0.85     0.95     1*
        0.89     0.95     1*
/
        0        0       1*
        0.2      0       1*
        0.3      0.2     1*
        0.4      0.38    1*
        0.6      0.42    1*
        0.7      0.45    1*
        0.8      0.55    1*
        0.85     0.8     1*
        0.89     0.95     1*
/
        0        0       1*
        0.2      0       1*
        0.3      0.2     1*
        0.4      0.38    1*
        0.6      0.42    1*
        0.7      0.45    1*
        0.8      0.55    1*
        0.85     0.8     1*
        0.89     0.95     1*
/
        0        0       1*
        0.2      0       1*
        0.3      0.2     1*
        0.4      0.38    1*
        0.6      0.42    1*
        0.7      0.45    1*
        0.8      0.55    1*
        0.85     0.8     1*
        0.89     0.95     1*
/
```

MS_INIT.INC

```
SALTVD
--
-- Salt v Depth
--
     3000     2309
     5000     2309
/
 EQUIL
--
-- Equilibration Data Specification
--
4560.36   1930 4560.36     0 4560.36     0    1*    1*    1* /

4724.4094488189 1984.25 4724.4094488189     0 4724.40   0    1*    1*    1*/

4816.27296587927 2037.53 4816.27296587927     0 4816.27   0    1*    1*    1*/

4967.19 2100.92 4967.19     0 4967.19     0    1*    1*    1*/

4986.87664041995 2109.19 4986.87664041995     0 4986.87   0    1*    1* 1*/

5055.77427821522 2138.13 5055.77427821522     0 5055.77   0    1*    1* 1*/

5085.30183727034 2150.53 5085.30183727034     0 5085.30   0    1*    1* 1*/

5129.59317585302   2169 5129.59317585302     0 5129.59   0    1*    1*    1*/

5177.16535433071 2189.1 5177.16535433071     0 5177.16   0    1*    1* 1*/

5278.87139107612 2231.83 5278.87139107612     0 5278.87   0    1*    1* 1*/

5278.87139107612   2231 5278.87139107612     0 5278.87   0    1*    1*    1*/

5337.92650918635 2256.6 5337.927     0 5337.92     0    1*    1*    1*/

5446.19422572178 2302.1 5446.19422572178     0 5446.19   0    1*    1*    1*/

5421.58792650919   2291 5421.58792650919     0 5421.58   0    1*    1*    1*/

5449.4750656168 2303.48 5449.4750656168     0 5449.47   0    1*    1*    1*/

5620.07874015748   2375 5620.07874015748     0 5620.07   0    1*    1*    1*/

5656.16797900262 2390.29 5656.16797900262     0 5656.16   0    1*    1* 1*/

5675.8530183727 2398.6 5675.8530183727     0 5675.85   0    1*    1*    1*/

5816.92913385827 2457.8 5816.92913385827     0 5816.92   0    1*    1*    1*/

5905.51181102362   2495 5905.51181102362     0 5905.51   0    1*    1*    1*/

6246.71916010499 2638.32 6246.71916010499     0 6246.71   0    1*    1*    1*/

6151.57480314961 2598.36 6151.57480314961     0 6151.57   0    1*    1*    1*/

6151.57480314961 2598.36 6151.57480314961     0 6151.57   0    1*    1*    1*/
```

```
5006.56167979003 2102.76 5006.56167979003    1* 5006.56    1*    1*   1*  1*/

5561.02362204724  2335.6 5561.02362204724    1* 5561.02    1*    1*   1*  1*/

5774.2782152231  2425.2 5774.2782152231     1* 5774.27    1*    1*   1*  1*/
ECHO
RPTSOL
--
-- Initialisation Print Output
--
'PRES' 'SOIL' 'SWAT' 'SGAS' 'RS' 'RV' 'RESTART=2' 'FIP=1' 'EQUIL' 'FIPVE'
'SWCO' 'SGCO' 'FIPTR=2' 'PD' 'KRW' 'KRG' 'PKRO' 'PKRW' 'PKRG' 'PPCW' 'PPCG'
/
```

MS_SCH.INC

```
WELSPECS
'5C' '1' 13 24 5095.30839895013 'GAS' 1* 'STD' 'SHUT' 'YES' 1 'SEG' 1* /
 /

RPTRST
'BASIC=5' 'FIP' 'FREQ=1' 'DRAIN=1' 'NORST=1' 'SAVE=5' 'ALLPROPS=1' /

TUNING
10* /
1* 0.05 0.01 0.01 1* 0.5 0.1 0.1 3* /
2* 100 1* 100 5* /

RPTSCHED
'RESTART=2' 'FIP=1' 'WELLS=2' 'SUMMARY=1' 'CPU=1' 'NEWTON=1' /

COMPDAT
'5C' 13 24 2 2 'SHUT' 1 1* 0.51 1* 2 1* 'Z' 1* /
 /
COMPDAT
'5C' 14 24 7 16 'SHUT' 2 1* 0.51 1* 2 1* 'Z' 1* /
 /
COMPDAT
'5C' 14 24 17 21 'SHUT' 2 1* 0.51 1* 2 1* 'Z' 1* /
 /
COMPDAT
'5C' 15 24 23 23 'SHUT' 3 1* 0.51 1* 2 1* 'Z' 1* /
 /
COMPDAT
'5C' 16 24 31 31 'SHUT' 4 1* 0.51 1* 2 1* 'Z' 1* /
 /
COMPDAT
'5C' 16 24 33 33 'OPEN' 5 1* 0.51 1* 5 1* 'Z' 1* /
 /
COMPDAT
'5C' 16 23 33 33 'OPEN' 5 1* 0.51 1* 5 1* 'Z' 1* /
 /
COMPDAT
'5C' 17 23 36 36 'OPEN' 6 1* 0.51 1* 5 1* 'Z' 1* /
 /
COMPDAT
'5C' 17 23 39 39 'OPEN' 7 1* 0.51 1* 5 1* 'Z' 1* /
 /
COMPDAT
'5C' 17 23 41 41 'OPEN' 8 1* 0.51 1* 5 1* 'Z' 1* /
 /
COMPDAT
'5C' 17 23 42 42 'OPEN' 9 1* 0.51 1* 5 1* 'Z' 1* /
 /
COMPDAT
'5C' 18 23 44 44 'OPEN' 10 1* 0.51 1* 5 1* 'Z' 1* /
 /
COMPDAT
'5C' 18 23 49 49 'OPEN' 11 1* 0.51 1* 5 1* 'Z' 1* /
 /
COMPDAT
'5C' 18 23 50 50 'OPEN' 11 1* 0.51 1* 5 1* 'Z' 1* /
```

```
/
COMPDAT
'5C' 18 23 51 51 'OPEN' 11 1* 0.51 1* 5 1* 'Z' 1* /
/
COMPDAT
'5C' 18 23 52 52 'OPEN' 11 1* 0.51 1* 5 1* 'Z' 1* /
/
COMPDAT
'5C' 18 23 53 53 'OPEN' 11 1* 0.51 1* 5 1* 'Z' 1* /
/
COMPDAT
'5C' 18 23 54 54 'OPEN' 11 1* 0.51 1* 5 1* 'Z' 1* /
/
COMPDAT
'5C' 18 22 58 58 'OPEN' 12 1* 0.51 1* 5 1* 'Z' 1* /
/
COMPDAT
'5C' 18 22 62 62 'OPEN' 13 1* 0.51 1* 5 1* 'Z' 1* /
/
COMPDAT
'5C' 18 22 64 64 'OPEN' 14 1* 0.51 1* 5 1* 'Z' 1* /
/
COMPDAT
'5C' 18 22 66 66 'OPEN' 15 1* 0.51 1* 5 1* 'Z' 1* /
/
COMPDAT
'5C' 18 21 71 71 'OPEN' 16 1* 0.51 1* 5 1* 'Z' 1* /
/
COMPDAT
'5C' 18 21 72 72 'OPEN' 16 1* 0.51 1* 5 1* 'Z' 1* /
/
COMPDAT
'5C' 18 21 73 73 'OPEN' 16 1* 0.51 1* 5 1* 'Z' 1* /
/
COMPDAT
'5C' 18 21 74 74 'OPEN' 16 1* 0.51 1* 5 1* 'Z' 1* /
/
COMPDAT
'5C' 18 21 75 75 'OPEN' 16 1* 0.51 1* 5 1* 'Z' 1* /
/
COMPDAT
'5C' 18 21 76 76 'OPEN' 16 1* 0.51 1* 5 1* 'Z' 1* /
/
COMPDAT
'5C' 18 21 80 80 'OPEN' 17 1* 0.51 1* 5 1* 'Z' 1* /
/
COMPDAT
'5C' 18 21 82 82 'OPEN' 18 1* 0.51 1* 5 1* 'Z' 1* /
/
COMPDAT
'5C' 17 20 96 96 'OPEN' 19 1* 0.51 1* 5 1* 'Z' 1* /
/
COMPDAT
'5C' 17 20 97 97 'OPEN' 19 1* 0.51 1* 5 1* 'Z' 1* /
/
COMPDAT
'5C' 17 20 98 98 'OPEN' 19 1* 0.51 1* 5 1* 'Z' 1* /
/
```

```
COMPDAT
'5C' 17 20 99 99 'OPEN' 19 1* 0.51 1* 5 1* 'Z' 1* /
 /
COMPDAT
'5C' 17 20 100 100 'OPEN' 19 1* 0.51 1* 5 1* 'Z' 1* /
 /
COMPDAT
'5C' 17 20 101 101 'OPEN' 19 1* 0.51 1* 5 1* 'Z' 1* /
 /
COMPDAT
'5C' 17 20 102 102 'OPEN' 19 1* 0.51 1* 5 1* 'Z' 1* /
 /
COMPDAT
'5C' 17 20 103 103 'OPEN' 19 1* 0.51 1* 5 1* 'Z' 1* /
 /
COMPDAT
'5C' 17 20 104 104 'SHUT' 19 1* 0.51 1* 5 1* 'Z' 1* /
 /
COMPDAT
'5C' 17 20 105 105 'SHUT' 19 1* 0.51 1* 5 1* 'Z' 1* /
 /
COMPDAT
'5C' 17 20 113 113 'OPEN' 20 1* 0.51 1* 5 1* 'Z' 1* /
 /
COMPDAT
'5C' 17 20 114 114 'OPEN' 20 1* 0.51 1* 5 1* 'Z' 1* /
 /
COMPDAT
'5C' 17 20 115 115 'OPEN' 20 1* 0.51 1* 5 1* 'Z' 1* /
 /
COMPDAT
'5C' 17 20 116 116 'OPEN' 20 1* 0.51 1* 5 1* 'Z' 1* /
 /
COMPDAT
'5C' 17 20 117 117 'OPEN' 20 1* 0.51 1* 5 1* 'Z' 1* /
 /
COMPDAT
'5C' 16 19 136 136 'OPEN' 21 1* 0.51 1* 5 1* 'Z' 1* /
 /
COMPDAT
'5C' 17 18 138 138 'OPEN' 22 1* 0.51 1* 5 1* 'Z' 1* /
 /
-- PROSPER Lift Curves For ECLIPSE Simulator    (Gas - Producer Well)  (Units System  - FIELD)

VFPPROD
3 6348.43 'GAS' 'WGR' 'OGR' 'THP' 1* 'FIELD' 'BHP' /
200 500 1000 5000 10000 20000 35000 55000 80000 100000 /
314.7 348 381.4 414.7 448 481.4 514.7 548 581.4 614.7 /
0.002 0.03 0.07 0.12 0.18 0.25 0.33 0.41 0.5 0.6 /
0 0.00277778 0.00555556 0.00833333 0.0111111 0.0138889 0.0166667 0.0194444
0.0222222 0.025 /
0 /
1 1 1 1 148 270.5 494.3 903.3 1487.5 2576.3 4079.5 6161.1 8837.4 11082.8
/
2 1 1 1 183.3 314 538 921.7 1499.1 2583.3 4083.1 6163.3 8838.6 11083.5
/
. . .
```

```
WCONPROD
'5C' 'SHUT' 'THP' 6* 620.1 3 1* /
 /

DATES
23 'JUN' 1996 /
/
. . .
/

DATES
1 'NOV' 1998 /
/

WCONPROD
'5C' 'OPEN' 'THP' 6* 677.2 3 1* /
 /

COMPDAT
'5C' 13 24 2 2 'OPEN' 1 1* 0.51 1* 2 1* 'Z' 1* /
 /
COMPDAT
'5C' 14 24 7 16 'SHUT' 2 1* 0.51 1* 2 1* 'Z' 1* /
 /
COMPDAT
'5C' 14 24 17 21 'SHUT' 2 1* 0.51 1* 2 1* 'Z' 1* /
 /
COMPDAT
'5C' 15 24 23 23 'OPEN' 3 1* 0.51 1* 2 1* 'Z' 1* /
 /
COMPDAT
'5C' 16 24 31 31 'OPEN' 4 1* 0.51 1* 2 1* 'Z' 1* /
 /
COMPDAT
'5C' 16 24 33 33 'OPEN' 5 1* 0.51 1* 5 1* 'Z' 1* /
 /
COMPDAT
'5C' 16 23 33 33 'OPEN' 5 1* 0.51 1* 5 1* 'Z' 1* /
 /
COMPDAT
'5C' 17 23 36 36 'OPEN' 6 1* 0.51 1* 5 1* 'Z' 1* /
 /
COMPDAT
'5C' 17 23 39 39 'OPEN' 7 1* 0.51 1* 5 1* 'Z' 1* /
 /
COMPDAT
'5C' 17 23 41 41 'OPEN' 8 1* 0.51 1* 5 1* 'Z' 1* /
 /
COMPDAT
'5C' 17 23 42 42 'OPEN' 9 1* 0.51 1* 5 1* 'Z' 1* /
 /
COMPDAT
'5C' 18 23 44 44 'OPEN' 10 1* 0.51 1* 5 1* 'Z' 1* /
 /
COMPDAT
'5C' 18 23 49 49 'OPEN' 11 1* 0.51 1* 5 1* 'Z' 1* /
 /
COMPDAT
```

```
'5C' 18 23 50 50 'OPEN' 11 1* 0.51 1* 5 1* 'Z' 1* /
 /
COMPDAT
'5C' 18 23 51 51 'OPEN' 11 1* 0.51 1* 5 1* 'Z' 1* /
 /
COMPDAT
'5C' 18 23 52 52 'OPEN' 11 1* 0.51 1* 5 1* 'Z' 1* /
 /
COMPDAT
'5C' 18 23 53 53 'OPEN' 11 1* 0.51 1* 5 1* 'Z' 1* /
 /
COMPDAT
'5C' 18 23 54 54 'OPEN' 11 1* 0.51 1* 5 1* 'Z' 1* /
 /
COMPDAT
'5C' 18 22 58 58 'OPEN' 12 1* 0.51 1* 5 1* 'Z' 1* /
 /
COMPDAT
'5C' 18 22 62 62 'OPEN' 13 1* 0.51 1* 5 1* 'Z' 1* /
 /
COMPDAT
'5C' 18 22 64 64 'OPEN' 14 1* 0.51 1* 5 1* 'Z' 1* /
 /
COMPDAT
'5C' 18 22 66 66 'OPEN' 15 1* 0.51 1* 5 1* 'Z' 1* /
 /
COMPDAT
'5C' 18 21 71 71 'OPEN' 16 1* 0.51 1* 5 1* 'Z' 1* /
 /
COMPDAT
'5C' 18 21 72 72 'OPEN' 16 1* 0.51 1* 5 1* 'Z' 1* /
 /
COMPDAT
'5C' 18 21 73 73 'OPEN' 16 1* 0.51 1* 5 1* 'Z' 1* /
 /
COMPDAT
'5C' 18 21 74 74 'OPEN' 16 1* 0.51 1* 5 1* 'Z' 1* /
 /
COMPDAT
'5C' 18 21 75 75 'OPEN' 16 1* 0.51 1* 5 1* 'Z' 1* /
 /
COMPDAT
'5C' 18 21 76 76 'OPEN' 16 1* 0.51 1* 5 1* 'Z' 1* /
 /
COMPDAT
'5C' 18 21 80 80 'OPEN' 17 1* 0.51 1* 5 1* 'Z' 1* /
 /
COMPDAT
'5C' 18 21 82 82 'OPEN' 18 1* 0.51 1* 5 1* 'Z' 1* /
 /
COMPDAT
'5C' 17 20 96 96 'OPEN' 19 1* 0.51 1* 5 1* 'Z' 1* /
 /
COMPDAT
'5C' 17 20 97 97 'OPEN' 19 1* 0.51 1* 5 1* 'Z' 1* /
 /
COMPDAT
'5C' 17 20 98 98 'OPEN' 19 1* 0.51 1* 5 1* 'Z' 1* /
```

```
/
COMPDAT
'5C' 17 20 99 99 'OPEN' 19 1* 0.51 1* 5 1* 'Z' 1* /
/
COMPDAT
'5C' 17 20 100 100 'OPEN' 19 1* 0.51 1* 5 1* 'Z' 1* /
/
COMPDAT
'5C' 17 20 101 101 'OPEN' 19 1* 0.51 1* 5 1* 'Z' 1* /
/
COMPDAT
'5C' 17 20 102 102 'OPEN' 19 1* 0.51 1* 5 1* 'Z' 1* /
/
COMPDAT
'5C' 17 20 103 103 'OPEN' 19 1* 0.51 1* 5 1* 'Z' 1* /
/
COMPDAT
'5C' 17 20 104 104 'SHUT' 19 1* 0.51 1* 5 1* 'Z' 1* /
/
COMPDAT
'5C' 17 20 105 105 'SHUT' 19 1* 0.51 1* 5 1* 'Z' 1* /
/
COMPDAT
'5C' 17 20 113 113 'OPEN' 20 1* 0.51 1* 5 1* 'Z' 1* /
/
COMPDAT
'5C' 17 20 114 114 'OPEN' 20 1* 0.51 1* 5 1* 'Z' 1* /
/
COMPDAT
'5C' 17 20 115 115 'OPEN' 20 1* 0.51 1* 5 1* 'Z' 1* /
/
COMPDAT
'5C' 17 20 116 116 'OPEN' 20 1* 0.51 1* 5 1* 'Z' 1* /
/
COMPDAT
'5C' 17 20 117 117 'OPEN' 20 1* 0.51 1* 5 1* 'Z' 1* /
/
COMPDAT
'5C' 16 19 136 136 'OPEN' 21 1* 0.51 1* 5 1* 'Z' 1* /
/
COMPDAT
'5C' 17 18 138 138 'OPEN' 22 1* 0.51 1* 5 1* 'Z' 1* /
/

DATES
6 'NOV' 1998 /
/

WCONPROD
'5C' 'SHUT' 'THP' 6* 677.2 3 1* /
/

DATES
1 'DEC' 1998 /
/

WCONPROD
'5C' 'SHUT' 'THP' 6* 14.7 3 1* /
```

```
 /

DATES
1 'JAN' 1999 /
 /

WCONPROD
'5C' 'SHUT' 'THP' 6* 435.2 3 1* /
 /

DATES
4 'JAN' 1999 /
 /

WCONPROD
'5C' 'OPEN' 'THP' 6* 435.2 3 1* /
 /
. . .
 /

DATES
25 'OCT' 2003 /
 /

WCONPROD
'5C' 'SHUT' 'THP' 6* 459.4 3 1* /
 /

RPTRST
'BASIC=2' 'DRAIN=1' 'NORST=0' 'SAVE=5' 'ALLPROPS=1' /

RPTSCHED
'RESTART=2' 'FIP=1' 'WELLS=2' 'CPU=1' /

DATES
1 'JUN' 2004 /
 /

-- PROSPER Lift Curves For ECLIPSE Simulator    (Gas - Producer Well)  (Units System  - FIELD)
VFPPROD
3 6348.43 'GAS' 'WGR' 'OGR' 'THP' 1* 'FIELD' 'BHP' /
200 500 1000 5000 10000 20000 35000 55000 80000 100000 /
314.7 348 381.4 414.7 448 481.4 514.7 548 581.4 614.7 /
0.002 0.03 0.07 0.12 0.18 0.25 0.33 0.41 0.5 0.6 /
0 0.00277778 0.00555556 0.00833333 0.0111111 0.0138889 0.0166667 0.0194444
0.0222222 0.025 /
0 /
1 1 1 1 148 270.5 494.3 903.3 1487.5 2576.3 4079.5 6161.1 8837.4 11082.8
/
2 1 1 1 183.3 314 538 921.7 1499.1 2583.3 4083.1 6163.3 8838.6 11083.5
/
. . .

WELSPECS
'MN2' '2' 20 30 5095.308 'GAS' 1* 'STD' 'SHUT' 'YES' 1 'SEG' 1* /
 /

RPTSCHED
```

'RESTART=2' 'FIP=1' 'WELLS=2' 'CPU=1' 'FIPTR=2' 'SALT' 'FIPSALT=2' 'VWAT'
/

RPTRST
'BASIC=5' 'FIP' 'FREQ=1' 'DRAIN=1' 'NORST=1' 'SAVE=5' 'ALLPROPS=1' /

TUNING
10* /
1* 0.05 0.01 0.01 1* 0.5 0.1 0.1 3* /
2* 100 1* 100 5* /

COMPDAT
'MN2' 20 30 7 7 'OPEN' 2 1* 0.51 1* 5 1* 'Z' 1* /
/
COMPDAT
'MN2' 20 30 8 8 'OPEN' 2 1* 0.51 1* 5 1* 'Z' 1* /
/
COMPDAT
'MN2' 20 30 9 9 'OPEN' 2 1* 0.51 1* 5 1* 'Z' 1* /
/
COMPDAT
'MN2' 20 30 10 10 'OPEN' 2 1* 0.51 1* 5 1* 'Z' 1* /
/
COMPDAT
'MN2' 20 30 11 11 'OPEN' 2 1* 0.51 1* 5 1* 'Z' 1* /
/
COMPDAT
'MN2' 20 30 12 12 'OPEN' 2 1* 0.51 1* 5 1* 'Z' 1* /
/
COMPDAT
'MN2' 20 30 13 13 'OPEN' 2 1* 0.51 1* 5 1* 'Z' 1* /
/
COMPDAT
'MN2' 20 30 14 14 'OPEN' 2 1* 0.51 1* 5 1* 'Z' 1* /
/
COMPDAT
'MN2' 20 30 15 15 'OPEN' 2 1* 0.51 1* 5 1* 'Z' 1* /
/
COMPDAT
'MN2' 20 30 16 16 'OPEN' 2 1* 0.51 1* 5 1* 'Z' 1* /
/
COMPDAT
'MN2' 20 30 17 17 'OPEN' 2 1* 0.51 1* 5 1* 'Z' 1* /
/
COMPDAT
'MN2' 20 30 18 18 'OPEN' 2 1* 0.51 1* 5 1* 'Z' 1* /
/
COMPDAT
'MN2' 20 30 19 19 'OPEN' 2 1* 0.51 1* 5 1* 'Z' 1* /
/
COMPDAT
'MN2' 20 30 20 20 'OPEN' 2 1* 0.51 1* 5 1* 'Z' 1* /
/
COMPDAT
'MN2' 20 30 21 21 'OPEN' 2 1* 0.51 1* 5 1* 'Z' 1* /
/
COMPDAT
'MN2' 21 30 23 23 'OPEN' 3 1* 0.51 1* 5 1* 'Z' 1* /

```
/
COMPDAT
'MN2' 21 29 31 31 'OPEN' 4 1* 0.51 1* 5 1* 'Z' 1* /
/
COMPDAT
'MN2' 21 29 33 33 'OPEN' 5 1* 0.51 1* 5 1* 'Z' 1* /
/
COMPDAT
'MN2' 21 29 34 34 'OPEN' 24 1* 0.51 1* 5 1* 'Z' 1* /
/
COMPDAT
'MN2' 21 29 39 39 'OPEN' 7 1* 0.51 1* 5 1* 'Z' 1* /
/
COMPDAT
'MN2' 21 28 41 41 'OPEN' 8 1* 0.51 1* 5 1* 'Z' 1* /
/
COMPDAT
'MN2' 21 28 42 42 'OPEN' 9 1* 0.51 1* 5 1* 'Z' 1* /
/
COMPDAT
'MN2' 21 28 44 44 'OPEN' 10 1* 0.51 1* 5 1* 'Z' 1* /
/
COMPDAT
'MN2' 21 27 49 49 'OPEN' 11 1* 0.51 1* 5 1* 'Z' 1* /
/
COMPDAT
'MN2' 21 27 50 50 'OPEN' 11 1* 0.51 1* 5 1* 'Z' 1* /
/
COMPDAT
'MN2' 21 27 51 51 'OPEN' 11 1* 0.51 1* 5 1* 'Z' 1* /
/
COMPDAT
'MN2' 21 27 52 52 'OPEN' 11 1* 0.51 1* 5 1* 'Z' 1* /
/
COMPDAT
'MN2' 21 27 53 53 'OPEN' 11 1* 0.51 1* 5 1* 'Z' 1* /
/
COMPDAT
'MN2' 21 27 54 54 'OPEN' 11 1* 0.51 1* 5 1* 'Z' 1* /
/
COMPDAT
'MN2' 21 27 58 58 'OPEN' 12 1* 0.51 1* 5 1* 'Z' 1* /
/
COMPDAT
'MN2' 20 26 64 64 'OPEN' 14 1* 0.51 1* 5 1* 'Z' 1* /
/
COMPDAT
'MN2' 20 26 69 69 'OPEN' 25 1* 0.51 1* 5 1* 'Z' 1* /
/
COMPDAT
'MN2' 20 25 71 71 'OPEN' 16 1* 0.51 1* 5 1* 'Z' 1* /
/
COMPDAT
'MN2' 20 25 72 72 'OPEN' 16 1* 0.51 1* 5 1* 'Z' 1* /
/
COMPDAT
'MN2' 19 25 73 73 'OPEN' 16 1* 0.51 1* 5 1* 'Z' 1* /
/
```

```
 COMPDAT
'MN2' 19 25 74 74 'OPEN' 16 1* 0.51 1* 5 1* 'Z' 1* /
 /
 COMPDAT
'MN2' 19 25 75 75 'OPEN' 16 1* 0.51 1* 5 1* 'Z' 1* /
 /
 COMPDAT
'MN2' 19 25 76 76 'OPEN' 16 1* 0.51 1* 5 1* 'Z' 1* /
 /
 COMPDAT
'MN2' 19 25 82 82 'OPEN' 18 1* 0.51 1* 5 1* 'Z' 1* /
 /
 COMPDAT
'MN2' 19 24 85 85 'OPEN' 26 1* 0.51 1* 5 1* 'Z' 1* /
 /
 COMPDAT
'MN2' 19 24 86 86 'OPEN' 26 1* 0.51 1* 5 1* 'Z' 1* /
 /
 COMPDAT
'MN2' 19 24 87 87 'OPEN' 26 1* 0.51 1* 5 1* 'Z' 1* /
 /
 COMPDAT
'MN2' 19 24 88 88 'OPEN' 26 1* 0.51 1* 5 1* 'Z' 1* /
 /
 COMPDAT
'MN2' 19 24 89 89 'OPEN' 26 1* 0.51 1* 5 1* 'Z' 1* /
 /
 COMPDAT
'MN2' 19 24 90 90 'OPEN' 26 1* 0.51 1* 5 1* 'Z' 1* /
 /
 COMPDAT
'MN2' 18 24 90 90 'OPEN' 26 1* 0.51 1* 5 1* 'Z' 1* /
 /
 COMPDAT
'MN2' 18 24 91 91 'OPEN' 26 1* 0.51 1* 5 1* 'Z' 1* /
 /
 COMPDAT
'MN2' 18 24 92 92 'OPEN' 26 1* 0.51 1* 5 1* 'Z' 1* /
 /
 COMPDAT
'MN2' 18 24 93 93 'OPEN' 26 1* 0.51 1* 5 1* 'Z' 1* /
 /
 COMPDAT
'MN2' 18 24 94 94 'OPEN' 26 1* 0.51 1* 5 1* 'Z' 1* /
 /

WCONPROD
'MN2' 'OPEN' 'THP' 6* 159.7 3 1* /
 /

WECON
'MN2' 1* 10 3* 'NONE' 'YES' 1* 'RATE' 1* 'NONE' 2* /
 /

TSTEP
91.25 /
. . .
```

Vitae

Manisa Rangponsumrit was born on December 30, 1975 in Chachoengsao, Thailand. She received her B.Eng. in Electrical Engineering from the Faculty of Engineering, Chiangmai University in 1997. She has been a graduate student in the Master's Degree Program in Petroleum Engineering of the Department of Mining and Petroleum Engineering, Chulalongkorn University since 2002.